

# Northumbria Research Link

Citation: Theodorou, Pavlos (2000) ATM optical wireless networks. Doctoral thesis, University of Northumbria at Newcastle.

This version was downloaded from Northumbria Research Link:  
<https://nrl.northumbria.ac.uk/id/eprint/15694/>

Northumbria University has developed Northumbria Research Link (NRL) to enable users to access the University's research output. Copyright © and moral rights for items on NRL are retained by the individual author(s) and/or other copyright owners. Single copies of full items can be reproduced, displayed or performed, and given to third parties in any format or medium for personal research or study, educational, or not-for-profit purposes without prior permission or charge, provided the authors, title and full bibliographic details are given, as well as a hyperlink and/or URL to the original metadata page. The content must not be changed in any way. Full items must not be sold commercially in any format or medium without formal permission of the copyright holder. The full policy is available online: <http://nrl.northumbria.ac.uk/policies.html>

Some theses deposited to NRL up to and including 2006 were digitised by the British Library and made available online through the [EThOS e-thesis online service](#). These records were added to NRL to maintain a central record of the University's research theses, as well as still appearing through the British Library's service. For more information about Northumbria University research theses, please visit [University Library Online](#).



**Northumbria  
University**  
NEWCASTLE



**UniversityLibrary**

# ATM Optical Wireless Networks

**Pavlos Theodorou** Ptychion (BEng), MSc

Thesis submitted to the University of Northumbria at Newcastle in partial fulfilment  
of the requirements for the degree of Doctor of Philosophy.

School of Engineering at the University of Northumbria, Newcastle, UK.

# Dedicated to The Most Holy Trinity

*... .. do not try to discover things that are beyond your power, for you can be misled by your own presumption and thus mislead others too.*

**(True Life In God, 7th Dec. 1989)**

*A skilled craftsman is admired for the things he makes, and a leader's wisdom is proved by his words.*

**(Sirach 9;17)**

## Acknowledgements

---

There were many people who, in the process of doing this research, provided me with invaluable help, support and encouragement. To the following people I am deeply indebted.

At the School of Engineering, University of Northumbria: Dr. Sexton Graham; Director of Studies, Dr. Jaafar Elmirghani; Director of studies, Prof. Robert Cryan; Second Director of Studies, Dr. Sean Danaher; Principal Lecturer.

In the mathematical department: Prof. Stan Scott; Retired Professor, Dr. Judith Akinbolu; Principal Lecturer.

Within the department of Engineering I extend my thanks to all those colleagues and friends who through their sharing, laughter and concern allowed me to persevere with this work.....names too numerous to mention but you all know who you are.....especially Dina, whose coffee I always refused but appreciated the daily question ☺

My friends outside the university who patiently tolerated the ups and downs of a PhD student...thanks guys!

The author is *especially* grateful to his Mama & Baba for the support, love and patience throughout this challenging task.

And...saving the Best for last, To Our Lord, God and Master, The Ultimate Educator for allowing me the skills of the craftsman and the wisdom to have made it all possible, to Him be The Glory.



# CONTENTS

---

<b>ABSTRACT</b>	<b>VI</b>
<b>LIST OF ACRONYMS AND SYMBOLS</b>	<b>VIII</b>
<b>LIST OF FIGURES</b>	<b>XIV</b>
 <b>OVERVIEW OF THE THESIS</b>	 <b>1</b>
<b>1 INTRODUCTION</b>	<b>2</b>
1.1 <i>Research Objectives</i>	4
1.2 <i>Organisation of the Report</i>	7
1.3 <i>Original Contributions</i>	9
 <b>BACKGROUND</b>	 <b>13</b>
<b>2 ASYNCHRONOUS TRANSFER MODE (ATM)</b>	<b>14</b>
2.1 <i>Introduction</i>	14
2.2 <i>ATM and the B-ISDN Protocol</i>	15
2.3 <i>The ATM Layer</i>	17
2.4 <i>The ATM Adaptation Layer (AAL)</i>	20
2.5 <i>ATM Cells</i>	22
2.6 <i>ATM Traffic Management</i>	26
2.7 <i>Summary</i>	29
 <b>3 INFRARED (IR) WIRELESS SYSTEMS</b>	 <b>31</b>
3.1 <i>Introduction</i>	31
3.2 <i>IR versus Radio Communication Systems</i>	32
3.3 <i>Types of IR Wireless Links</i>	34
3.4 <i>IR Wireless Channel Characterisation</i>	37
3.5 <i>IR Radiation and Eye Safety</i>	41

3.6	<i>Current IR Communication Systems</i>	43
3.7	<i>Summary</i>	46
<b>NEW HYBRID LAN</b>		<b>47</b>
<b>4</b>	<b>THE PROPOSED ATM IR WIRELESS LAN</b>	<b>48</b>
4.1	<i>Introduction</i>	48
4.2	<i>Network Scenario</i>	49
4.3	<i>The Protocol Stack Model</i>	53
4.4	<i>The Medium Access Control (MAC) Protocol</i>	56
4.5	<i>Wireless ATM Cell Format</i>	59
4.6	<i>Technical Challenges of Employing ATM over Diffused IR Links</i>	62
4.7	<i>Summary</i>	63
<b>5</b>	<b>ANALYSIS AND PERFORMANCE OF THE MAC PROTOCOL</b>	<b>65</b>
5.1	<i>Introduction</i>	65
5.2	<i>Speech Source Model</i>	65
5.3	<i>Steady-State Probability</i>	67
5.4	<i>Packet Dropping Probability</i>	70
5.5	<i>System Throughput</i>	74
5.6	<i>Average Access Delay</i>	75
5.7	<i>Statistical Multiplexing Gain</i>	76
5.8	<i>Numerical Results</i>	76
5.9	<i>Summary</i>	83
<b>6</b>	<b>ANALYSIS AND PERFORMANCE OF THE HANDOVER PRIORITY-BASED MAC PROTOCOL</b>	<b>86</b>
6.1	<i>Introduction</i>	86
6.2	<i>Steady-State Probability</i>	87
6.3	<i>Packet Dropping Probability</i>	97
6.4	<i>System Throughput</i>	99
6.5	<i>Average Access Delay</i>	100
6.6	<i>New Call Blocking Probability</i>	100

6.7	<i>Handover Blocking Probability</i>	101
6.8	<i>Forced Termination Probability</i>	102
6.9	<i>Performance</i>	103
6.10	<i>Summary</i>	109
<b>7</b>	<b>SIMULATION OF THE MODEL</b>	<b>112</b>
7.1	<i>Introduction</i>	112
7.2	<i>Block Diagram of the Simulation Model</i>	113
7.3	<i>The Source</i>	118
7.4	<i>The MAC Protocol</i>	122
7.5	<i>Comparison of Analysis and Simulation Results</i>	128
7.6	<i>Summary</i>	132
	<b>DISCUSSION</b>	<b>133</b>
<b>8</b>	<b>PROPOSED EXTENDED WORK</b>	<b>134</b>
8.1	<i>Introduction</i>	134
8.2	<i>Dynamic Slot Allocation of the MAC Protocol</i>	134
8.3	<i>MAC Performance Under Hybrid FEC/ARQ Techniques</i>	135
8.4	<i>Co-channel Interference for Various Reuse Factors</i>	136
8.5	<i>Handover Request Initiation</i>	137
8.6	<i>Simulation Including Mobility and IR Channel Impairments</i>	138
8.7	<i>Summary</i>	139
<b>9</b>	<b>CONCLUSIONS</b>	<b>141</b>
	<b>APPENDIX A</b>	<b>145</b>
	<b>APPENDIX B</b>	<b>146</b>
	<b>APPENDIX C</b>	<b>147</b>
	<b>REFERENCES</b>	<b>148</b>

## ABSTRACT

---

The aim of the research is to propose, design and evaluate a new wireless communication, local area network (LAN). Such a LAN will be able to extend the asynchronous transfer mode (ATM) wireline technology into indoor optical wireless networks.

To date many studies have been conducted in order to extend the ATM capabilities into radio wireless systems. Due to high bandwidths, which are required for wireless broadband platforms, radio is not the most conducive medium to deliver these because of various technical impairments. Impairments such as spectrum regulations, low antenna gain, and high-noise floor due to multi-user interference once market penetration is achieved. However, since diffused infrared (IR) technology offers mobility in indoor environments and high bandwidth channels it is potentially a more favourable alternative medium.

This thesis presents the network scenario and the protocol structure design of the IR wireless LAN in a way that it provides seamless interworking with the wired ATM network. Using mathematical analysis, its statistical performance parameters for variable bit rate packet (VBR) services, such as voice and video, is investigated. It is shown that for packet dropping probability ( $P_{\text{drop}}$ ) equal to 1%, the system is capable of supporting 15 voice terminal units (TUs) simultaneously. The utilisation of the IR channel is 0.68 and the statistical multiplexing gain is 1.7 conversations per time slot. If there are less than 14 TUs, the variance of them has no effect on the average access delay but if the TUs exceed 14, the system is said to be in a sensitive region, and therefore the access delay increases rapidly. The multiaccess interference at the correlative receiver is found to be approximately  $10^{-8}$ , a satisfactory value.

To support mobile ATM voice services over the IR wireless LANs a hybrid handover priority-based medium access control (MAC) protocol is designed.



Carrying out mathematical analysis, its performance parameters are derived for fixed slot assignment. When VBR voice TUs are served it is shown that the forced termination probability improved over the nonpriority handover scheme in return of increasing the new call blocking probability. For  $P_{\text{drop}} = 1\%$  the new call blocking probability is less than 1% while the forced termination probability is less than 0.05%. Moreover, the value of the system throughput parameter is slightly changed over the nonpriority scheme only for high new call arrival rates demonstrating a general improved performance of the network.

Discrete time and event simulation process is used to evaluate the system performance. The simulation model is divided into two main phases, the traffic generation (talkspurts and silences) and the MAC mechanism. Performance parameters such as packet dropping probability, throughput, average access delay and statistical multiplexing gain are simulated and compared with those derived from an operative mathematical analysis. The results of both processes are in close agreement.

# LIST OF ACRONYMS AND SYMBOLS

---

## Acronyms

AAL	ATM Adaptation Layer
ACK	Acknowledgement Slot
AEL	Accessible Emission Limit
ARQ	Automatic Repeat Request
ATM	Asynchronous Transfer Mode
BER	Bit Error Rate
B-ISDN	Broadband Integrated Services Digital Network
BS	Base Station
CAC	Connection Admission control
CBR	Constant Bit rate
CI	Confidence Interval
CLP	Cell Loss Priority
CRC	Cyclic Redundancy Check
CS	Convergence Sublayer
DATA	Data Field of an IWC
DD	Direct Detection
DLC	Data Link Control
FCC	Federal Communication Commission
FDD	Frequency Division Duplex
FEC	Forward Error Control
GFC	Generic Flow Control
H	Header
HEC	Head Error Control
HF	Header Field
HLR	Home Location Register
I	Information Slot

---

IM	Intensity Modulation
ISI	Intersymbol Interference
IEEE	Institution of Electrical & Electronic Engineering
IEC	International Electrotechnical Commission
IR	Infrared
IrDA	Infrared Data Association
ISDN	Integrated Services Digital Network
ISI	Intersymbol Interference
ITU-T	International Telecommunication Union (Standardisation Sector)
IWC	Infrared Wireless Cell
LAN	Local Area Network
LD	Laser Diode
LED	Light Emitting Diode
LOS	Line-of-Sight
MAC	Medium Access Control
MVCC	Metasignaling Virtual Channel Connection
NNI	Network-to Network Interface
OOK	ON-OFF keying modulation
PHY	Physical Layer
PRMA	Packet Reservation Multiple Access
PT	Payload Type Identifier
QoS	Quality of Service
R	Reservation Slot
RZ	Return Zero Pulse Modulation
SAAL	Signalling ATM Adaptation Layer
SAR	Segmentation and Reassembly
SDH	Synchronous Digital Hierarchy
SIG	Signalling Layer
SNR	Signal-to-Noise Ratio
SONET	Synchronous Optical Network
SVCC	Signalling Virtual Channel Connection



TDD	Time Division Duplex
TDMA	Time Division Multiple Access
TF	Tail Field
TU	Terminal Unit
UNI	User-to-Network Interface
UPC	Usage Parameter Control
VBR	Variable Bit Rate
VC	Virtual Channel
VCC	Virtual Channel Connection
VCI	Virtual Channel Identifier
VP	Virtual Path
VPC	Virtual Path Connection
VPI	Virtual Path Identifier

## Symbols

### Roman

$B_c$	Allocated bandwidth within a downlink/uplink frame
$B_v$	Statistical bandwidth for the VBR video source
$C$	Number of slots in the common group
$C_d(M)$	All distributions of $T$ TUs to the $Z$ cells with exactly $M$ TUs remaining in the cell under consideration
$\bar{D}$	Delay experienced by a terminal
$D_{\max}$	Maximum delay limit for voice packets
$d_{\min}$	Distance cover by a TU during $t_{\min}$
$d_{\text{rms}}$	Channel rms delay spread

$d_s$	Distance between two neighbouring cells
$E[x]$	Statistical expected value of the random variable $x$
$F_D(D, t_1)$	Derivative of probability density function of delay
$F_{tot}$	The total circular area of the cell
$F_1$	The cell area where each covered distance is smaller than $d_{min}$
$f(D, t, t_1)$	Joint probability density function of $D$ and message duration of $t$ seconds with average message duration of $t_1$ seconds
$f_D(D, t_1)$	Probability density function of delay
$f_t(t, t_1)$	Probability density function of message duration
$G$	Statistical multiplexing gain
$H$	Number of bits for header information
$H(0)$	IR wireless channel dc gain
$H(f)$	Fourier transform of $h(t)$
$h(t)$	Impulse response
$J$	Channel reuse factor
$L$	Number of TUs in the system
$L_q$	Number of TUs in the queue
$M$	Number of TUs within a cell
$M_{max}$	Maximum Number of TUs supported within a channel frame
$\mu_d$	Channel mean delay spread
$N$	Number of slots per frame
$N_p$	Number of packets in a message
$N_s(t)$	Signal-independent additive noise
$n$	Number of TUs in the system
$n_c$	Number of contending TUs
$n_r$	Number of reserved slots in the channel frame
$P$	Optical prime code
$P_b$	New call blocking probability
$P_d$	Number of dropped packets in a TU
$P_{drop}$	Packet dropping probability for a VBR voice TU
$P_F$	Forced call termination probability

$P_H$	Probability that a call needs a handover
$P_{HB}$	Total handover blocking probability
$P_{hb}$	Handover blocking probability when $M_{\max}$ TUs are in the system
$P_{hb'}$	Handover blocking probability due to $t_{\min}$
$P_{\text{loos}}$	Packet loss probability for a VBR video TU
$P_M$	Average probability of M TUs stay within a cell
$P_N$	Average probability that exactly M TUs stay in the cell
$P_n$	State probability of n in the system
$P_r$	Average received optical power
$P_t$	Average transmitted optical power
$P_0$	State probability of 0 in the system
$q$	Number of information bits within a time slot
$q_n$	This variable relates the general-time probability $P_n$ to the probability that an arrival finds n TUs in the system
$R$	Photodetector responsivity
$R_c$	Channel bit rate
$R_s$	Source rate
$r$	Cell radius
$T$	Total number of TUs within the LAN
$T_c$	Average call duration without any prematurely termination
$T_d$	Downlink timing signal
$T_{cf}$	Channel frame duration
$T_f$	Uplink/downlink frame duration
$T_h$	Mean sojourn time of a TU in the cell
$T_r$	Average time between call arrivals
$t_1$	Talkspurt duration
$t_2$	Silence duration
$t_{\min}$	Minimum tolerant time between two consecutive handovers
$v$	Speed of a mobile TU
$V_N$	Required number of slots per channel frame for the VBR video TU

$X(t)$	Instantaneous optical power of the IR emitter
$Y(t)$	Instantaneous current in the receiving photodetector
$Z$	Number of hexagonal cells

### Greek

$\alpha$	Number of cell crossings per unit time
$\beta$	Speech source burstiness
$\gamma$	Transition probability from talking to silent state during a channel frame
$\delta$	Speech source activity ratio
$\eta$	System throughput
$\lambda$	Mean arrival rate (independent of the system size)
$\lambda_H$	Mean value of the handover arrival rate
$\lambda_N$	Mean value of the new talkspurt arrival rate
$\lambda_n$	Mean arrival rate when there are $n$ TUs in the system
$\mu$	Mean service rate (independent of the system)
$\mu_n$	Mean service rate when there are $n$ TUs in the system
$\sigma$	Transition probability from silent to talking state during a channel frame



## LIST OF FIGURES

---

<i>Fig. 2-1 B-ISDN protocol reference model</i>	15
<i>Fig. 2-2 ATM connection structure</i>	17
<i>Fig. 2-3 Service classification for AAL</i>	21
<i>Fig. 2-4 ATM cell format</i>	22
<i>Fig. 2-5 ATM cell headers</i>	23
<i>Fig. 2-6 HEC field operation</i>	25
<i>Fig. 3-1 Configuration of wireless optical links</i>	36
<i>Fig. 3-2 IR wireless channel model</i>	38
<i>Fig. 4-1 Network configuration representing the attached wireless LAN onto the wired ATM network</i>	49
<i>Fig. 4-2 Cellular topology. a) Using a channel reuse factor of seven in a cellular system, b) axes to specify the position of a cell relative to its nearest neighbour.</i>	51
<i>Fig. 4-3 Protocol stack configuration for the user and control plane</i>	54
<i>Fig. 4-4 Timing organisation for the uplink and downlink frame of the MAC protocol</i>	58
<i>Fig. 4-5 The IR wireless cell format, a) the new DLC frame and b) the final form of the wireless cell after the MAC layer</i>	61
<i>Fig. 5-1 Two-state Markovian model for speech source</i>	66
<i>Fig. 5-2 Packet dropping probability versus the number of voice TUs when there is a) no video TU and b) one video TU, in the system</i>	79
<i>Fig. 5-3 System throughput versus the number of voice TUs when there is a) none video TU and b) one video TU, in the system</i>	80

<i>Fig. 5-4 Average access delay versus the number of voice TUs when there is a) none video TU and b) one video TU, in the system</i>	81
<i>Fig. 5-5 Statistical multiplexing gain of the MAC protocol while <math>P_{drop} = 1\%</math></i>	82
<i>Fig. 6-1 Arrivals and departures within a cell</i>	89
<i>Fig. 6-2 One dimensional Markov-chain state transition diagram</i>	90
<i>Fig. 6-3 Forced termination probability versus new call arrival rate /TU/min</i>	105
<i>Fig. 6-4 New call blocking probability versus new call arrival rate /TU/min</i>	106
<i>Fig. 6-5 Packet dropping probability versus new call arrival rate /TU/min</i>	107
<i>Fig. 6-6 Average access delay versus new call arrival rate /TU/min</i>	108
<i>Fig. 6-7 Throughput versus new call arrival rate /TU/min</i>	109
<i>Fig. 7-1 Basic block diagram of the discrete time simulation model</i>	114
<i>Fig. 7-2 Basic block diagram of the discrete event simulation model</i>	117
<i>Fig. 7-3 Flow chart for arranging talkspurt and silence streams of each TU on the same time axis</i>	120
<i>Fig. 7-4 Flow chart that replaces the value of each random number with 1s and 0s.</i>	121
<i>Fig. 7-5 Flow chart diagram for the discrete time MAC mechanism</i>	124
<i>Fig. 7-6 Flow chart diagram for the discrete event MAC mechanism</i>	127
<i>Fig. 7-7 Simulation and analysis results for the packet dropping probability</i>	129
<i>Fig. 7-8 Simulation and analysis results for the throughput system</i>	130
<i>Fig. 7-9 Simulation and analysis results for the average access delay</i>	131
<i>Fig. 7-10 Simulation and analysis results for the statistical multiplexing gain</i>	132



# OVERVIEW OF THE THESIS

## CHAPTER ONE: INTRODUCTION



# 1 INTRODUCTION

The past three centuries have each been dominated by a single technology. The 18<sup>th</sup> century was the time of the great mechanical systems accompanying the industrial revolution. The 19<sup>th</sup> century was the age of the steam engine. During the 20<sup>th</sup> century, the key technology has been information gathering, processing, and distribution through telecommunication networks. Nowadays in the field of telecommunications, developments are proceeding along two main lines: the world-wide wired infrastructure using optical fibres and the wireless services. The optical wired infrastructure of broadband integrated services digital networks (B-ISDNs) deploys the asynchronous transfer mode (ATM) packet format which has brought us to the beginning of a new era in telecommunications networking [1-21]. ATM is designed to support high-bandwidth multimedia applications, to provide bandwidth on demand, traffic integration, cost effectiveness and flexible data networking.

Although ATM was designed for optical wired networks, several studies since the early '90s have been conducted to extend ATM into outdoor/indoor wireless networks [22,23]. The challenge is to extend the ATM capabilities into the wireless medium, a medium that does not promise the same quality of service as optical fibres. This is because a wireless link is subject to several impairments arising from noisy environments, multipath dispersion, inherent user mobility and unavoidable changes caused by motion of the surrounding environment. These impairments often result in a high bit-error-rate communication channel that is unable to meet the needs for multimedia applications.

There are two viable media which we can consider to implement indoor wireless B-ISDN systems, radio and infrared. Radio (including the band of microwaves) is already used in cellular phone systems, but such links will always find it difficult to deliver mobile high bandwidths which are required for multimedia broadband platforms. Oppositely, the very high carrier frequency associated with infrared systems (e.g. 300 THz at  $1\mu\text{m}$  wavelength) promises high bandwidth channels in the GHz region. Moreover, IR transmission neither interferes with existing radio systems or falls under any regulation of the Federal Communication Commission (FCC) and therefore there is no need for any licence. Also, the fact that infrared signals do not penetrate walls enables an indoor wireless network to provide both a considerable degree of privacy within an area, and a very large spatial bandwidth at the same spectrum because the same wavelength can be reused in adjacent areas.

Wireless networking using IR technology was first proposed over 17 years ago and has recently become a commercial reality, with a few companies marketing IR modems operating at different data rates. However, prior to this decade very little had been published by the research community. Over the last five years the situation has changed drastically and there has been a great deal of research activity that has examined the extent to which IR can support future requirements for high bit rate services and methods for mitigating the inherent problems associated with the physical layer only. However, research activity regarding protocols that stand above the physical layer and they are responsible to share the IR medium to users, carry out

mobility management, interface the wireless local network (LAN) with existing broadband wired networks (e.g. ATM) is still in its infancy.

This project aims to integrate the ATM protocol with the infrared wireless technology in a new hybrid communication system. Such a system will facilitate to extend the broadband wired networks into indoor optical wireless LANs. The primary objectives have been to establish both requirements and strategies to employ the ATM protocol into optical wireless links. This has resulted in an original design, mathematical analysis, simulation and evaluation of the prototype model that is capable of supporting variable bit rate ATM services in fully mobile indoor wireless LANs.

### **1.1 Research Objectives**

To acquire an insight into the wired B-ISDN protocol model and to appreciate the aspects needed to support high performance voice, video, and text services. Because both wired and wireless networks will use ATM to transfer information it is of interest to appreciate the merits and requirements of traffic and congestion control in this technology.

To review and identify the merits and limitations of the optical wireless technology, and compare them with the radio communications. Further, to identify the technical



challenges and the obstacles of optical wireless ATM service delivery in addition to techniques for mitigating these effects.

To keep complexity and time processing between the wired and wireless network at minimum. Therefore, the overall protocol stack of the model was designed to provide seamless interworking with the wired network. This kind of “native approach” transports the ATM cells between ATM node and mobile terminal units as transparently as possible.

To identify and propose a suitable medium access control (MAC) protocol suitable for small sized cell networks. This established the requirement to adopt a packet reservation multiple access (PRMA) protocol and modify it to operate under time division duplex (TDD) mode. The original PRMA protocol was also modified to a contention free slot reservation protocol by assigning each terminal user a unique orthogonal optical prime code. Subsequently, a new hybrid MAC protocol was designed to share the IR wireless medium to mobile terminal units and keep the pre-assigned quality of service for each type of service.

To design the format of the IR wireless cells (IWCs) which holds a vital role in the total performance of the network. The IWC must allocate space for the payload field as well as for signalling information and error correction codes. Here, the challenge is to keep the overhead size at minimum in order to increase the efficiency of the medium channel and to reduce header-processing time for the system.

To carry out a rigorous mathematical treatment of the MAC protocol. Initially, it was modelled as a  $M/M/N/\infty/M$  queuing model consisting of exponentially distributed durations of arrivals and departures,  $N$  parallel servers, infinite storage, and  $M$  users. Using variable bit rate speech and video sources, expressions for the state probabilities, system throughput, packet dropping probability, average access delay, and statistical multiplexing gain were derived. Hence, an original evaluation of the performance parameters for the model was carried out and the results accommodate the statistical behaviour of the MAC protocol. Then the MAC protocol was modelled as a  $M/M/N/\infty/M_{\max}$  queuing model consisting of two main service groups. The first group is the common group and its responsibility is to serve both new and handover arriving calls. The second group is the guard group and its responsibility is to exclusively serve handover requests. By employing only variable bit rate speech sources in the network, expressions for the state probabilities, system throughput, packet dropping probability, new call blocking probability, handover blocking probability, forced termination blocking probability and average access delay were derived. Hence, original numerical results of the performance parameters are given for a range of LAN specifications.

The mathematical treatment of the MAC protocol was validated by using a simulation process. The simulation model was split into two distinct phases, the data generation consisting of talkspurts and silences and the MAC mechanism. The

duration of a speech packet is taken to be the basic time unit or event for every process in the MAC hence, both discrete time and event simulation process are used.

## **1.2 Organisation of the Report**

Following the introduction in Chapter 1, the rest of the report is organised as follows:

Chapter 2 presents a review of the ATM technology. The protocol model and the format of the cells, which are used to convey user/signalling information across the network, are briefly presented. Also, the ATM layer with its traffic management and the ATM adaptation layer (AAL) with its service classification are discussed in some detail.

In chapter 3, the infrared (IR) wireless communication technology is briefly introduced. The advantages and drawbacks are compared to those of radio media. The different types of IR links as well as the fundamental properties of the IR medium using intensity modulation with direct detection (IM/DD) are presented. The eye safety problem that arises due to high optical powers is discussed while some of the currently available wireless IR links and LANs are described.

Chapter 4 presents the proposed scenario for an ATM optical wireless network. The original structures of the two plane protocol stacks as well as the new hybrid MAC



protocol to serve the need of sharing the medium channel to mobile terminal units (TUs) are presented. Finally, the author describes an original design of the optical wireless cell to convey information between the base station and TUs in the user plane.

The mathematical treatment of the MAC protocol is presented in Chapter 5. Using queuing theory, and specifically the birth-death theory, expressions for the steady-state probability, system throughput, packet dropping probability, average access delay, and statistical multiplexing gain of the system are derived. Original numerical results evaluating the system performance for typical model parameters are given as well. For a particular number of TUs staying in the cell the results depict the statistical behaviour of the MAC protocol for voice and video sources.

Chapter 6 is devoted to the mathematical treatment of the MAC protocol when handover-priority service is supported. Initially, the departure and arrival rates within a cell are derived and after using the birth-death theory to identify the statistical behaviour of the protocol the performance parameters are derived. Such parameters are packet dropping probability, new call blocking probability, handover blocking probability, forced termination blocking probability, system throughput and average access delay. Using the information in link design original numerical results of a LAN example, in which variable bit rate voice TUs are served, are presented.



Chapter 7 deals with the simulation process of the MAC protocol. Since the protocol can be characterised as a discrete time or event queuing model (its operation is synchronised on a slot basis), the simulation algorithm can be either discrete time or discrete event process. Performance parameters such as packet dropping probability, throughput, average access delay and statistical multiplexing gain are simulated and then compared with those taken by the mathematical analysis in Ch. 5. To implement the simulation model the mathematical program MATHCAD 8.0 Prof. by MathSoft, Inc. was used.

Lastly, chapter 8 addresses related areas for further investigation of the prototype model while chapter 9 summarises this report.

### **1.3 Original Contributions**

The author has

1. Presented a seamless interworking ATM overall protocol stack for ATM optical wireless networks and has proposed a general format for ATM optical wireless cells to carry the information between the base station and mobile terminal units.
2. Designed a new hybrid MAC protocol for sharing the IR channel to mobile terminal units.

3. Used queuing theory to carry out a mathematical analysis of the system and has therefore obtained expressions that characterise the performance of the system.
4. Established original results for system throughput, packet dropping probability, average access delay, and statistical multiplexing gain for ATM services in optical wireless systems.
5. Used queuing theory to carry out original mathematical analysis for a hybrid handover-priority mechanism in the MAC protocol.
6. Reported original results for packet dropping probability, new call blocking probability, handover-blocking probability and forced termination blocking probability of a fully mobile infrared wireless LAN.
7. Carried out discrete time simulation of the MAC protocol and compared the simulation results with those taken by the mathematical analysis.

These original contributions are supported by the following publications:

1. Pavlos Theodorou, J.M.H Elmirghani, R.A. Cryan, “*Concept and architecture for Indoor Optical Wireless Multimedia Systems*”, The International Society for Optical Engineering (SPIE), All-Optical Communication Systems: Architecture,

- Control and Network Issues Conference, Vol. 3230, pp. 104-108, Dallas, Texas, November 1997.
2. Pavlos Theodorou, J.M.H Elmirghani and R.A. Cryan, “*Packet Voice Transmission for Indoor Optical wireless Networks*”, Proc. IEEE Global Communications Conference (GLOBECOM'98), Sidney, Australia, Vol. 1, pp.288-233, 1998.
  3. Pavlos Theodorou, J.M.H Elmirghani, and R.A. Cryan “*ATM Infrared Wireless LANs: A proposed architecture*”, IEEE Communications Magazine, Vol. 36, No. 12, pp. 118-123, Dec. 1998.
  4. Pavlos Theodorou, J.M.H. Elmirghani, and R.A. Cryan, “*Broadband Optical Wireless ATM LANs With Fixed Time Slot Assignment*”, 3rd IEEE International Workshop on Broadband Switching Systems, Queen's University, Kingston, Ontario, Canada, June 1-3, 1999.
  5. Pavlos Theodorou, J.M.H. Elmirghani, and R.A. Cryan, “*Performance Analysis of ATM Traffic on Optical Wireless LANs*”, Proc. IEE Colloquium on Optical Wireless Communications, pp. 11/1-11/6, London 1999.
  6. Pavlos Theodorou, J.M.H Elmirghani, and R.A. Cryan “*Performance of ATM Optical Wireless LANs with Fixed Channel Assignment*”, Accepted for

publication at IEEE Global Communications Conference (GLOBECOM'99), Rio de Janeiro, Brazil, 5-9 December 1999.

7. Pavlos Theodorou, J.M.H Elmirghani, and R.A. Cryan “*Performance of Fixed Slot Assignment MAC Protocol for ATM Infrared Wireless LANs*”, Accepted for publication in the Journal of Optical Communications, 1999.

# BACKGROUND

## CHAPTER TWO:

### ASYNCHRONOUS TRANSFER MODE (ATM)



## **2 ASYNCHRONOUS TRANSFER MODE (ATM)**

### **2.1 Introduction**

This chapter provides an overview of the Asynchronous Transfer Mode (ATM) which has been agreed world-wide through the ITU-T as the transfer mode for broadband integrated services networks (B-ISDNs) [2-4]. All services including voice, video and data share both the same transmission and switching fabrics throughout the entire network. ATM is a packet switching based protocol, but with a number of differences from standard packet protocols e.g. frame relay and X.25. It involves the partition of user information into fixed length packets for transmission across the network. The fixed length packet known as a cell comprises a fixed block of information and a short fixed-length header which is just sufficient to identify the connection.

The enthusiasm that exists for ATM by users as well as network operators and equipment vendors is demonstrated by the popularity of the ATM Forum [21], which is the industry driven body. Several hundred member organisations have joined to define specific implementation options for a range of technical issues. These are known as Implementation Agreements.

The next section provides a brief description of the B-ISDN protocol model, as published by the ITU-T. Section 2.3 focuses on the ATM layer and explains the aim of the virtual channels and virtual paths. The role of the ATM adaptation layer is

examined in section 2.4 while the structure of the ATM cell is examined in section 2.5. Finally, in section 2.5 emphasis is placed on the ATM traffic management which is responsible for maintaining a certain quality of service (QoS) between network and users.

## 2.2 ATM and the B-ISDN Protocol

For B-ISDNs, the transfer of information across the user-network interface (UNI) is done by using ATM. That means that a B-ISDN is a packet-based network, however, the recommendation by ITU-T states that B-ISDN will support circuit-mode applications as well. This is done over a packet-based transport mechanism [3]. Therefore, ISDN, which began as an evolution from the circuit-switching networks and supports channels based on a primary bit-rate, has transformed itself into a packet-switching mode network as it takes on broadband services. The protocol architecture for B-ISDN is shown in Fig. 2-1.

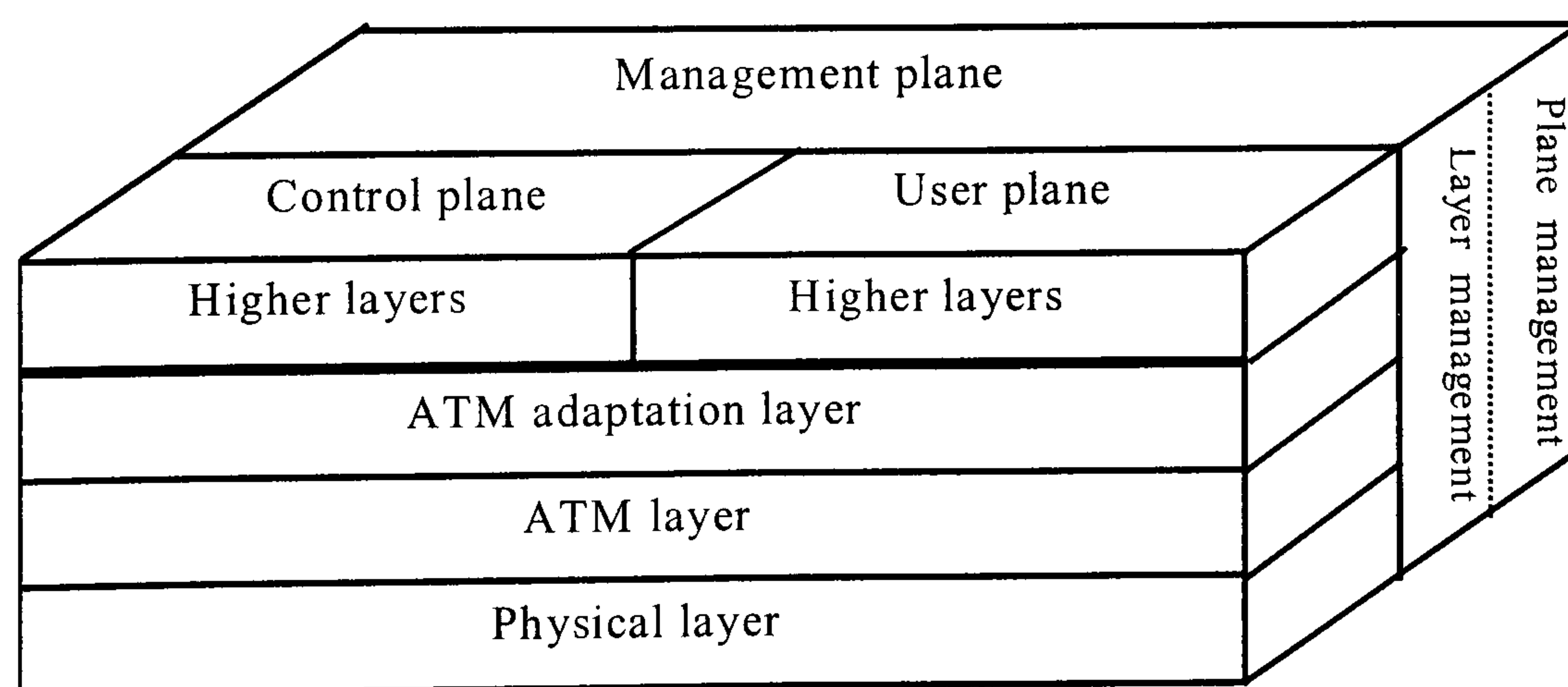


Fig. 2-1 B-ISDN protocol reference model



The physical layer is responsible for the physical connection of the nodes and users as well as for transmitting and receiving a continuous flow of bits. It can be implemented with SONET/SDH, DS3, FDDI physical layer, CEPT4 and others. However, for large public networks, SONET/SDH is the preferred physical layer. The ATM layer is independent of the physical medium and its responsibility is the management of sending and receiving cells between the user node and the network node. It adds and processes the 5-byte cell header. Directly above the ATM layer is the ATM adaptation layer (AAL). The primary function of the AAL is to organise the data from the higher layers of the terminal into units that will fit within the information field of the ATM cell (48 bytes). For example, if a block of computer data is too large for the information field it must be divided into two or more segments (cells) at the source and reassemble from those segments at the destination. The higher layers can serve signalling protocols for connection admission control (CAC) and support mobility functions for user handover assignments in a wireless environment. The user plane transports the information cells from/to the users while the control plane transports signalling information. The overall management of the protocol is divided into management for the layers and management for the control and user planes.

The transfer mode is asynchronous in the sense that the rate of transmission of cells for a particular connection can be variable and it depends on the source rather than

any clock reference within the network. Thus a B-ISDN, or ATM, network is bandwidth transparent. The benefits of this are:

- The ability to handle efficiently variable mixtures of services at different bandwidths.
- The potential to introduce new services in a gradual manner.
- Insensitivity to inaccuracies in predictions of the mix in service demand.
- The ability to handle variable bit rate traffic.
- The inherent statistical multiplexing.

### 2.3 The ATM Layer

As depicted in Fig. 2-2 the ATM layer consists of virtual channel and virtual path levels, and it is responsible for the routing of the cells using the identification fields in the headers. A virtual channel (VC) is a connection between two end users through the network where a full-duplex flow of cells at variable rates can be exchanged.

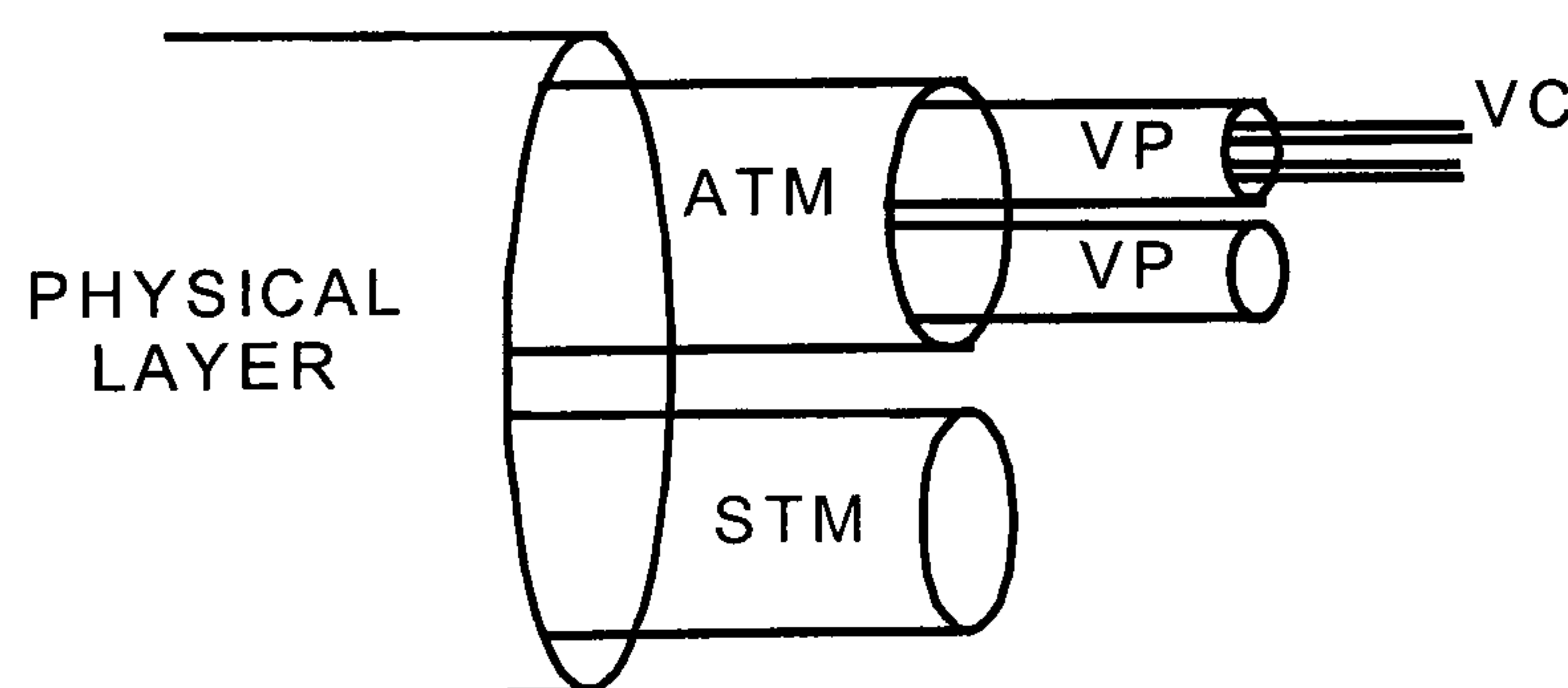


Fig. 2-2 ATM connection structure

A virtual channel connection (VCC) is the concatenation of VC links defined by the translation, or usually referred as look-up, tables in the switching points. Translation tables in each node provide link and virtual channel identifier (VCI) translation information for each cell that input to a switch. The routing information in these translation tables is established at the set-up of a connection, and remains constant for the duration of the connection. Therefore it can be said that ATM is a connection oriented service since there is only one possible path through the network for each connection. Thus a VCC is an end-to-end connection and the endpoints can be end users, network entities, or an end user and a network entity.

A virtual path (VP) is a bundle of virtual channels that have the same endpoints. More precisely, virtual path connections are defined in a similar way as for virtual channels above, except that the routing field used for switching is restricted to the virtual path identifier (VPI) part of the cell header. Since the VPI field is a subset of the routing field used for a virtual channel another way of viewing this is to consider that two layers of ATM connections exist: the virtual path layer and the virtual channel layer. The switching elements of the lower layer (virtual path switches) examine only the VPI part of the header whereas the switching elements of the upper layer (virtual channel switches) examine the whole routing field, i.e. VPI and VCI.

The purpose of a VP is to provide direct routes, shared by many VCs, between switching nodes via intermediate cross-connect nodes. It provides the logical



equivalent of a link between two switching nodes that are not necessarily directly connected by a single physical link. Thus, it makes a distinction between physical and logical network structure. This technique helps to control cost by grouping connections sharing common paths through the network. So that, network management actions can be applied to a small number of groups of connections rather than to a large number of individual connections. In general, VPs exhibit the following advantages:

- Simplified network architecture, since network transport operations separated into those related to virtual channels and those related to virtual paths.
- Network performance and reliability are improved, because the network deals with fewer aggregated entities.
- The connection set-up time for VCs is reduced. When a VP is set-up it reserves a certain capacity from the network in anticipation of later connection arrivals. New virtual channel connections can be established by executing simple control functions at the endpoints of the virtual path connection, without requiring any special call processing. Therefore, establishing new VCs to an existing VP takes a minimal processing.

The establishment and release of the virtual connections is performed using a primary ATM connection named the signalling virtual channel connection (SVCC). It is a point-to-point connection between a terminal and the connection handling function. The allocation of a SVCC to a terminal is not permanent. It is performed during the metasignalling phase that can take place for instance at terminal

activation. Communication during the metasignalling phase uses a predefined virtual channel connection called the Metasignalling VCC (MVCC). The MVCC is a broadcast connection [10].

## **2.4 The ATM Adaptation Layer (AAL)**

From Fig. 2-1 it is evident that the AAL acts as the interface between the user applications and the ATM layer. It plays a key role in the ability of an ATM network to support multiapplication operations. The type of user payload is identified at the AAL. Therefore, AAL must be able to accommodate to a wide variety of traffic, from connectionless, asynchronous data to connection-oriented, synchronous voice and video applications. At first glance it may appear that the integration of different services is a simple matter. If we examine the transmission requirements of video, voice and data, we find that they are quite different. Yet the AAL standards do not define completely how to manage and support these requirements, these important functions are defined in other standards.

Voice and lower quality video transmissions exhibit a high tolerance for errors. For example, if a cell is lost or distorted the quality of the voice or video reproduction is not severely effected. However, data transmissions have a low tolerance for errors since they involve retransmissions or many times no tolerance at all. Another major difference is that voice and video cells can not tolerate long delays while data delay can vary considerably. Indeed, data can be transmitted asynchronously through the



network without any precise timing arrangements between the sender and the receiver.

The AAL layer is organised in two logical sublayers: the convergence sublayer (CS) and the segmentation and reassembly sublayer (SAR). The CS provides the functions needed to support specific user applications using AAL, this sublayer is service depended. The segmentation and reassembly sublayer is responsible for packaging information received from CS into cells for transmission and unpacking the information at the other end. Since a cell consists of a 5-byte header and a 48-byte information field the SAR must pack any SAR headers and trailers plus CS information into 48-byte field.

ITU-T has defined four classes of services that cover a broad range of requirements, for each different service there is a particular AAL protocol, named type 1 through type 4.

	Class A	Class B	Class C	Class D
Timing relation Betwee source and destination	Required		Not required	
Bit rate	Constant	Variable		
Connection	Connection oriented			Connectionless
AAL protocol	Type 1	Type 2	Type ¾, Type 5	Type ¾,

Fig. 2-3 Service classification for AAL

The classification shown in Fig. 2-3 is based on whether a timing relationship must be maintained between source and destination, whether the application requires a constant bit rate and whether the transfer is connection-oriented or connectionless. For example, classes A and B require timing relationship between the source and destination. Therefore, clocking mechanisms are utilised for this traffic. Since ATM does not specify any type of synchronisation, it could be a timestamp and/or a synchronous clock. This function is performed in the application running on top of AAL. Last, the ATM Forum has specified class X, which is an unrestricted service where the requirements are defined by the user.

## 2.5 ATM Cells

The fixed-size cell, which is used for ATM, has a length of 53 bytes and consists of a 5-byte header and 48-byte payload (or information field) as shown in Fig. 2-4.

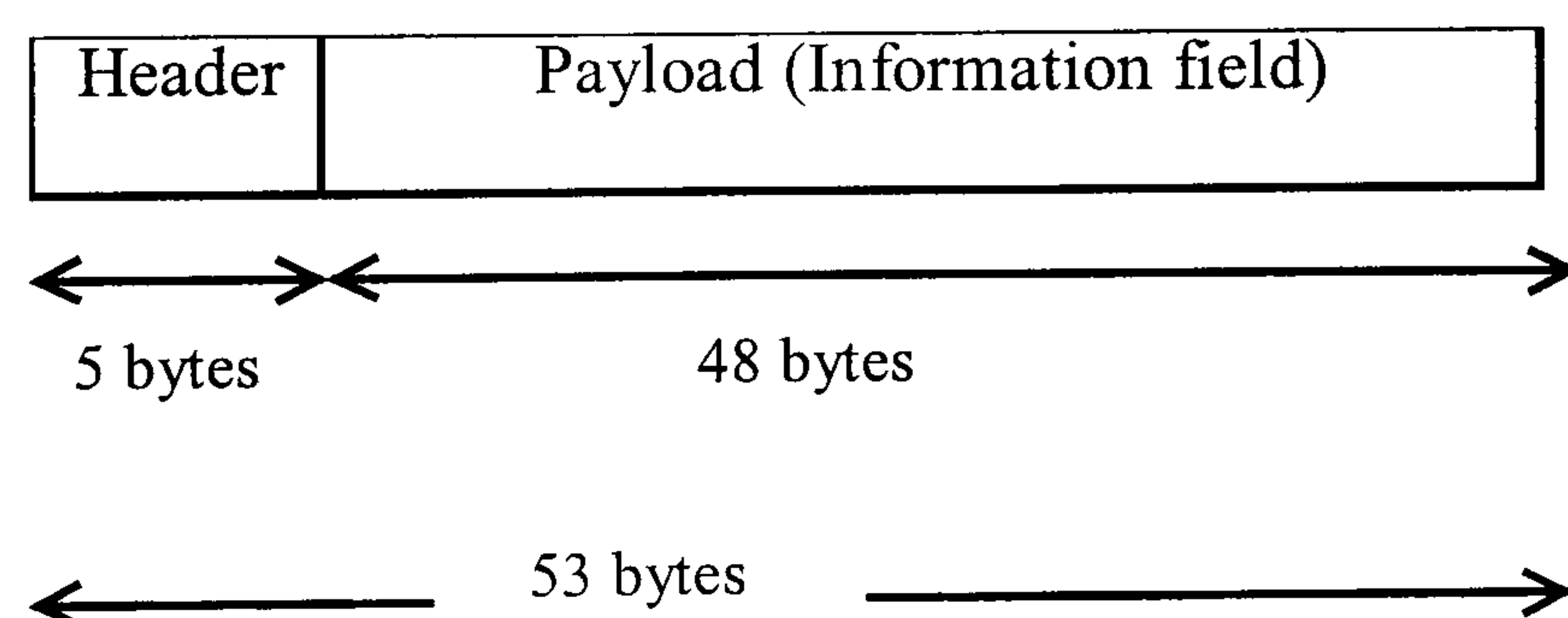


Fig. 2-4 ATM cell format

An advantage of the use of such small fixed-size cells is that the queuing delay for a high priority cell (when it arrives slightly behind a lower priority cell) is not long. Another advantage is that fixed-size cells can be switched more efficiently than variable length cells and this is very important for high data rates.

The header carries sufficient information to route the cell across the network so that cells from different sources can be multiplexed together on the same bearer. At the switch, the cell header is used to address a look-up table to determine the switch outlet required. The contents of the look-up table are pre-set by the management and control system [11].

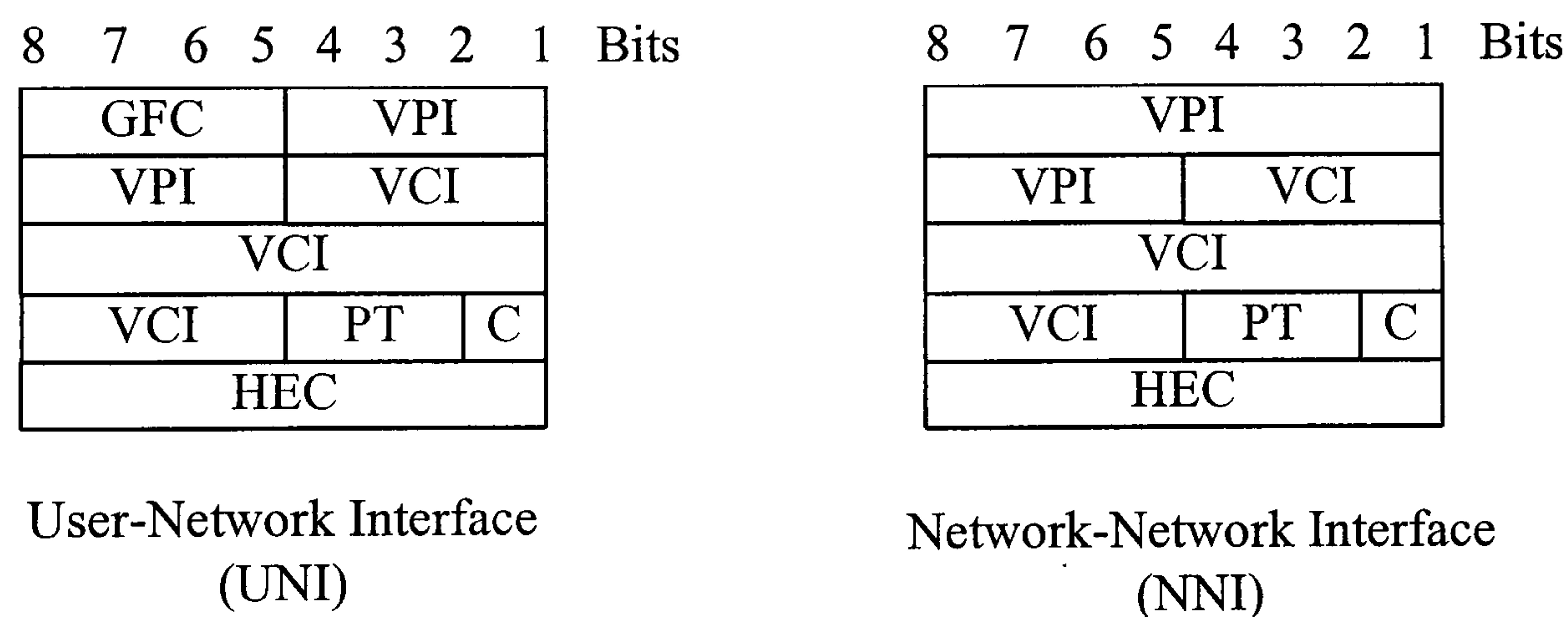


Fig. 2-5 ATM cell headers

As shown in Fig. 2-5 there are two slightly different forms of the ATM header, one used on user to network interface (UNI) and the other on the network to network interface (NNI). The generic flow control (GFC) is 4 bits and its use is still not fully defined. It is indented to be used by access mechanisms that implement different

levels of priorities, and can be used either by the customer premises network, or at the access to the network, in the case where several UNIs share a common resource.

The GFC field value is not transported across the network, and it does not appear at NNI headers. The VPI is 8 bits long at the UNI and 12 bits at the NNI, as its name suggests is the identity of the virtual path that this cell is to be carried on. The VCI is 2 bytes and is used to identify the virtual channel that this cell is to be carried on. The payload type (PT) is 3 bits and indicates if cells are normal traffic cells or used for internal control or management purposes.

The cell loss priority (CLP), denoted as C in the figure, part identifies if the cell is high priority (CLP = 0) and not to be discarded or is low priority (CLP = 1) and can be discarded when it encounters network congestion. This part of the cell critically affects certain aspects of traffic engineering and design. It deals with the conditions under which a cell is allowed to enter a buffer. A buffer, which is full for low priority cells can still allow high priority cells to enter. The effect is to increase the likelihood of loss for low priority cells compared with that for high priority cells. So, network nodes may not just be simple first-in first-out buffers but they can also implement some form of priority scheme.

The header error control (HEC) checks the validity of the data only in the header and not the 48-byte information field. It consists of 8 bits and allows correction of a single bit error and detection of multiple errors.



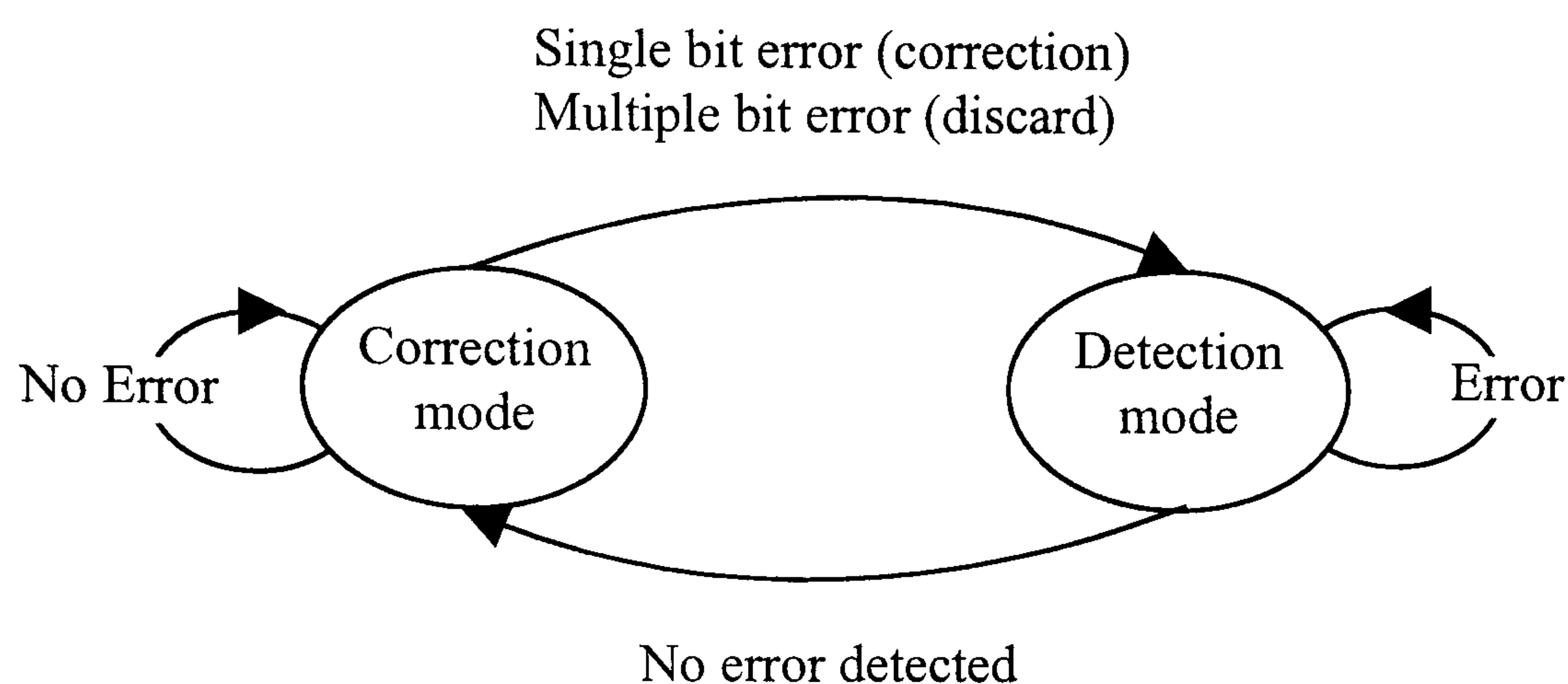


Fig. 2-6 HEC field operation

Fig. 2-6 depicts the operation of the HEC at the receiver. When cells are received without errors the receiver remains in error-correction mode. If it detects either a single bit error or a multiple bit error in the header, it moves to the detection mode. A single bit error is corrected and a multiple bit error results in the discarding of the cell. The receiver remains in the detection mode as long as errored cells are received. When a cell with no error is detected, the receiver switches back to correction mode. The HEC is also used as an alignment mechanism to identify cell header and therefore cells on a new link, or one that has lost alignment. Finally, the information field uses 48 bytes in order to transfer the user information. This information is loaded into the cell by the ATM adaptation layer (AAL).

ATM cell error checking and correction is only carried out on the header and not on the payload, this luck arises from the following two reasons. First, the error rate of the communication network is expected to be very low, e.g.  $10^{-10}$ , and second the

extra overhead and delay in correcting errors in ATM layer is undesirable in a high speed service carrying delay sensitive services. When error correction is required then it is carried out at higher protocol layers [24-26].

## **2.6 ATM Traffic Management**

An effective ATM network must be designed with an understanding that both user and the network assume responsibility for certain quality of service (QoS) between them. The user is responsible for agreeing to a service contract, with the ATM network, which stipulates rules on the use of the network such as the amount of traffic that can be submitted in a measured time period. In turn, the network assumes the responsibility of providing the user QoS requirements [27-29].

ATM networks present difficulties in effectively controlling congestion not found in other types of networks, which mostly carry non-real data traffic by using variable length packets. The complexity of the problem is compounded by the limited number of overhead bits available for exerting control over the flow of user cells. So that, traffic and congestion control techniques are vital to the successful operation of the network.

The design of traffic control strategy is based on determining whether a new ATM connection can be accommodated and agreeing with the subscriber on the performance parameters that will be supported. The subscriber and the network enter

into a contract. The network agrees to support traffic at a certain level on this connection, and the subscriber agrees not to exceed performance limits. Traffic control functions are concerned with establishing these traffic parameters and take care to avoid congestion conditions or to minimise congestion effects in the network.

These functions can be divided into the following categories:

- Network resource management. The concept behind network resource management is to allocate network resources in such a way as to separate traffic flows according to service characteristics. The QoS parameters that are primary concern for network resource management are the cell loss ratio, cell transfer delay and cell delay variation. All of these parameters are effected by the amount of the resources devoted to the VPC by the network.
- Connection admission control (CAC). It is a set of procedures that operate at the UNI, encompassing actions taken by the network to grant or deny a connection to a user. When a new VPC or VCC is requested, the user must specify the traffic characteristics for that connection. In other words, the user has to select traffic characteristics by selecting a QoS from among the QoS classes that the network provides, Fig. 2-3. The network accepts the connection only if it can support that traffic level and at the same time maintaining the agreed QoS of existing connections.
- Usage parameter control (UPC). After a connection is accepted from the network, the UPC monitors this connection. This operation checks on the validity of the traffic entering the network to determine whether the traffic conforms to the traffic contract between the user and the network. UPC can be done at both the



VP and VC levels. Of these, the more important is VPC level control, since network resources are initially allocated on the basis of virtual paths, with the virtual path capacity shared among the member virtual channels. Main UPC mechanisms are [30]: the leaky bucket, jumping window, the triggered jumping window and the moving window.

- Priority control. When the network, at some point beyond the UPC function, starts discarding cells (CLP=1) then the priority control comes into the play. Its role is to discard lower priority cells in order to protect the performance of higher priority cells.
- Traffic shaping. It is used to smooth out a traffic flow and reduce cell clumping. This can result in a fairer allocation of resources and a reduced average delay time. A simple approach to traffic shaping is to use a form of the leaky bucket algorithm known as the token bucket [12].

Traffic control functions are concerned with congestion avoidance. If it fails in certain instances then congestion control functions are invoked to minimise the intensity spread and duration of congestion. These functions are divided into the following categories:

- Selective cell discarding. In the priority control function excess cells with CLP=1 are discarded to avoid congestion. Once congestion actually occurs, the network is no longer bound to meet all performance objectives and is free to discard any cell, even if when CLP=0, that are not complying with their traffic contract.



- Explicit forward congestion indication. This is a function in which any network node that is experience congestion may send an indication. This indication, in the cell header of cells on congestion passing through the node, notifies the user to invoke actions to reduce the cell rate of the connection. Note that the GFC field is not involved. The GFC has only local significance and cannot be communicated across the network.

## 2.7 Summary

ATM has been agreed world-wide through the ITU-T as the transfer mode for B-ISDNs, it is a packet switching technique and makes use fixed-size packets, called cells. Each cell consists of a 5-byte header and 48-byte payload. Because of the small size cell ATM provides limited error detection and few operations are performed on the short header. The intention of this approach is to implement a network that is fast enough to support high bit rates. The ATM layer consists of virtual channel and virtual path levels and carries out the routing of the cells using the identification fields of the headers. The AAL layer performs convergence as well as segmentation and reassembly operations on different types of traffic. Due to lack of flow and error control mechanisms in the ATM layer there is need for using traffic and control techniques on higher layers in order to guarantee a successful operation of the network.

# CHAPTER THREE:

## INFRARED (IR) WIRELESS SYSTEMS

### **3 INFRARED (IR) WIRELESS SYSTEMS**

#### **3.1 Introduction**

As portable palmtop computers and other communication terminals become more widely employed, the demand for more research on wireless digital links and local area networks is increasing. Although, the majority of currently available wireless communications are based on radio waves, the desire for inexpensive high-speed links has motivated recent interest in infrared (IR) wireless technology. The idea of using the IR medium for wireless communications is not new, it has been proposed as a means for indoor communications two decades ago [31]. However, the last few years have seen an explosive interest in the potential for free space systems to provide portable data communications [32-64]. Wireless IR represents an attractive choice for many sort range applications and particularly its use is encouraged for environments where radio and microwave radiation is not suitable.

This chapter is intended as a brief introduction to the technology of the IR wireless communications. In section 3.2, advantages and drawbacks of the IR medium are compared to those of radio media. The different types of IR links to implement indoor local area networks (LANs) are discussed in section 3.3. Physical characteristics of IR channels using intensity modulation with direct detection (IM/DD) including the ambient noise and multipath responses are presented in section 3.4. The eye safety problem that arises due to high optical powers is

discussed in section 3.5 while currently available IR links and LANs are described in the final section 3.6.

### **3.2 IR versus Radio Communication Systems**

Infrared communication has significant differences from radio communication, some may be advantageous and other disadvantageous when implementing indoor wireless local area networks (LANs). Radio systems are already used in cellular phone networks, but such links will always find difficult to deliver the high bandwidths that are required for multimedia broadband platforms. In contrast, the very high carrier frequency associated with IR systems (300 THz at  $1\mu\text{m}$ ) promises high bandwidth wireless links. Because IR transmission does not interfere with existing radio systems it does not fall under any regulation of the Federal Communication Commission (FCC) and therefore there is no need for any licence, this feature can help keep the cost low. Moreover, the fact that IR signals do not penetrate walls enables an indoor wireless network to provide both a considerable degree of privacy within an area and a very large spatial bandwidth at the same spectrum, as the same frequency can be reused in adjacent areas. Therefore, IR wireless LANs can potentially achieve a very high aggregate capacity and their design may be simplified in some cases where transmissions in different rooms need not be co-ordinated.



The only practical technique to transmit information over IR wireless links is intensity modulation with direct detection (IM/DD). Because of this, the short carrier wavelength and large-area square-law detector lead to efficient spatial diversity that prevents multipath fading. Freedom from multipath fading greatly simplifies the design of the system. Also, a significant part of the cost of radio systems attributed to frequency conversion or quadrature demodulation can be avoided. Furthermore, only IR technology can be used in some areas where radio signal use is not encouraged, for example in radiology departments, aeroplanes etc.

Some of the characteristics of the IR communication are disadvantageous compared to radio communication. Because IR radiation does not propagate through walls and other opaque objects communication in such a scenario requires the installation of wireless access points that are interconnected via a wired backbone, thus increasing complexity and cost. With IM/DD being the only practical transmission mode, the signal-to-noise ratio (SNR) is proportional to the square of the received optical power, implying that such links can tolerate only a comparatively limited path loss. Outdoor applications using diffused IR links are impossible due to intense solar radiation that induces noise in the receiver. Moreover, in many indoor environments there exists intense infrared noise that arises not only from sunlight but other artificial light sources such as incandescent and fluorescent light. This noise significantly reduces the SNR and calls for high transmitter powers. Here, high powers can be problematic due to eye safety standards that have to be obeyed and are governed by International Electrotechnical Commission (IEC) standards. Diffuse



IR links also suffer from technical problems in terms of multipath and inter-symbol interference (ISI) which limit the data rate to speeds much lower than those of the line-of-sight (LOS) topology. Typically, data rates up to 100 Mb/s can be achieved [42]. Although these are much lower than what can be achieved in a LOS link, yet the data rates for diffuse IR systems are much higher than those of radio systems. The properties of radio and infrared as the medium for indoor wireless LAN applications differ significantly and are summarised in Table 3-1.

Property of medium	Radio	IM/DD Infrared
Bandwidth regulated?	Yes	No
Passes through walls?	Yes	No
Multipath fading	Yes	No
Multipath distortion?	Yes	Yes
Path loss	High	High
Dominant noise	Other users	Background light
Input signal represents	Amplitude	Power
Range/coverage	High	Low
Security	?	High
Technology cost	?	Potentially low

Table 3-1 Main basic differences between radio and IM/DD infrared wireless systems

### 3.3 Types of IR Wireless Links

IR links are classified according to two criteria. The first criterion relates to the degree of directionality of the transmitter and receiver while the second criterion



relates to whether the link relies on the existence of an uninterrupted line-of-sight (LOS) path between the transmitter and receiver. Directed links employ directional transmitters and receivers that must point each other to establish a link. On the contrary non-directed links employ wide-angle transmitters and receivers, alleviating the need for such pointing.

An advantage of direct links is that they require relatively low transmit power requirements since the power is concentrated into a narrow optical beam which maintains a high power flux density at the receiver. A further benefit of direct links is that they do not suffer the effects of a multipath environment. Also the receiver does not require a large field of view and so the effective gain of the concentrator can be exploited to improve the link budget. In addition, narrowband thin film optical filters can be readily employed because the angular dependence of the filter response is not an issue [36]. Finally, direct links can handle bi-directional communication links better than non-directed links. However, such systems require accurate alignment and are particularly susceptible to blocking. It is also possible to have hybrid links that combine transmitters and receivers having different degrees of directionality. Six different configurations for optical wireless links are shown in Fig. 3-1. LOS links rely upon such directionality while non-LOS links, which is often referred to as diffuse links, rely upon reflection of the light from the ceiling, walls or other reflecting objects in the work area.



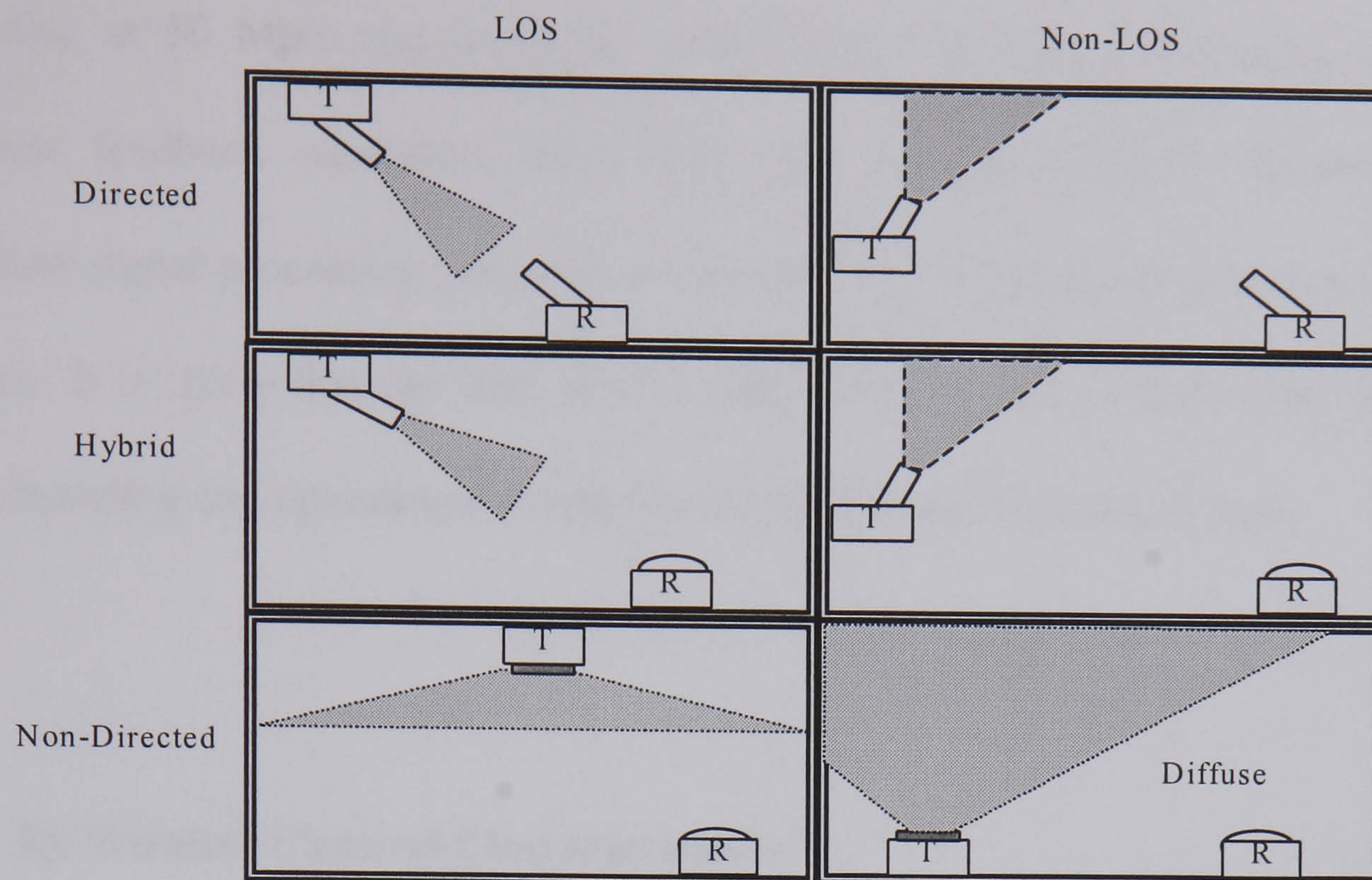


Fig. 3-1 Configuration of wireless optical links

Diffuse systems overcome the blocking probability problem but at the same time only a significant fraction of the receiver signal arrives at the receiver from a number of angles. As a result, this mode of transmission is well suited for applications requiring mobility such as cordless phones, palmtop computers or other portable digital assistants. However, the ultimate bit rate that can be supported by the link is limited by the intersymbol interference and it is much lower than that of direct systems. In addition, optical losses associated with the link are much greater than those for LOS cases. The receiver design is made more demanding because of the high dynamic range requirements due to the large variations in received signal level. Diffuse systems operating at 1-4 Mb/s are already a commercial reality and the IEEE 802.11 wireless standard includes a diffuse infrared physical layer definition, in addition to those for radio systems [69]. Laboratory demonstrations of systems



operating at 50 Mb/s and feasibility studies for 100 Mb/s, both using adaptive decision feedback equalisers, have also been reported [39,42]. However, the equaliser signal processing functions at the receiver will incur a power consumption penalty. It is likely that the data rates in these systems will be limited by practical manufacturing and operational constraints rather than any theoretical limit.

### **3.4 IR Wireless Channel Characterisation**

For wireless IR links, the most viable modulation is intensity modulation (IM) in which the desired waveform is modulated onto the instantaneous power of the carrier. The most practical down-conversion technique is direct detection (DD), in which a photodetector produces a current proportional to the received instantaneous power, i.e. proportional to the square of the received electric field.

The modelling of IR wireless channels with IM/DD is illustrated in Fig. 3-2. The input signal  $X(t)$  is the instantaneous optical power of the emitter, and the output of the channel  $Y(t)$  is the instantaneous current in the receiving photodetector.  $Y(t)$  is the product of the photodetector responsivity ( $R$ ) and the integral over the photodetector surface of the total instantaneous optical power at each location.  $h(t)$  is the impulse response which is fixed for a certain physical configuration of receiver, reflectors and transmitter [54].

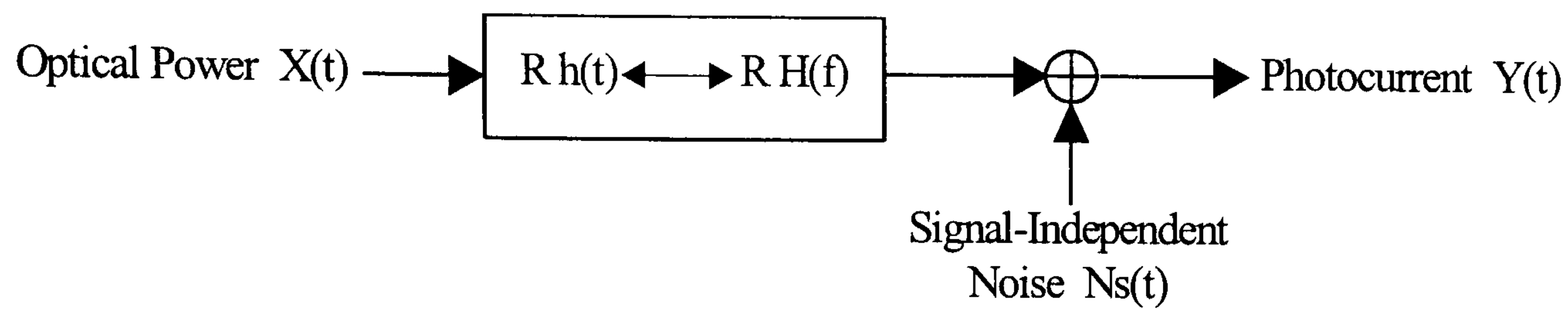


Fig. 3-2 IR wireless channel model

The received electric field generally displays spatial variations of magnitude and phase so that multipath fading would be experienced if the detector areas were smaller than a wavelength. However, usual detector areas are millions of square wavelengths and consequently multipath fading is prevented.

As the optical signal  $X(t)$  propagates to the receiver there are two principal limitations caused by interference from ambient light and multipath propagation. The multipath propagation causes time dispersion of the transmitted digital symbol and the resulting intersymbol interference (ISI) limits the maximum digital transmission rate, just as it does on a radio channel. As room dimensions became larger, the multipath spread increases and the maximum supportable bit rate decreases. The channel can also be described in terms of the frequency response by utilising the Fourier transform of  $h(t)$

$$H(f) = \int_{-\infty}^{\infty} h(t) e^{-j2\pi ft} dt \quad (3.1)$$

The  $h(t)$  is quasistatic due to the high signalling rates, high-order diversity of the large-area receiver and the low speeds at which indoor objects move. The linear relationship between  $X(t)$  and  $Y(t)$  is a consequence of the fact that the received signal consists of many electromagnetics modes [45]. By contrast, when IM/DD is employed in dispersive single-mode optical fibres, the relationship between  $X(t)$  and  $Y(t)$  is sometimes non-linear.

Received ambient light, which can be minimised by introducing optical filtering, results in additive, white, nearly Gaussian shot noise  $N_s(t)$  and independent of  $X(t)$ . When there is little or no ambient light present the dominant noise source is the receiver preamplifier noise, which is also signal independent, and Gaussian. Therefore, the noise  $N_s(t)$  is usually modelled as Gaussian and signal-independent and this is in contrast to the signal dependant Poisson noise considered in optical wired channels. The baseband channel model can now be written as

$$Y(t) = R X(t) \otimes h(t) + N_s(t) \quad (3.2)$$

Where  $\otimes$  denotes convolution. Because  $X(t)$  represents instantaneous optical power, the channel input is nonnegative  $X(t) \geq 0$ , which stands in contrast to conventional electrical and radio systems. The average transmitted optical power  $P_t$  is given by

$$P_t = \lim_{T \rightarrow \infty} \frac{1}{2T} \int_{-T}^T X(t) dt \quad (3.3)$$

and the average received optical power is written as

$$P_r = H(0)P_t \quad (3.4)$$

Where  $H(0)$  is the channel dc gain and is defined as

$$H(0) = \int_{-\infty}^{\infty} h(t) dt \quad (3.5)$$

Assuming that  $N_s(t)$  is dominated by a white Gaussian component having double-sided power-spectral density  $N_{s_0}$  and knowing the channel bit rate  $R_c$  then the performance of the digital link in terms of the SNR at the receiver is given by

$$\text{SNR} = \frac{R^2 P_r^2}{R_c N_{s_0}} = \frac{R^2 H^2(0) P_t^2}{R_c N_{s_0}} \quad (3.6)$$

From (3-6) we see that the SNR depends on the square of the received optical average power, implying that IR links must transmit at a relatively high power and can tolerate only a limited path loss. This again stands in contrast to the case of conventional channels, where the SNR is proportional to the first power of the received average power.



The temporal dispersion of an impulse response  $h(t)$ , which is translated to ISI, can be expressed by the channel rms delay spread ( $d_{\text{rms}}$ ) and is calculated from the impulse response as [53]

$$d_{\text{rms}} = \left[ \frac{\int_{-\infty}^{\infty} (t - \mu_d)^2 h^2(t) dt}{\int_{-\infty}^{\infty} h^2(t) dt} \right]^{1/2} \quad (3.7)$$

Where  $\mu_d$  is the mean delay and is given by

$$\mu_d = \frac{\int_{-\infty}^{\infty} t h^2(t) dt}{\int_{-\infty}^{\infty} h^2(t) dt} \quad (3.8)$$

Since  $h(t)$  is fixed for a given configuration, so is the rms delay spread. In [53] is shown that in the absence of shadowing, LOS channels, whose impulse response is dominated by a short initial pulse  $d_{\text{rms}}$  is ranging between 1.3 ns and 12 ns while shadowed LOS channels exhibit a larger  $d_{\text{rms}}$  that lies between 7 and 13 ns.

### 3.5 IR Radiation and Eye Safety

Because the human eye acts similarly to a camera, focusing the energy density of the incident light onto the retina by a factor of 100.000 or more, eye safety is one of the

primary constraints in any optical wireless system. Consequently, the maximum permissible exposure levels must be quite low to prevent thermal damage. The eye safety limit is described by the accessible emission limit (AEL), which is a function of the viewing time, wavelength and size of the optical source. A distinction is drawn between point sources, which the eye can focus, and large area or extended sources which form an extended image on the retina.

The outer layer of the eye, the cornea, acts as an optical bandpass filter passing wavelengths ranging roughly from  $0.4\ \mu\text{m}$  to  $1.4\ \mu\text{m}$ . Light energy at wavelengths outside this range is absorbed by the cornea and does not pass through to retina. Thus, wavelengths of  $1.5\ \mu\text{m}$  and higher are relatively safe for the human eye. However, the photodiodes presently available at this band are more expensive and exhibit a higher capacitance per unit area than their silicon counterparts where operate between  $0.8$  and  $0.95\ \mu\text{m}$ . Light emitting diodes (LEDs) are currently used in all commercial systems due to very low cost and because most LEDs emit light from a sufficient large surface area are considered eye-safe. Laser diodes (LDs) are generally more expensive than LEDs but offer advantages such as 1) better electro-optic conversion efficiency 2) high modulation bandwidths and 3) very narrow spectral widths. However, to overcome the strict power limitations that apply to point sources, such as LDs, the beam must go through some holographic diffusers that destroys its spatial coherence and spreads the radiation over a sufficient emission angle [34,47,48,65,66]. The AELs for extended sources can be an order of magnitude greater than those for a point source. In practice, the limiting constraint

on transmitted power from such an extended source will be due to the power in undiffracted beam from the diffuser. Thus, the power emitted in the zero-order mode, where point source AELs will apply, will set the maximum transmit power. For example, the acceptable emission limit for a point source at  $0.84\ \mu\text{m}$  is  $0.24\ \text{W}$  [68] and the undiffracted zero beam is much below this value. The eye safety of IR transmitters is governed by International Electrotechnical Commission standards [67].

### **3.6 Current IR Communication Systems**

Today there are commercially available IR wireless communication systems which utilise both direct links and diffuse links. They operate between  $0.85$  and  $1\ \mu\text{m}$ , this wavelength matches the responsivity peak of silicon p-i-n photodiodes which are available at very low cost. Direct-LOS and hybrid-LOS links have been used for many years in remote-control units, IR headphones and other unidirectional low-bit-rate applications.

One of the most successful and widely adopted standards to date is the Infrared Data Association (IrDA) [60] standard. IrDA is an industrial organisation, which was formed in 1993, and up to date has established standards for short-range half-duplex LOS links operating at a maximum bit rate of  $4\ \text{Mb/s}$ . Using four-pulse position modulation (4-PPM) for  $4\ \text{Mb/s}$  the link is specified to support bit error rates (BER)



$<10^{-9}$  at ranges of about two meters. The field of view is specified between a minimum of  $\pm 15^\circ$  to a maximum of  $\pm 30^\circ$ . Although the initial functionality of this system is modest, it has proved successful in its intention to provide wireless cable replacement and gain acceptance of infrared technology. Two of the key features of IrDA links are low power consumption, which is vital for portable units, and low cost. IrDA transceivers have now become a standard feature of numerous mobile and fixed information devices, such as computers, printers, mobile telephones, cameras and many other personal and industrial digital assistants. Also, in the future infrared points in public telephones may enable wireless access to the Internet, while infrared links in automatic teller machines might allow one to download “digital cash”.

IrDA systems use direct-LOS and hybrid-LOS links and therefore cannot provide fully mobile links within a LAN. However, it might be possible to build a hub capable of establishing simultaneous point-to-point links with several portable devices. One technical challenge to building such a hub is cochannel interference between different inbound transmissions. For fully mobile services diffuse IR transmission must be utilised together with a suitable medium access control (MAC) protocol that shares the IR medium to users and provides mobility management when they move from one cell to another.

Diffuse IR technology is still in its infancy (however, it is included as part of the IEEE 802.11 standard for wireless LANs [69]), because of this there are very few manufacturers of this technology. An example of such a network is the



SpectrixLite™, made by the Spectrix Corporation [70]. The system utilises a base station which can provide an aggregate capacity (on 16 wireless access points) of only 4 Mb/s, employing OOK with RZ pulses. The base station connects to a wired network which can be an Ethernet or a Token Ring. The IR medium is shared to mobile users by utilising the deterministic CODIAC (Centralised Operation Deterministic Interface Access Control) protocol. The protocol is employed under time division duplex (TDD) mode and therefore a single wavelength is used for both uplink and downlink. The diffused links of the system target a BER of  $10^{-6}$  and can cover a range of about 15 meters. Table 3-2 summarises the current available IR wireless communication systems and compares them with their radio equivalents.

Medium	System	Bit Rate	Range	Roaming
Optical	JVC	10 Mbit/s	10 m	No
	Spectrix	4 Mbit/s	10 m	Yes
	IrDA	4 Mbit/s	1 m	No
Radio	WaveLAN	8 Mbit/s	100 m	Yes
	HiperLAN	26 Mbit/s	50 m	Yes
	Bluetooth	1 Mbit/s	10 m	Yes

Table 3-2 Comparison of currently available wireless communication systems for indoor environments

To date recent research work suggests that using new techniques it is possible to enhance the technology of diffused IR communication significantly as far as the physical layer is concerned. However, need arises for research into higher layers in



these systems to enable the support of multimedia services such as ATM that is believed to be the feature in the optical wired networks.

### **3.7 Summary**

Although, the majority of currently available wireless communication services are based on radio waves, indoor IR wireless technology is receiving increased attention due to its many advantages over radio. Such advantages are unregulated high bandwidth, no multipath fading, no interference with radio, and spectral reuse within a room or building.

Diffused IR links are well suited for applications requiring portability because such links rely upon reflection of the light of any reflecting object in the work area. As the optical signal propagates to the receiver there are two principal limitations caused by interference from ambient light and multipath propagation. The ambient light significantly reduces the SNR and calls for high transmitter powers. High powers can be problematic due to eye safety standards that have to obey. Diffuse IR technology is still in its infancy and most of the available systems today employ mainly direct-LOS or hybrid-LOS links.

# NEW HYBRID LAN

## CHAPTER FOUR:

### THE PROPOSED ATM IR WIRELESS LAN

## **4 THE PROPOSED ATM IR WIRELESS LAN**

### **4.1 Introduction**

As mentioned in the introduction of the thesis, the project aims to integrate the ATM facilities with diffuse optical wireless technology. Such a combination will extend the B-ISDN wireline networks into indoor optical wireless, fully mobile, local area networks (LANs). Therefore, some of the areas for immediate consideration are the overall structure of the protocol stack, the medium access control (MAC), the wireless ATM cell format, set-up connection management, and mobility management.

The chapter is organised as follows. Section 4.2 presents the network scenario where the wireless LAN is integrated into the ATM wired network. It is important that the protocol stack of the wireless network to be designed in a way that provides seamless interworking with the wired network. Such a design will reduce the complexity between the wired and wireless network as well as processing time, hence the wireless network is less dependant on the wired one. The organisation and analysis of the protocol reference model are considered in section 4.3 Section 4.4 is devoted to the structure and analysis of the MAC sublayer which holds a primary role of the overall performance of the LAN. Its responsibility is to share the IR wireless medium to mobile TUs on a packet based transmission and support mobility management, such as handover control, when active TUs change cells. In



section 4.5 the format of the wireless ATM cell is examined. Finally, in section 4.6 technical challenges concerning the employment of ATM over diffused IR wireless LANs are discussed.

## 4.2 Network Scenario

The network configuration representing the proposed concept of the attached wireless LAN onto the wired ATM network is illustrated in Fig. 4-1 [58,56,59].

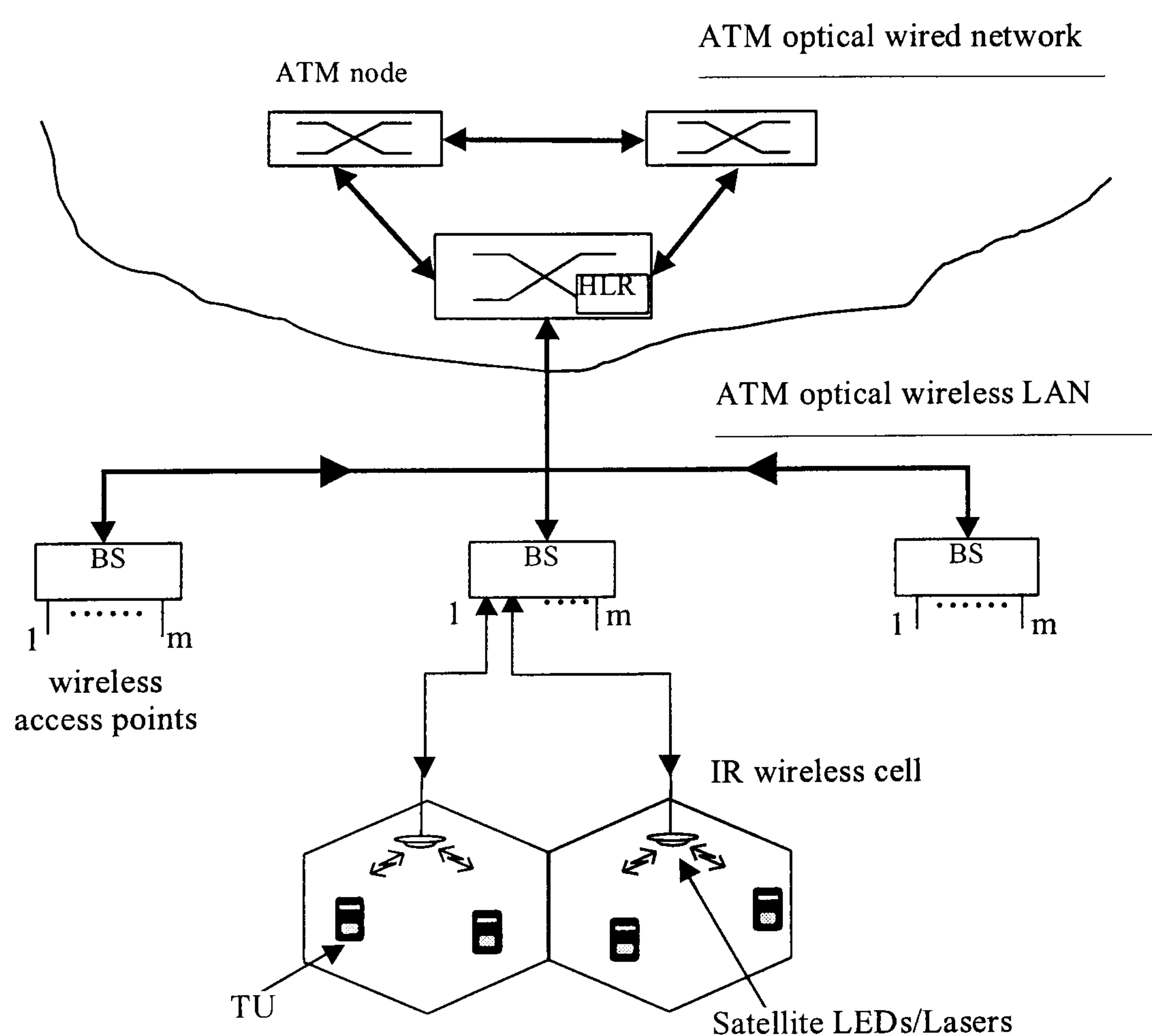


Fig. 4-1 Network configuration representing the attached wireless LAN onto the  
wired ATM network

Optical fibre is used to connect the ATM nodes in the wired regime with the base stations (BSs) of the LAN. Each ATM node is equipped with a home location registered (HLR) database in which the identification of each TU in the wireless LAN is registered.

A large area such as an open plan office needs to be divided into small communication zones, usually hexagonal cells. Here a cell is the area covered by a wireless access point and must not be confused with an ATM cell. Recalling that the SNR for a direct-detection IR receiver is proportional to the square of the received power then the covered area of a cell cannot be more than a few meters. Typical values of the cell diameter lay in the range of 5 to 10 meters. At any given time a TU belongs to exactly one cell and is associated with the BS at which the wireless access point of the cell is connected. Since BSs are designed to support up to a certain number of wireless access points it is convenient for the designer to consider that mobility functions and handoff procedures can be allocated in the BSs instead in the ATM nodes. This feature can help the wireless LAN to be less dependant on the fixed ATM network.

In order to prevent cochannel interference between adjacent cells the MAC protocol assigns the IR medium to each cell at a different time. This is done by dividing the downlink/uplink bandwidth into a number of equal time partitions, each time partition is referred to as IR channel. The number of the time partitions is equal to the number of the considered neighbouring cells and is called the channel reuse

factor. As an example, Fig. 4-2(a) shows the layout of a topology using a channel reuse factor of seven. The location of the first neighbour is specified using the co-ordinate axes shown in Fig. 4-2(b), and the rest are determined from symmetry.

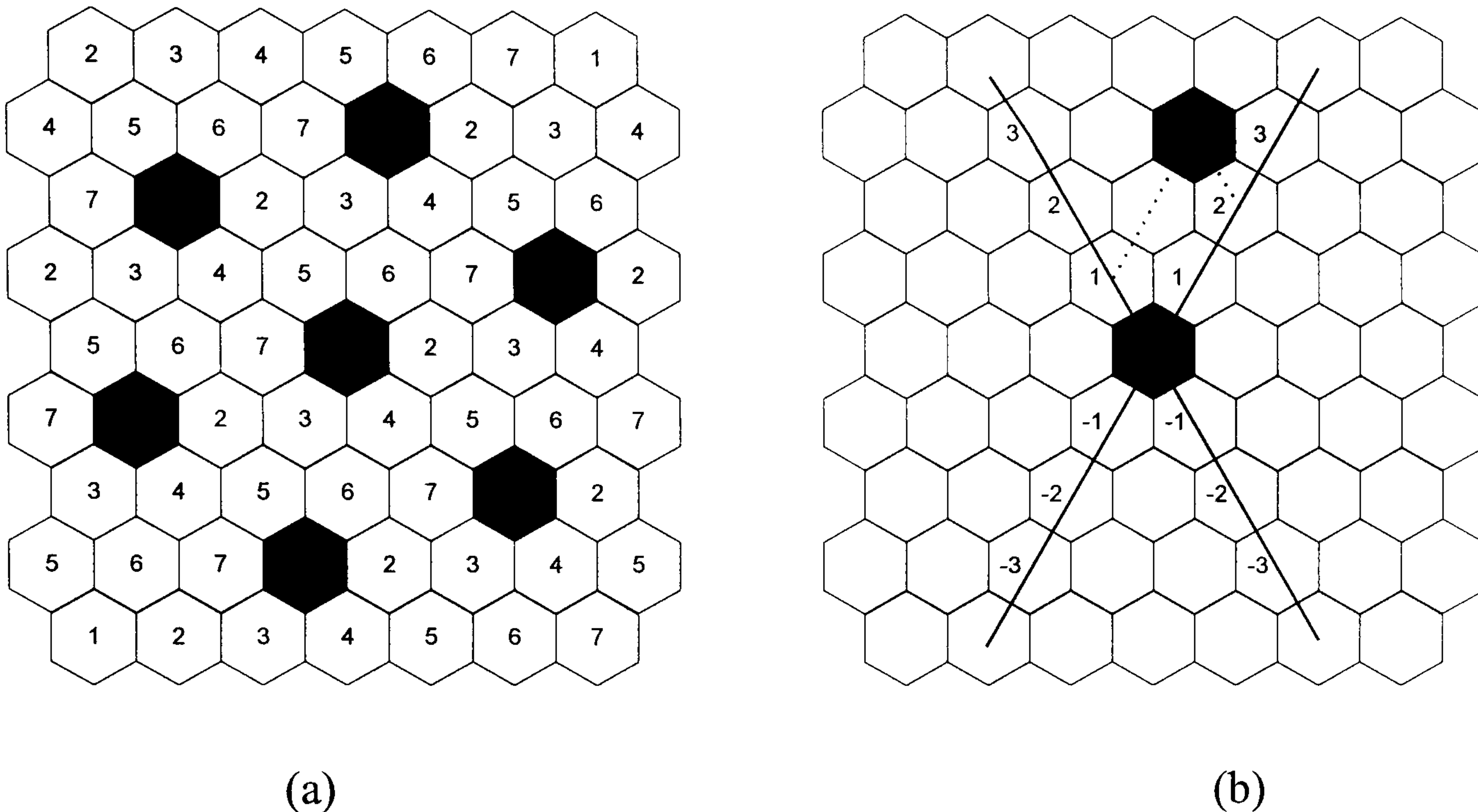


Fig. 4-2 Cellular topology. a) Using a channel reuse factor of seven in a cellular system, b) axes to specify the position of a cell relative to its nearest neighbour.

If the first nearest neighbour is located at co-ordinates (k,l) then the channel reuse factor is given by

$$J = k^2 + l^2 + kl \quad (4.1)$$

Given the radius (r) of a cell as measured from its centre to a vertex then the distance between a cell and its nearest neighbours is the reuse distance and is given by

$$ds = r\sqrt{3J} \quad (4.2)$$

Using the lowest possible reuse factor we can maximise the capacity of the LAN, however, this would cause an increase of the cochannel interference and consequently of the bit error rate (BER). Therefore, the optimum channel reuse factor must be based on the targeted BER and required capacity of the network in order to support ATM services. Higher capacity can be achieved by dynamically allocating the IR medium to cells, depending upon the number of TUs in each of them, though at the price of increased complexity.

The radius of a cell is taken to be 3 meters and to prevent cochannel interference the first nearest neighbour is located at (1, 2), resulting in a reuse channel factor  $J = 7$  and a distance between two neighbouring cells of 13.7 meters. This distance is large enough to ignore cochannel interference since the latter is much lower than the noise produced by the ambient and artificial light sources according to [57]. The communication path between TUs and wireless access points is established via diffused IR links where OOK modulation is used at a bit rate of 10 Mb/s. It has been shown that when the transmission bit rate is low enough,  $\leq 10 \text{ Mb/s}$  then intersymbol interference effects can be ignored [53].



### 4.3 The Protocol Stack Model

The protocol stack model illustrating how the wireless network can be integrated with the fixed ATM network is shown in Fig. 4-3. It is composed of two planes, the user plane that is responsible for providing user information transfer and the control plane which is responsible for setting up and releasing a connection. The user plane does not involve any ATM adaptation layer (AAL) at the BS and therefore ATM cells are transported from the ATM nodes to TUs as transparently as possible. This kind of "native approach" treats ATM cells as a payload data field for the data link control (DLC) layer. The AAL, which is found in the protocol stack of the TUs, is designed to act as the interface between user applications and the ATM layer. As such, it is expected to enhance the service provided by the ATM layer, based on the specific requirements of various applications such as voice, video and data. The ATM layer consists of virtual channel and virtual path levels and is responsible for the routing of the cells using identification fields in the cell header. Among the other tasks, the transmitting ATM layer adds the 5-byte header on the ATM cell and the receiving ATM layer processes this header, then strips it away before passing the rest of the cell to the AAL.

Below the ATM layer the DLC and MAC layers are allocated, these two layers are used to enhance the physical layer transport capability. The DLC layer is introduced to improve the throughput performance degradation due to the bit error degradation

in a diffused IR link, while the MAC layer is responsible for sharing the IR wireless medium to TUs according to their bandwidth requirements.

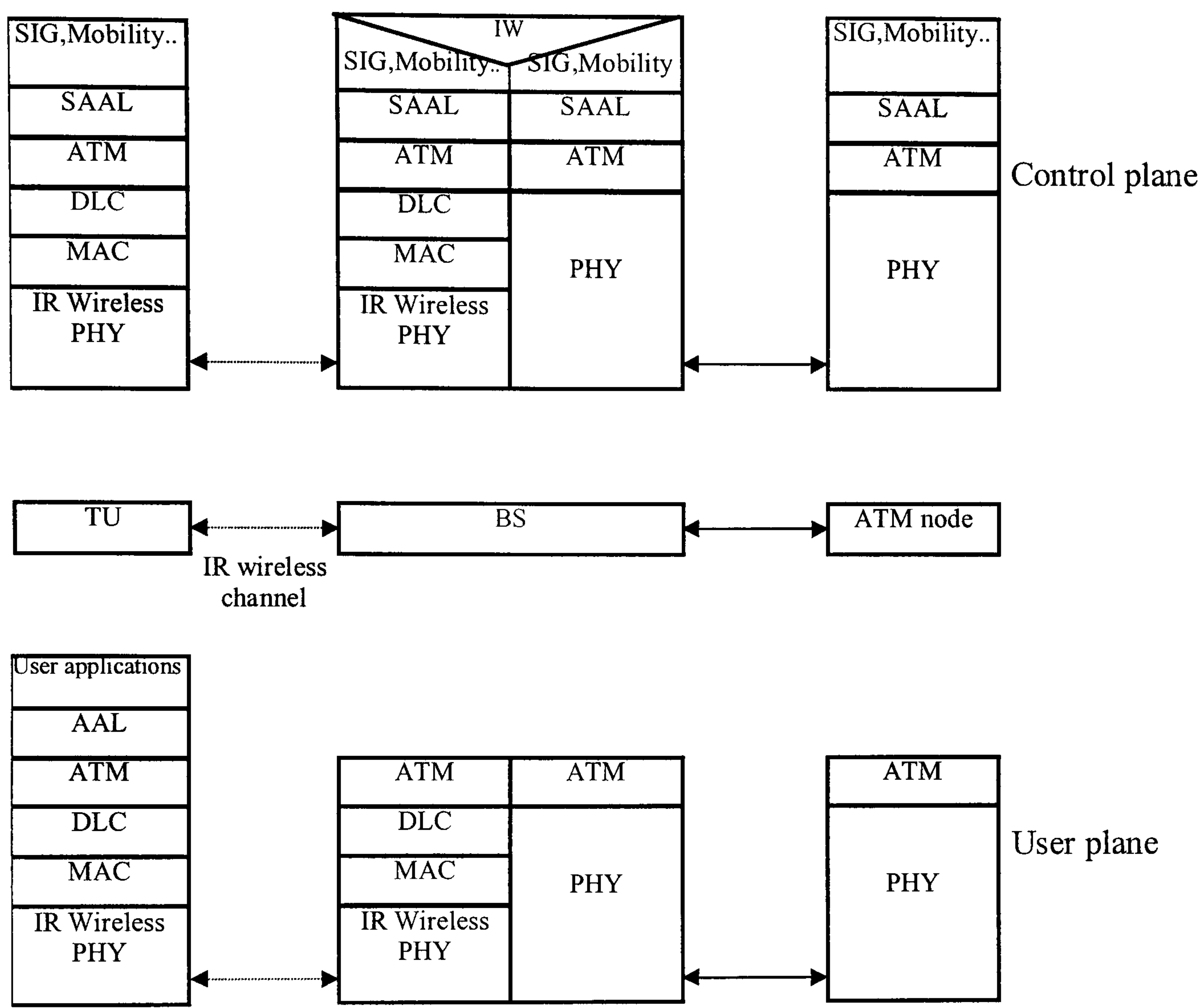


Fig. 4-3 Protocol stack configuration for the user and control plane

To utilise the IR medium efficiently, connections need to be set up on demand. Connections on demand simply mean that the ATM user-to-network interface (UNI) must support switched channel connections. These connections, or virtual channels, are established and released with signalling procedures (based on Q.2931 or any ATM Forum UNI signalling protocol) in the signalling (SIG) layer in the control plane [71]. The BS terminates control signalling to/from TUs and carries out call

admission control then sends the SETUP message to the ATM node after interworking at the BS. Among the fields of SETUP in the signalling protocol, there is also a destination address. The ATM node to determine the route that is to be established for the connection uses this address. Each node accepts the SETUP request message from the TUs, examines the destination address and then consults a routing table to determine the next node that should receive the message. The same operations will be performed by the BS to set-up connection routes between two or more BSs within the LAN. These operations are significantly dependent on the type of the TUs. For instance when the BS is called to serve a TU with a constant bit rate application then a link-to-link basis set-up is adopted. In contrast, when the BS is called to serve a TU with an available bit rate application (e.g. email low priority) then the BS may need to search for available bandwidth through different routes till the application is completely served.

Call admission control (CAC) is a set of procedures that operate at the user-to-network interface encompassing actions taken by both networks (wired/wireless) to grant or deny a connection [72,73]. A connection is granted when the traffic contract (contains information such as peak cell rate, maximum cell delay, sustainable cell rate, burst tolerance, etc.) of a TU is examined revealing that the connection can be supported through both networks (wired/wireless) at its required quality of service level. Based on this information the BS carries out IR channel control for the TUs. The layer below the SIG is the signalling ATM adaptation layer (SAAL) and supports the transport of the signalling protocol and mobility function protocol.



The structure of the overall protocol does not call for the ATM node to carry any function related to the IR channel control. However, the BS gets more complex because it needs to terminate the SAAL, to carry out connection admission control, IR channel control and mobility management. Thus, the BS is equivalent to a small ATM switch and this makes it easy to add the proposed wireless LAN to existing ATM networks.

#### **4.4 The Medium Access Control (MAC) Protocol**

To date many studies have focused on time division multiple access (TDMA) protocols to support ATM services only on radio based wireless systems [22,23,75-95]. Among them PRMA, a modified reservation ALOHA protocol [74], exploits talkspurts-silences statistical character of speech stream. This is done by means of a speech activity detector in order to serve more speech TUs. Packet-based transmission facilitates PRMA to accommodate information from diverse sources and to act in harmony with other packet networks, such as ATM which is commonly believed to be the future in long-haul networks.

In this project, the MAC protocol is a modified PRMA version and enables the dispersed TUs to transmit packetised information to BSs over a time division duplex (TDD) mode channel. The original PRMA considers that cellular communication



networks operate under frequency division duplex (FDD). The main difference between FDD and TDD is that upstream and downstream are conveyed on different carriers under FDD and therefore they can be transmitted simultaneously. By contrast upstream and downstream are conveyed on the same carrier under TDD and therefore they can only be transmitted in sequence. In a recent study [92] it was shown that a PRMA protocol is highly efficient under TDD mode and has almost the same performance as the original PRMA under FDD. Furthermore, in the original PRMA slotted ALOHA is used for contention and packet collisions will occur when more than one TU tries to access the network at the same time. Consequently, this results in an increase in the packet loss probability in the system. While for other protocols such as RAMA [77] and R-GRAP [85], collisions are reduced or prevented because orthogonal address codes are used for reservations. Still one TU will be successful at once in RAMA, and collisions occur while several TUs select the same orthogonal code in R-GRAP.

The emergence of optical communications has resulted in a growing interest in multiple-access techniques for optical wired LANs. These techniques make use of optical codes and are capable of achieving a very low multiple-access interference, though at the price of bandwidth that is needed for the codes. Such codes are; optical orthogonal codes, prime codes,  $2^n$  prime codes, and  $2^n$  extended-prime codes [96-103]. Therefore, to prevent collisions when TUs try to access the base station to request reservation, optical prime codes are used. Before a TU transmits or receives any information connection admission control takes place. When a TU is accepted it



is dispatched with a unique address code (an optical prime code) that is considered as the virtual path identifier (VPI).

Fig. 4-4 depicts the time organisation of the uplink and downlink frame of the MAC protocol. Each frame is divided into  $J$  channel frames. An uplink channel frame is composed of one reservation (R) slot and  $N$  information (I) slots. TUs request a reservation by transmitting their codes through the R slot.

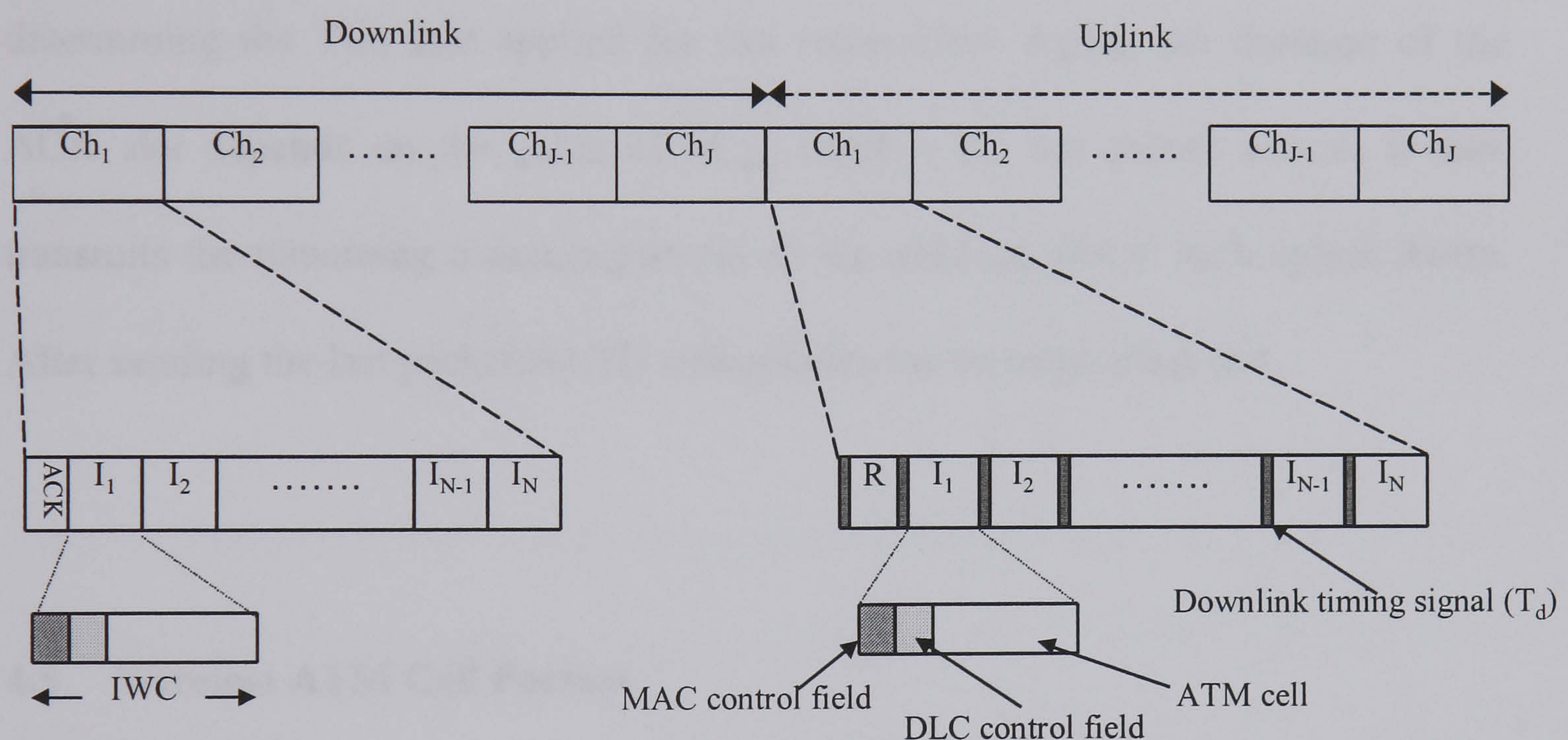


Fig. 4-4 Timing organisation for the uplink and downlink frame of the MAC protocol

Because the chip rate of the codes is the same as the channel bit rate, the duration of the R slot is defined by the maximum number ( $M_{\max}$ ) of TUs that will be supported within the channel frame. An I slot is the transmission time of an IR wireless cell (IWC). Each TU is synchronised to transmit in its own time slot by means of a short downlink timing signal (T<sub>d</sub>) which the base station broadcasts exactly before the slot.



For instance, the TU that has been allocated the first slot will start transmitting after the end of the reservation slot and the second  $T_d$  while the TU that has been allocated the  $n^{\text{th}}$  slot will start transmitting after the  $n^{\text{th}+1} T_d$ . The timer in each TU resets at the end of each downlink frame.

A downlink channel frame is composed of an acknowledgement (ACK) slot and  $N$  information (I) slots. The ACK slot is used by the BS to broadcast messages regarding the state for each downlink slot, for instance reservation messages after determining the TUs that applied for slot reservation. Again, the duration of the ACK slot depends on the value of  $M_{\text{max}}$ . Once a TU has gained access, it then transmits the remaining message packets on the reserved slot in each uplink frame. After sending the last packet the TU relinquishes the corresponding slot.

#### **4.5 Wireless ATM Cell Format**

This section shows a possible structure of the cells that convey information within the user plane. The structure represents a generic approach and is based on the requirement to keep the total overhead at minimum without degrading the service quality. When an ATM cell arrives to the base station, it firstly goes through the DLC layer. The layer compresses the header of the ATM cell and divides the 48-byte payload into portions that fit within the payload field of the DLC frame. The latter is shown in Fig. 4-5 (a). The size of the DLC payload field is analogous to the

amount of the speech information that is produced by a TU during a roundtrip. A roundtrip is the time for transmitting an uplink and a downlink frame. Therefore, the size of the DLC payload is given by

$$\text{DLC\_payload} = \frac{R_c T_{cf}}{N} - H \quad (4.3)$$

Where  $T_{cf}$  is the channel frame duration and  $N$  is the number of slots within a channel frame, these two parameters are derived in the next chapter.  $R_c$  is the channel bit rate and  $H$  the total overhead of the cell. After the DLC payload is finished the layer adds the DLC control header and the cyclic redundancy check (CRC) fields, the CRC field is used for error detection in all bits of the frame.

The next stage of the frame now is to go through the MAC layer in which it will get its final format for transmission, this cell is referred to as IR wireless cell (IWC), and is shown in Fig. 4-5 (b). It is composed of the header field (HF) that contains information about the destination of the cell and its sequence number. The sequence number is used at the receiver during the building of the voice talkspurt. It is used to note the first speech packet in the talkspurt as well as to note if a speech packet has been lost. The value is incremented by 1 for each subsequent speech packet in the signal. The HF is followed by the DATA field which accommodates one DLC voice frame.



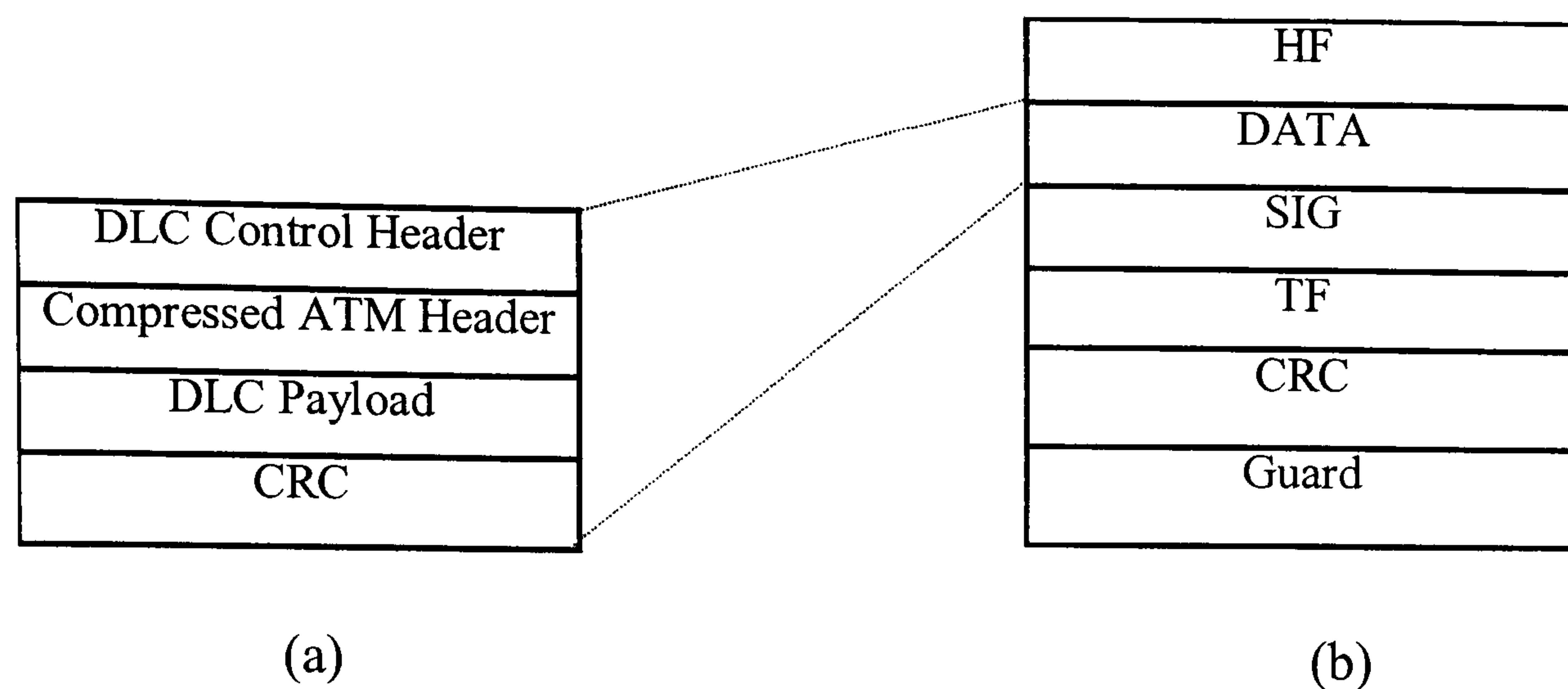


Fig. 4-5 The IR wireless cell format, a) the new DLC frame and b) the final form of the wireless cell after the MAC layer

The SIG field is used to piggyback signalling information such as handover requests, instantaneous bandwidth requirements or other acknowledgements from the TU to the base station. Information regarding changes of the required bandwidth of the TU is used for dynamic slot allocation. After the SIG layer the tail field (TF) follows which can be used to carry details such as the number of bytes residing in the DATA field and the level of background noise that is to be played in the absence of packets, since an active speech detector is used. Finally, a CRC field for error detection and a guard band no longer than a byte complete the structure of the IWC. The value of the total added overhead in the cell (DLC layer + MAC layer) lies between 70-80 bits. The structure of IWCs that are used in the control plane for CAC, mobility, and other control signalling functions is expected to be different and smaller in size compared to that above.

#### **4.6 Technical Challenges of Employing ATM over Diffused IR Links**

Since ATM was designed for a medium whose BER is very low, namely optical fibre, it is challenging to extend its capabilities onto an IR diffuse link, a medium that does not promise the same quality of service as optical fibres. This is because an IR diffuse link is subject to several impairments arising from the noise due to ambient and artificial light, multipath propagation, time-varying ISI, cochannel interference (in a multi-cell topology), inherent user mobility and unavoidable changes caused by motion of the surrounding environment. These impairments increase the BER of the communication link and often make it unable to meet the quality standards needed for ATM multimedia applications.

As in the case with radio communications, a data link control (DLC) layer is introduced in the IR wireless protocol stack for error recovery. It will possibly involve the employment of a forward error control (FEC) for time sensitive services and automatic repeat request (ARQ) for time insensitive services. Although several hybrid ARQ/FEC techniques have been reported in the literature concerning radio wireless systems [e.g., 104,105], fundamental differences between radio and the diffuse IR links may change many of the boundary conditions. Hence, more research under the particularities of diffuse IR links is required. IR links are capable of delivering much higher bandwidths than radio links yet their capacity is much lower than optical wired links due to the various impairments mentioned above. Hence, the employed MAC protocol, which shares the wireless bandwidth to mobile TUs,



exhibits many differences comparing to the one of wired networks. Finally, to support mobility when a TU is moving from one cell to another adding mobility functions in the protocol stack is indispensable. Because a communication area cell for IR wireless LANs can practically be no more than a few meters in radius we expect that in an indoor environment with high user mobility the signalling load due to handover requests to be quite heavy. Therefore, it is highly desirable that the MAC protocol to support handover service for ongoing calls with priority over new calls, so that the agreed quality of service contract with the TU is maintained.

#### **4.7 Summary**

In this chapter, the author proposed an approach for a wireless LAN that integrates the ATM capabilities with the features of diffuse IR wireless technology. The network scenario was presented and the structure of the protocol stack that attaches the wireless part onto the wired ATM network was analysed. To reduce complexity and processing time between the two networks the wireless part is designed to provide seamless interworking with the wired ATM network. Emphasis was placed on the structure of the MAC protocol, which uses optical prime codes to prevent collisions when TUs apply for slot reservations. Finally, the format of the IR wireless cells for voice services was considered and some of the most basic challenges of employing ATM over diffuse IR local area networks were revealed.

# CHAPTER FIVE:

## ANALYSIS AND PERFORMANCE OF THE MAC PROTOCOL



## **5 ANALYSIS AND PERFORMANCE OF THE MAC PROTOCOL**

### **5.1 Introduction**

This chapter presents the mathematical analysis and evaluation of the MAC protocol, which was described in the previous chapter. The analysis considers that the base station has to serve an indoor LAN, with small-sized cells (picocells), and in each cell there are  $M$  homogeneous TUs. The protocol is examined under statistical slot allocation for variable bit rate (VBR) speech services. The various IR channel impairments are not taking into account, therefore it is assumed that there is a perfect physical connection between TUs and BS. Under this condition, the performance of the LAN is mainly dependant on the MAC structure.

Section 5.2 describes the speech source model that each TU employs. The steady-state probability of the queuing model, which represents the MAC protocol, is revealed in section 5.3. The formulas of the MAC performance parameters such as throughput, packet dropping probability, average access delay, and statistical multiplexing gain are derived in sections 5.4-5.7 respectively. Finally, in section 5.8 numerical results of the performance parameters are given for a range of LAN specifications.

### **5.2 Speech Source Model**

In literature it has been shown that a speech source has ON-OFF patterns, and that

all talkspurts (ON) and silences (OFF) are exponential distributed [75]. Therefore, the behaviour of a voice TU that employs a slow speech activity detector can be modelled as a two-state (ON-OFF) Markov chain. Such a source model is shown in Fig. 5-1. Where  $\gamma$  denotes the transition probability from talking to silent state during a channel frame while  $\sigma$  denotes the transition probability from silent to talking state during a channel frame. Talkspurt duration is equivalent to message length or service time of each TU in the uplink channel frame, likewise gap duration is equivalent to inter-arrival time of messages. The probability of more than two transitions, from talking to silent state or vice versa, during one channel frame is taken to be zero. This is due to the big difference between channel frame duration and speech patterns duration.

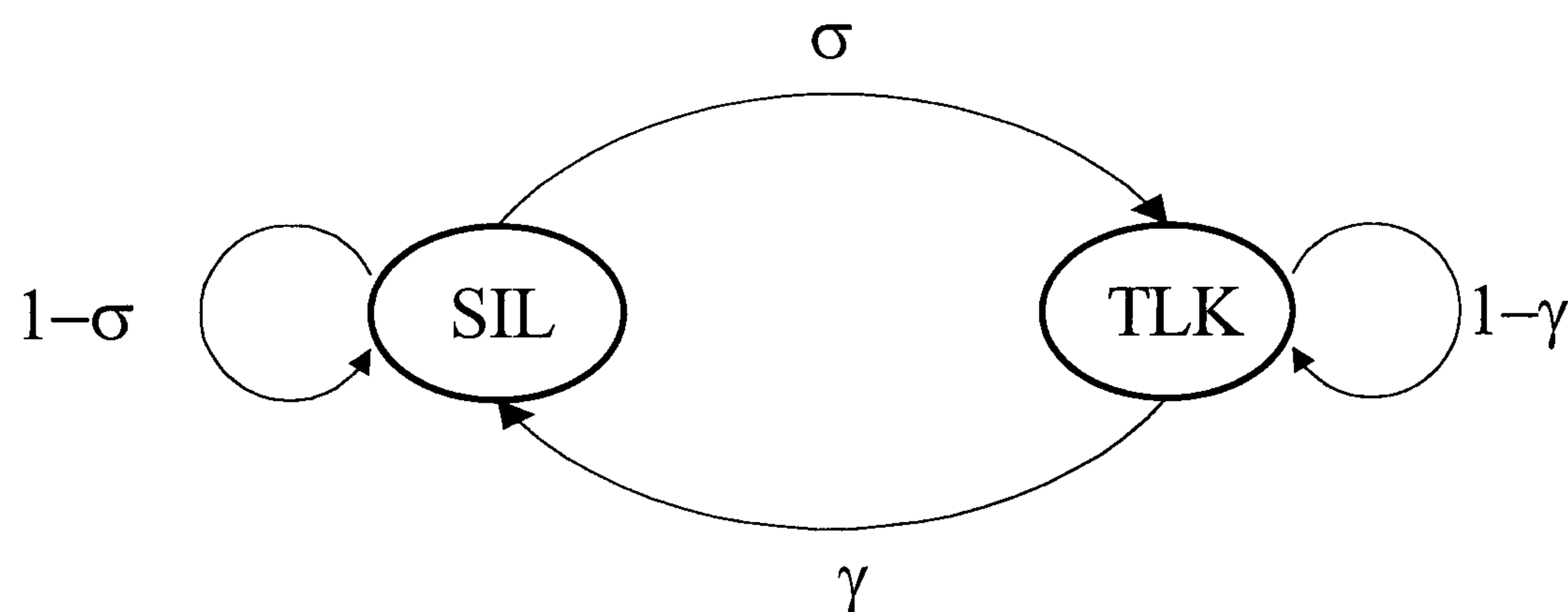


Fig. 5-1 Two-state Markovian model for speech source

Knowing the channel frame duration ( $T_{cf}$ ) and the mean duration of talkspurts ( $t_1$ ), silences ( $t_2$ ) then



$$\gamma = 1 - \exp(-T_{cf} / t_1) \quad (5.1)$$

$$\sigma = 1 - \exp(-T_{cf} / t_2) \quad (5.2)$$

Other description parameters of the ON/OFF speech source are the activity ratio  $\alpha$  and source burstiness  $\beta$ , which are defined as follows.

$$\alpha = \frac{t_1}{t_1 + t_2} \quad (5.3)$$

$$\beta = \frac{t_1 + t_2}{t_1} \quad (5.4)$$

### 5.3 Steady-State Probability

Considering the time slots within a channel frame as a bunch of parallel servers and recalling that a TU with a reservation will be served once for the whole channel frame the MAC protocol can be modelled as a  $M/M/N/\infty/M$  queuing system. The latter consists of exponentially distributed durations of all spurts and gaps,  $N$  parallel servers, infinite storage and  $M$  users. Obviously, in a real system the storage must be finite with its size depending on parameters such as tolerant storage time for time sensitive services. However, assuming infinite storage can simplify the analysis and still be of value in describing the queuing behaviour.

To find the steady-state probability, which is the probability of finding  $n$  customers in the system at an arbitrary point of time after the process has reached statistical equilibrium, first the transition rates of arrivals and departures within a cell must be defined. The transition rate from a state  $n$  to a state  $n+1$ , which denotes an arrival, is given by

$$\lambda_n = \begin{cases} (M - n)\lambda & 0 \leq n < M \\ 0 & n \geq M \end{cases} \quad (5.5)$$

Where  $\lambda$  is defined as the number of packets arriving per unit time and is given by  $\lambda = 1/t_2$ . The transition rate from a state  $n$  to a state  $n-1$ , which denotes a departure, is written as

$$\mu_n = \begin{cases} n\mu & 0 \leq n < N \\ N\mu & n \geq N \end{cases} \quad (5.6)$$

Where  $\mu$  is the rate of service in terms of completions per unit time and is given by  $\mu = 1/t_1$ . Following to the birth-death theory [106] the state probability ( $P_n$ ) can be expressed as

$$P_n = \begin{cases} \binom{M}{n} \left(\frac{\lambda}{\mu}\right)^n P_0 & 0 \leq n < N \\ \binom{M}{n} \frac{n!}{N^{n-N} N!} \left(\frac{\lambda}{\mu}\right)^n P_0 & N \leq n \leq M \end{cases} \quad (5.7)$$



Where

$$\binom{M}{n} = \frac{M!}{(M-n)! n!} \quad (5.8)$$

is the binomial coefficient. With the uplink channel frame rate to be identical to the arrival rate of voice packets the number of slots (N) per channel frame is given by

$$N = \text{int} \left[ \frac{(R_c T_{cf})}{(2 J T_{cf} R_s + H)} \right] \quad (5.9)$$

Where  $\text{int}[x]$  is the largest integer smaller than or equal to  $x$ ,  $R_c$  is the channel bit rate,  $R_s$  is the source bit rate,  $J$  is the number of channel frames (or channel reuse factor) in the uplink/downlink frame, and  $H$  is the header size of an IR wireless cell.

Where  $T_{cf}$  is the duration of a channel frame and is given by

$$T_{cf} = \frac{T_f}{J} - \frac{\text{ACK}}{R_c} \quad (5.10)$$

Transmission delays between TUs and the base station are negligible. In (5.7)  $P_0$  can be derived by normalisation as

$$\sum_{n=0}^M p_n = 1 \quad (5.11)$$

Hence substituting (5.7) into (5.11)

$$P_0 = \left[ \sum_{n=0}^{N-1} \binom{M}{n} \left( \frac{\lambda}{\mu} \right)^n + \sum_{n=N}^M \binom{M}{n} \frac{n!}{N^{n-N} N!} \left( \frac{\lambda}{\mu} \right)^n \right]^{-1} \quad (5.12)$$

#### 5.4 Packet Dropping Probability

Packets that convey real time information, such as speech, require to be promptly delivered. If the packets are delayed over a time limit ( $D_{\max}$ ), they are discarded. Therefore, an important performance measure for voice TUs is the probability that generated speech packets waited more than a specified time limit. This probability is referred to as packet dropping probability ( $P_{\text{drop}}$ ) and the expression can be derived from the statistical particularities of the MAC protocol. A TU starts dropping packets if its very first packet experiences a delay over  $D_{\max}$ . Hence, the number of dropped packets ( $P_d$ ) in the TU that suffers a delay more than  $D_{\max}$  can be written as

$$P_d = \left( \frac{D - D_{\max}}{2T_f} \right) \quad (5.13)$$

Where  $D$  is the delay experienced by the TU. The number of packets ( $N_p$ ) in a message with duration of  $t$  seconds is written as



$$N_p = \left( \frac{t}{2T_f} \right) \quad (5.14)$$

Hence, the packet dropping probability for a message with length of  $t$  seconds and experienced delay of  $D$  seconds is

$$P_{\text{drop}} = f(D, t, t_1) \frac{\left( \frac{D - D_{\text{max}}}{2T_f} \right)}{\left( \frac{t}{2T_f} \right)} \Delta D \Delta t = f(D, t, t_1) \frac{D - D_{\text{max}}}{t} \Delta D \Delta t \quad (5.15)$$

Where  $f(D, t, t_1)$  is the joint probability density function (pdf) of delay  $D$  and message duration of  $t$  seconds with average message duration of  $t_1$  seconds. Since both the suffered delay and message duration are statistically independent  $P_{\text{drop}}$  is written as

$$P_{\text{drop}} = f_D(D, t_1) f_t(t, t_1) \frac{D - D_{\text{max}}}{t} \Delta D \Delta t \quad (5.16)$$

Where  $f_D(D, t_1)$  is the pdf of delay and  $f_t(t, t_1)$  is the pdf of message duration. Finally, the average packet dropping probability expression is written as

$$P_{\text{drop}} = \int_{t=2T_f}^{\infty} \int_{(D=D_{\text{max}}+2T_f)}^{(D_{\text{max}}+t)} f_D(D, t_1) f_t(t, t_1) \frac{D - D_{\text{max}}}{t} dD dt \quad (5.17)$$

The cumulative distribution function of the delay, denoted by  $F_D(D, t_1)$ , is written as [106]

$$F_D(D, t_1) = 1 - \sum_{n=N}^{M-1} \frac{(M-n)p_n}{M-L} \sum_{i=0}^{n-N} \frac{(\mu ND)^i}{i!} \exp(-\mu ND) \quad (5.18)$$

while  $f_D(D, t_1)$  is the derivative of the  $F_D(D, t_1)$  and is given by

$$f_D(D, t_1) = \frac{(e^{-\mu ND}) \mu N}{M-L} \sum_{n=N}^{M-1} p_n (M-n) \frac{(\mu ND)^{n-N}}{(n-N)!} \quad (5.19)$$

Knowing that the message duration follows the negative exponential distribution, the pdf of message duration is

$$f_t(t, t_1) = \frac{\exp(-t/t_1)}{t_1} = \lambda \exp(-\lambda t) \quad (5.20)$$

Hence, substituting (5.20) and (5.19) into (5.17) we can calculate the  $P_{\text{drop}}$ . However, the resulting function cannot be easily computed and the alternative simplified function is used [107]

$$P_{\text{drop}} = \int_{(D_{\text{max}}+2T_f)}^{(D_{\text{max}}+t_1)} f_D(D, t_1) \frac{D - D_{\text{max}}}{t_1} dD \quad (5.21)$$



In (5.19)  $L$  is the average number of TUs in the system (served and contending TUs) and is given by

$$L = \sum_{n=0}^M nP_n \quad (5.22)$$

Substituting (5.7) into (5.22) gives

$$L = p_0 \left[ \sum_{n=0}^{N-1} n \binom{M}{n} \left( \frac{\lambda}{\mu} \right)^n + \sum_{n=N}^M n \binom{M}{n} \frac{n!}{N^{n-N} N!} \left( \frac{\lambda}{\mu} \right)^n \right] \quad (5.23)$$

This is the neatest expression for  $L$ ,  $P_0$  must first be calculated and then multiplied by the two series one of  $N$  terms and the other of  $M-(N+1)$  terms. The number of the TUs that are waiting in the queue  $L_q$  to be served is a function of  $L$  and can be obtained as

$$L_q = L - N + \sum_{n=0}^{N-1} (N - n)P_n \quad (5.24)$$

Substituting (5.23) into (5.24) gives

$$L_q = L - N + P_0 \sum_{n=0}^{N-1} (N - n) \binom{M}{n} \left( \frac{\lambda}{\mu} \right)^n \quad (5.25)$$

Although an increase in  $P_{\text{drop}}$  reduces the received voice quality at the same time it reduces the average message duration as

$$t_1^{u+1} = (1 - P_{\text{drop}}^u) t_1^u \quad (5.26)$$

$$\text{with } P_{\text{drop}}^0 = 0$$

Therefore, to calculate the exact value of the packet dropping probability and the rest of the performance parameters we need to use (5.26) for a number of iteration steps to give a desired accuracy.

## 5.5 System Throughput

System throughput ( $\eta$ ) is another important measure of the system performance and is defined as the number of the reserved slots in the uplink channel frame over the average number of total slots in the same channel frame. We can calculate the throughput using the equilibrium states as follows

$$\eta = \frac{\text{the number of reserved slots in the uplink frame}}{\text{the number of slots in the uplink frame}} \quad (5.27)$$

or

$$\eta = \frac{E[n_r]}{N} = \frac{1}{N} \sum_{n_r=0}^N \sum_{n_c=0}^{M-n_r} P(n_r, n_c) n_r \quad (5.28)$$



Where  $E[x]$  is the statistical expected value of the random variable  $x$ ,  $n_r$  is the number of reserved slots in the channel frame,  $n_c$  is the number of contenting TUs,  $P(n_r, n_c)$  is the probability that there are  $n_c$  contenting TUs in the system and  $n_r$  reserved slots. Since a TU that waits in the queue will be served as soon as a slot becomes free, the throughput of the system can be expressed as

$$\eta = \frac{\text{Average number of reserved slots} + \text{Average number of contenting TUs}}{N} \quad (5.29)$$

or

$$\eta = \frac{1}{N} \left( \sum_{n=0}^{N-1} nP_n + N \sum_{n=N}^M P_n \right) \quad (5.30)$$

## 5.6 Average Access Delay

The total delay for a TU in the system is the sum of waiting time in the queue plus the service time. Therefore, the average access delay ( $\bar{D}$ ) is the delay that is experienced by a TU while waiting in the queue and is directly calculated by utilising Little's formula

$$\bar{D} = \frac{L}{\lambda(M-L)} - \frac{1}{\mu} \quad (5.31)$$

## 5.7 Statistical Multiplexing Gain

Statistical multiplexing gain ( $G$ ) is the maximum number of simultaneous conversations per uplink slot when  $P_{\text{drop}} \leq 1\%$ . The statistical multiplexing gain is given by

$$G = \frac{M_{\text{max}}}{N} \quad (5.32)$$

Where  $M_{\text{max}}$  is the maximum number of TUs supported within a channel frame.

## 5.8 Numerical Results

To obtain numerical results of the performance parameters the LAN specifications in Table 5-1 are used. The radius of a cell is taken to be  $r = 3$  meters, this is a satisfactory size between the interference-limited region and noise-limited region according to [57]. To prevent performance degradation due to cochannel interference the channel reuse factor is taken to be  $J = 7$ , recalling (4.2) this results in a distance of 13.7 meters between two neighbouring cells. Such a distance is large enough to ignore cochannel interference because the latter is much lower than the noise produced by the ambient and artificial light sources. Using OOK modulation at a transmission bit rate  $\leq 10 \text{ Mb/s}$ , the intersymbol interference (ISI) effects due to multipath phenomenon can be ignored [53]. Therefore, ensuring that the physical layer transmits and receives data at a desired BER, usually  $10^{-9}$ , the LAN



performance depends mainly on the MAC protocol structure. The bandwidth allocated during the uplink/downlink frame within a cell is given by

$$B_c = (T_{cf} R_c) / 2 T_f \tag{5.33}$$

This bandwidth can be used to serve constant bit rate (CBR), variable bit rate (VBR), unspecified bit rate (UBR) and available bit rate (ABR) ATM services. For ABR/UBR services, (such as text) free slots are assigned by means of a dynamic slot allocation algorithm. The average duration of speech activities taken from [108] and video activities (e.g. videoconference) taken from [93] are shown in Table 5-1.

Variable	Notation	Value
Channel bit rate	$R_c$	10 Mb/s
Source peak bit rate	$R_s$	64 kb/s
Video peak bit rate (coded)	$R_v$	320 kb/s
Uplink/downlink frame duration	$T_f$	3.1 ms
R slot duration	$R$	256 bits
ACK slot duration	ACK	$R+T_d(N+1)$
Downlink timing signal	$T_d$	4 bits
Speech mean ON duration	$t_1$	1 s
Speech mean OFF duration	$t_2$	1.35 s
Speech cell maximum time delay	$D_{max}$	20 ms
Video mean ON duration	$Vt_1$	33 ms
Video mean OFF duration	$Vt_2$	67 ms
Video cell maximum time delay	$VD_{max}$	150 ms
Channel reuse factor	$J$	7
Number of identical superimposed ON/OFF sources to model the video traffic	$N_s$	15
Header of an IWC (compressed ATM header, DLC field, MAC field, guard band)	$H$	70 bits

Table 5-1 The LAN specifications

A VBR video source can be described as a superposition of  $X$  independent identical ON/OFF sources, however, the calculation of the statistical bandwidth (or equivalent capacity) to guarantee the quality of service becomes very complicated. In [93] the statistical bandwidth for the video source has been calculated and found  $B_v > 130$  kb/s for packet loss probability  $(P_{\text{loss}}) \leq 10^{-4}$ . Thus, the number of time slots is required per channel frame for the video source is

$$V_N = \frac{(2 T_f B_v)}{q} \quad (5.34)$$

Where  $q$  is the number of information bits (excluding the header) conveyed per time slot and is given by

$$q = \frac{R_c T_{cf}}{N} - H \quad (5.35)$$

Where  $H$  is the size of the IWC header.

Fig. 5-2 shows the  $P_{\text{drop}}$  versus the number ( $M$ ) of voice TUs for two cases *a*) when no video TU is in the system and *b*) when one video TU is in the system. For both cases it is observed that after a particular value of  $M$  the packet dropping probability is no longer zero but starts increasing rather rapidly. This is because  $M$  becomes



greater than the number of slots and consequently the TUs start dropping packets due to lack of free slots within the channel frame.

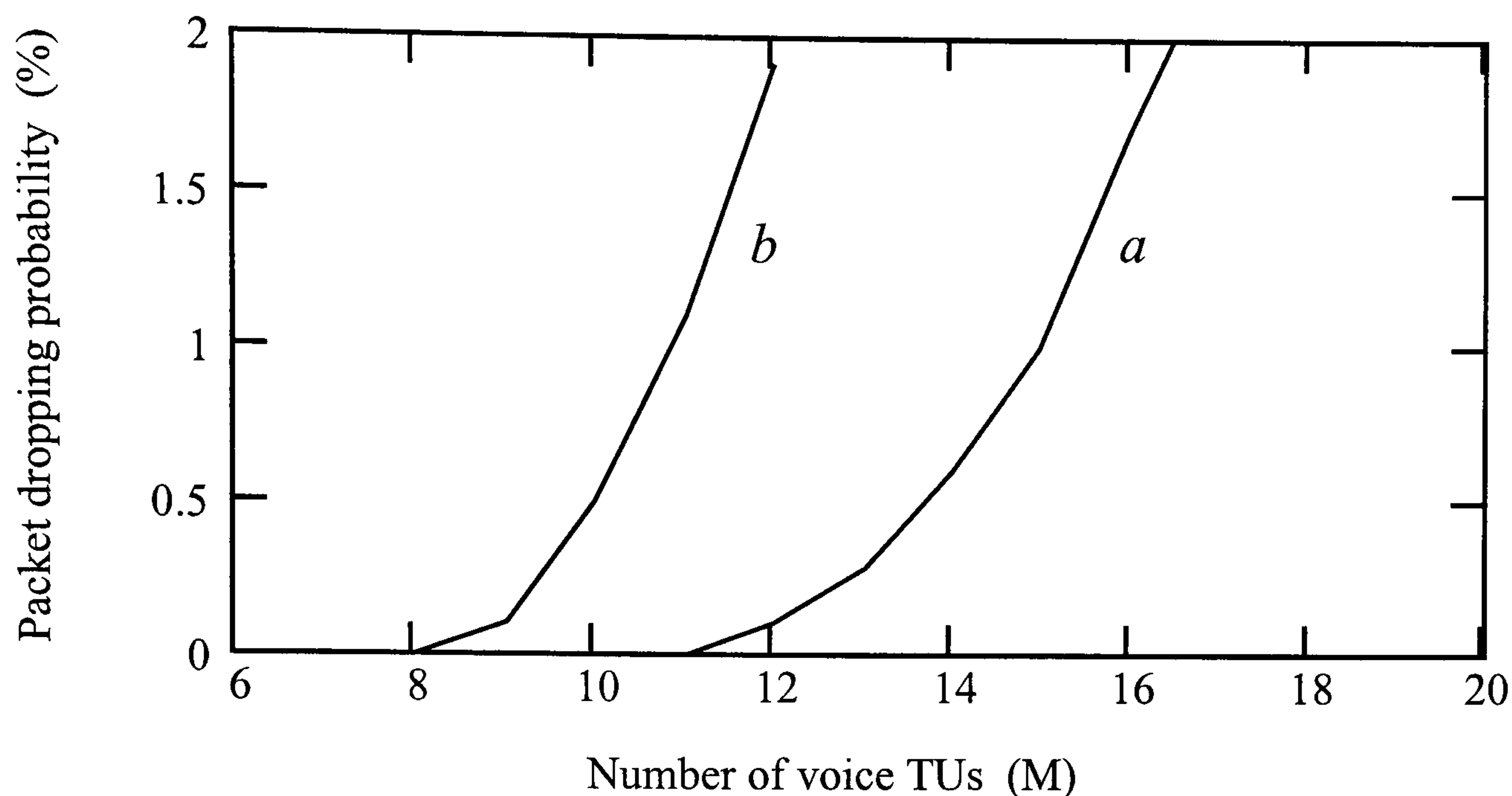


Fig. 5-2 Packet dropping probability versus the number of voice TUs when there is  
*a)* no video TU and *b)* one video TU, in the system

Speech  $P_{\text{drop}}$  with which speech quality degradation is almost not perceptible must be  $\leq 1\%$  [75]. Curve (a) shows that for  $P_{\text{drop}} = 1\%$  the system is capable of supporting up to 15 TUs simultaneously. If  $M$  is above 15 the quality of service performance is not satisfied. While curve (b) shows that  $M$  is equal to 11 for  $P_{\text{drop}} = 1\%$ , this is because the video TU engages two slots, according to (5.34), in each channel frame.

Although the performance of a VBR video source may be satisfied when its statistical bandwidth is assigned, however, the statistical bandwidth does not exactly describe the traffic of the source. In order to precisely allocate the bandwidth for such a source and therefore improve the performance of the system in terms of

capacity, dynamic slot allocation based on the instantaneous bandwidth requirements of the source must be employed.

Fig. 5-3 depicts numerical results of the system throughput ( $\eta$ ). In both cases increasing the value of  $M$  the throughput increases to a maximum value, which is 0.76 when there is not any video TU in the system and 0.74 with one video TU in the system. Beyond the saturation point the throughput is not increased even if the number of voice TUs keeps increasing, this indicates a good stability of the MAC protocol. For 15 TUs in the system  $\eta = 0.68$  while with one video and 11 voice TUs the throughput slightly drops to 0.64. Obviously, these values are not very close to unity and the reason for this is the small number ( $N = 9$ ) of slots per frame. For higher values of  $N$  the probability of the reserved slots within a channel frame, Eq (5.30), increases asymmetrically resulting in a higher system throughput.

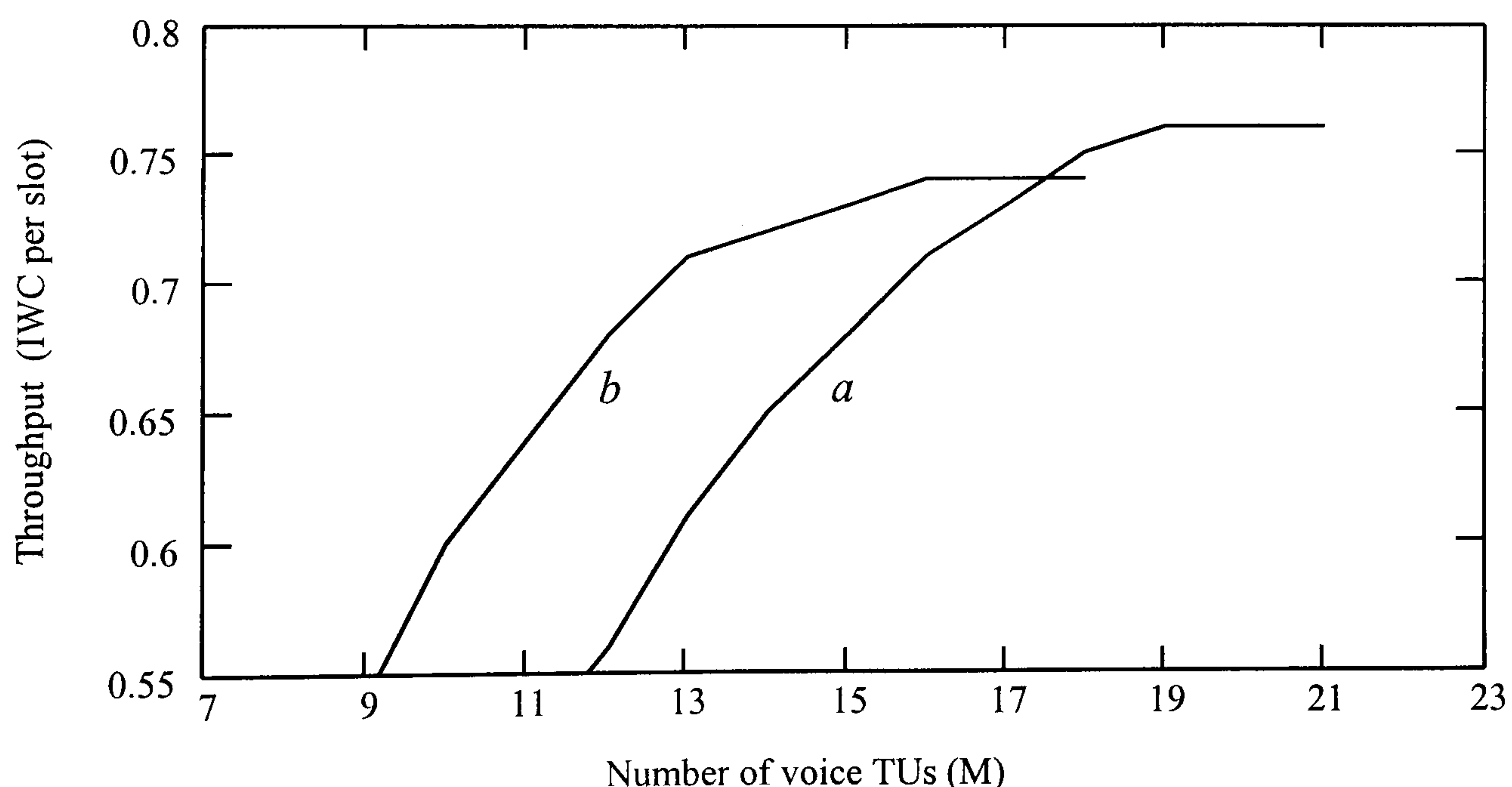


Fig. 5-3 System throughput versus the number of voice TUs when there is *a*) none video TU and *b*) one video TU, in the system



As the number of TUs increases the average access delay ( $\bar{D}$ ) also increases and this is depicted in Fig. 5-4. For both cases there is a particular number of  $M$  where  $\bar{D}$  starts to increase rapidly. For example, looking at curve (a) for  $M$  less than 12 the system is in an insensitive region and variation of  $M$  has no significant effect. However, when  $M$  exceeds 12 the value of  $\bar{D}$  increases rapidly and the system is said to be in a sensitive region. In this region, the addition of even one more TU changes significantly the value of the access delay.

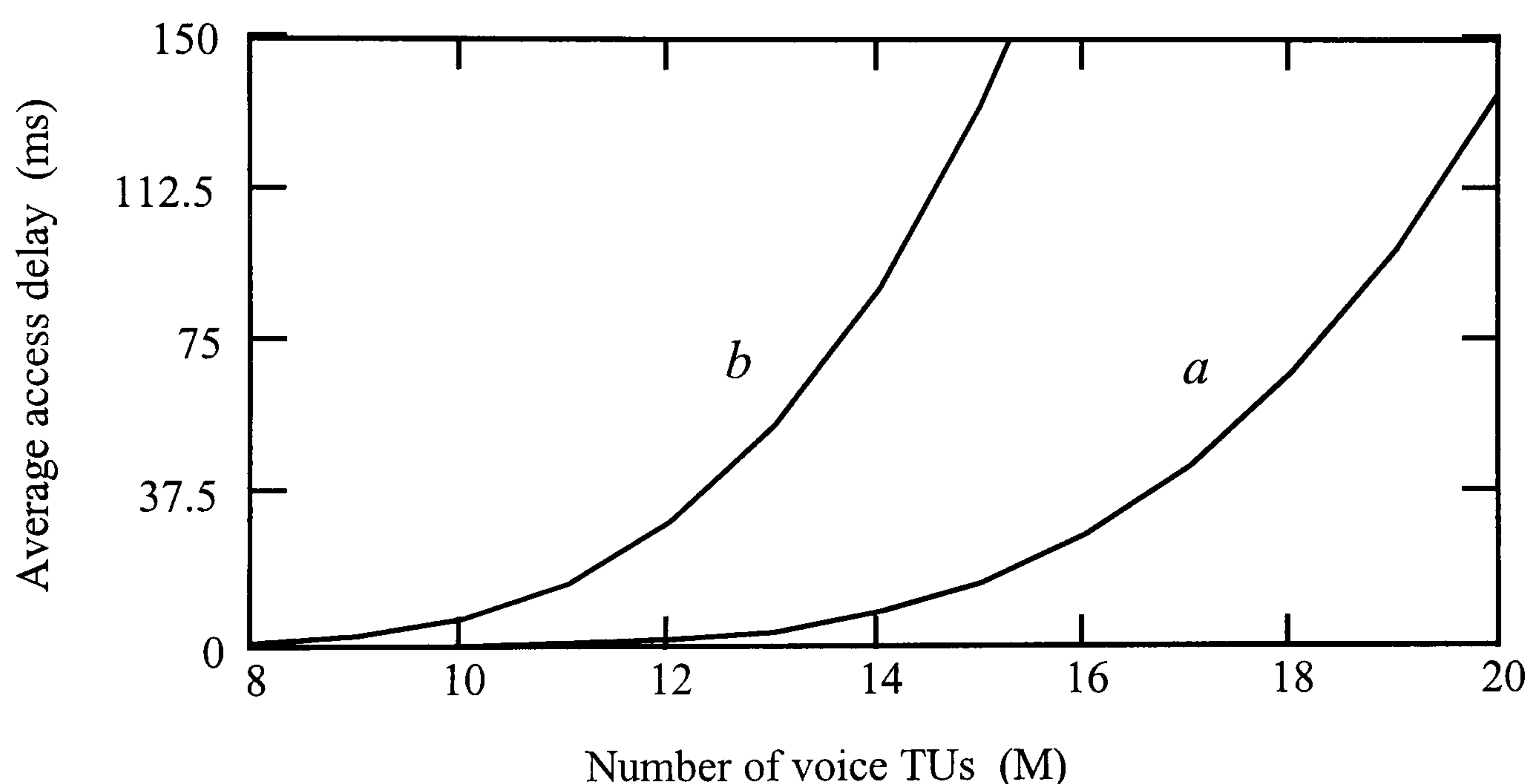


Fig. 5-4 Average access delay versus the number of voice TUs when there is *a*) none video TU and *b*) one video TU, in the system

Fig. 5-5 shows the statistical multiplexing gain of the MAC versus the number of slots ( $N$ ) per channel frame when  $P_{\text{drop}} = 1\%$ . It is observed that as  $N$  increases the gain increases too, implying that more voice packets can be accommodated within a

time slot. Using the specifications in Table 5-1 N equals to 9 and therefore from the figure it is seen that the MAC can accommodate 1.7 conversations per uplink time slot.

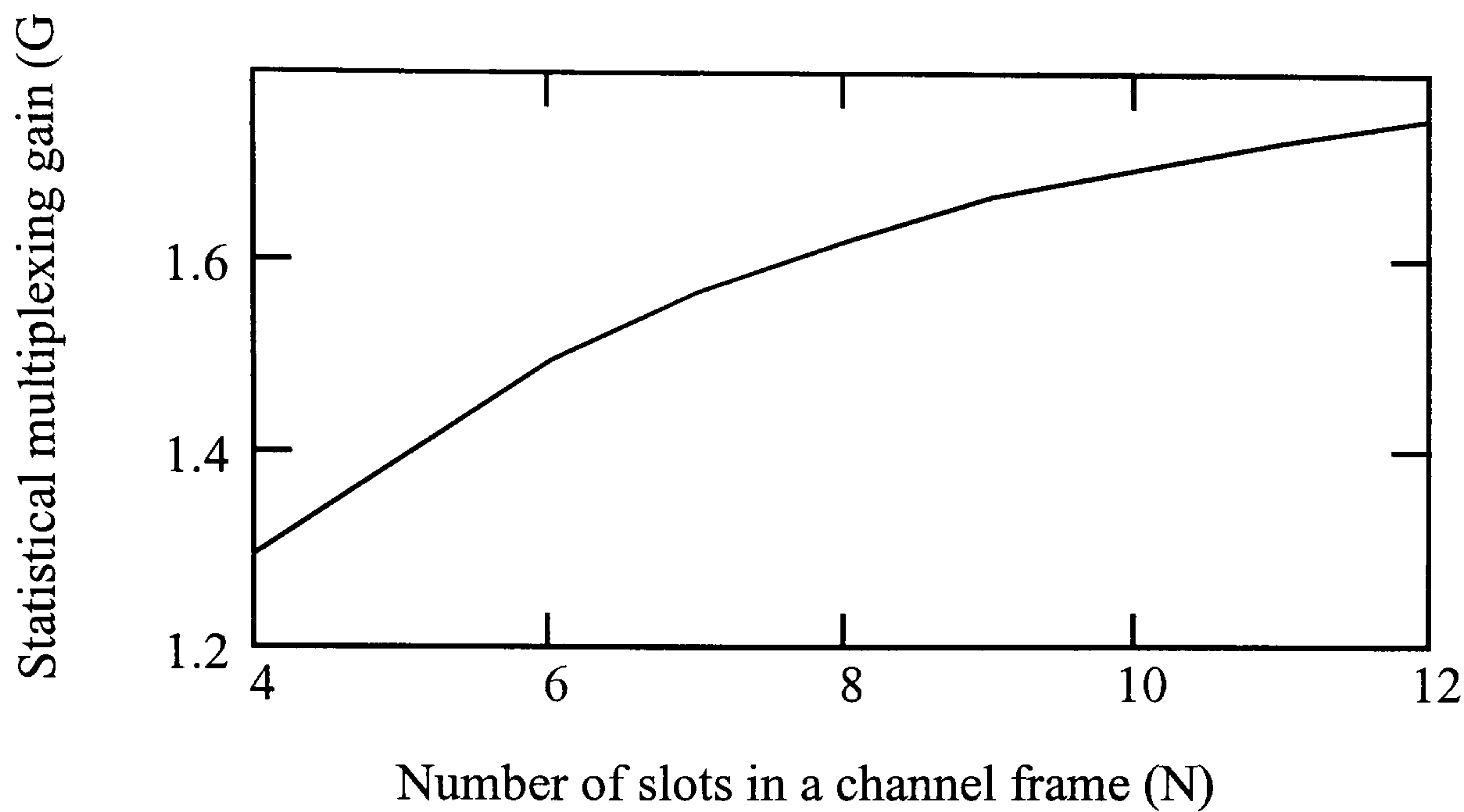


Fig. 5-5 Statistical multiplexing gain of the MAC protocol while  $P_{\text{drop}} = 1\%$

Finally, because each TU uses its own code for slot reservation the BS must assign  $M$  optical prime codes ( $P$ ), each of length  $P^2$ . Now when more than one TU transmit simultaneously to reserve a slot there is multi-access interference at the receiver and consequently the BER increases. If this BER is high then the BS cannot distinguish the TUs and this results in a further delay of service, which in turn is translated into a higher  $P_{\text{drop}}$  rate. Using Gaussian approximation the BER formula is written as

$$\text{BER} = \frac{1}{\sqrt{2\pi}} \int_{-\infty}^{-\frac{\sqrt{\text{SNR}}}{2}} \exp\left(-\frac{x^2}{2}\right) dx \quad (5.36)$$



Where SNR is the signal to noise ratio and according to [111] is written as

$$\text{SNR} = \frac{4P^2}{1.5(m-1)} \quad (5.37)$$

Where  $m$  is the number of TUs that simultaneously transmit their codes. The average value of  $m$  can be approximated to the average value of TUs in the system ( $L$ ) that is given by (5.23). From (5.36) it is found that the BER due to multiaccess interference at the correlative receiver to be approximately  $10^{-8}$ , which is a satisfactory performance.

## 5.9 Summary

In this chapter the MAC protocol was modelled as a  $M/M/N/\infty/M$  queuing system consisting of exponentially distributed durations of all spurts and gaps,  $N$  parallel servers, infinite storage and  $M$  TUs. The steady-state probability was derived using the birth-death theory and then the performance parameters such as throughput, average access delay, packet dropping probability, and statistical multiplexing gain were derived based on the statistical behaviour of the MAC. Using statistical slot allocation it was revealed that for  $P_{\text{drop}}$  equal to 1% the MAC is capable of supporting 15 voice TUs simultaneously while the system throughput is 0.68.

For  $M$  less than 14 the system is in an insensitive region and the variance of TUs has no effect on the average access delay. When  $M$  exceeds 14 the system is in a sensitive region and the access delay increases rapidly. Finally, the statistical multiplexing of the MAC is 1.7 conversations per each uplink time slot for  $P_{\text{drop}} = 1\%$  while the multiaccess interference at the correlative receiver is approximately  $10^{-8}$ .



# CHAPTER SIX:

## ANALYSIS AND PERFORMANCE OF THE HANDOVER PRIORITY-BASED MAC PROTOCOL

## 6 ANALYSIS AND PERFORMANCE OF THE HANDOVER PRIORITY-BASED MAC PROTOCOL

### 6.1 Introduction

By introducing small radius cells (3 to 5 meters) for IR wireless LANs the system capacity per unit area increases but at the same time both the cochannel interference from the neighbouring cells and the number of handovers per call increase too. For a good speech service, network performance parameters such as new call blocking probability ( $P_b$ ) and forced call termination probability ( $P_F$ ) should be low for quite high traffic loads. While the packet dropping probability ( $P_{drop}$ ) should not degrade the voice quality. From the TU's point of view  $P_{drop}$  is the most important parameter while  $P_F$  is more important than  $P_b$ . Giving priority to handover calls over new calls the handover blocking probability ( $P_{HB}$ ), and hence  $P_F$ , are decreased while  $P_b$  is increased. This trade-off is inevitable in handover priority-based schemes and has been observed by many studies in the literature [e.g. 112,113].

There are three basic schemes for handover priority: 1) the guard slot scheme where a number of slots is reserved (either in a fixed way or dynamically) exclusively for handovers, 2) the queuing scheme where a handover call is queued to be served when no available slot is free to serve it immediately, and 3) the subrating scheme where certain slots are temporarily divided into two slots to accommodate handover calls. Among the three schemes, here the guard one is adopted because it provides a



good performance as far as the parameter  $P_F$  is concerned [114] and it also exhibits low complexity and cost.

The rest of the chapter is organised as follows. In section 6.2 first the arrival and departure rates within a cell are derived and then the queuing model of the handover priority MAC protocol is formed in order to derive the steady-state probability. Expressions of the performance parameters such as throughput, packet dropping probability, average access delay, new call blocking probability, handover blocking probability and forced termination blocking probability are derived in sections 6.3-6.8 respectively. In section 6.9 numerical results of the performance parameters are given for a range of LAN specifications.

## 6.2 Steady-State Probability

To proceed with the derivation of the steady-state probability and hence the other performance parameters the plan of a LAN that covers an area of  $Z$  hexagonal cells with a total number of  $T$  TUs is considered. Each TU employs a slow speech activity detector with talkspurts ( $t_1$ ) and silences ( $t_2$ ) to obey the exponential distribution. Providing that the channel frame of the MAC is short enough and knowing that a TU with a reservation will be served once for the whole channel frame we can consider the time slots in a channel frame as a bunch of parallel servers. Under these features the MAC protocol can be modelled as a  $M/M/N/\infty/M_{\max}$  queuing model with arrival and service rates to follow the Poisson distribution,  $N$  parallel servers and infinite

storage. Of course, in a real system the system storage must be finite with its size depending on parameters such as tolerant storage time for time sensitive services. However, assuming infinite storage can simplify the analysis and still be of value in describing the queuing behaviour. Where  $M_{\max}$  is the maximum number of voice TUs that can be supported within a channel frame. With the uplink channel frame rate to be identical to the arrival rate of voice packets the number of slots per channel frame is given by

$$N = \text{int} \left[ \frac{(R_c T_{cf})}{(2 J T_{cf} R_s + H)} \right] \quad (6.1)$$

Where  $\text{int}[y]$  is the largest integer smaller than or equal to  $y$ ,  $R_c$  is the channel bit rate, and  $R_s$  is the source bit rate.  $J$  is the number of channel frames (or channel reuse factor) in the uplink/downlink frame, and  $H$  is the header size of the IR wireless cell.  $T_{cf}$  is the duration of a channel frame and is given by

$$T_{cf} = \frac{T_f}{J} - \frac{\text{ACK}}{R_c} \quad (6.2)$$

Where  $T_f$  is the uplink/downlink frame duration and ACK is the length of the acknowledgement slot. Transmission delays between TUs and the base station (BS) are negligible.



Since we assume a homogenous mobile network every cell in the network is statistically identical and independent to each other. Therefore, analysing the performance of one single cell we can characterise the performance of the whole network. To study a cell it is essential to take into account the interaction between the cell under investigation and its neighbouring cells. This interaction can be modelled by considering the handover call arrivals from the neighbouring cells into the cell under investigation as well as the departures from the cell into its neighbouring cells. This is depicted in Fig. 6-1. Here, we must mention that for a homogeneous system at the steady-state the total arrival rate is equal to the total departure rate.

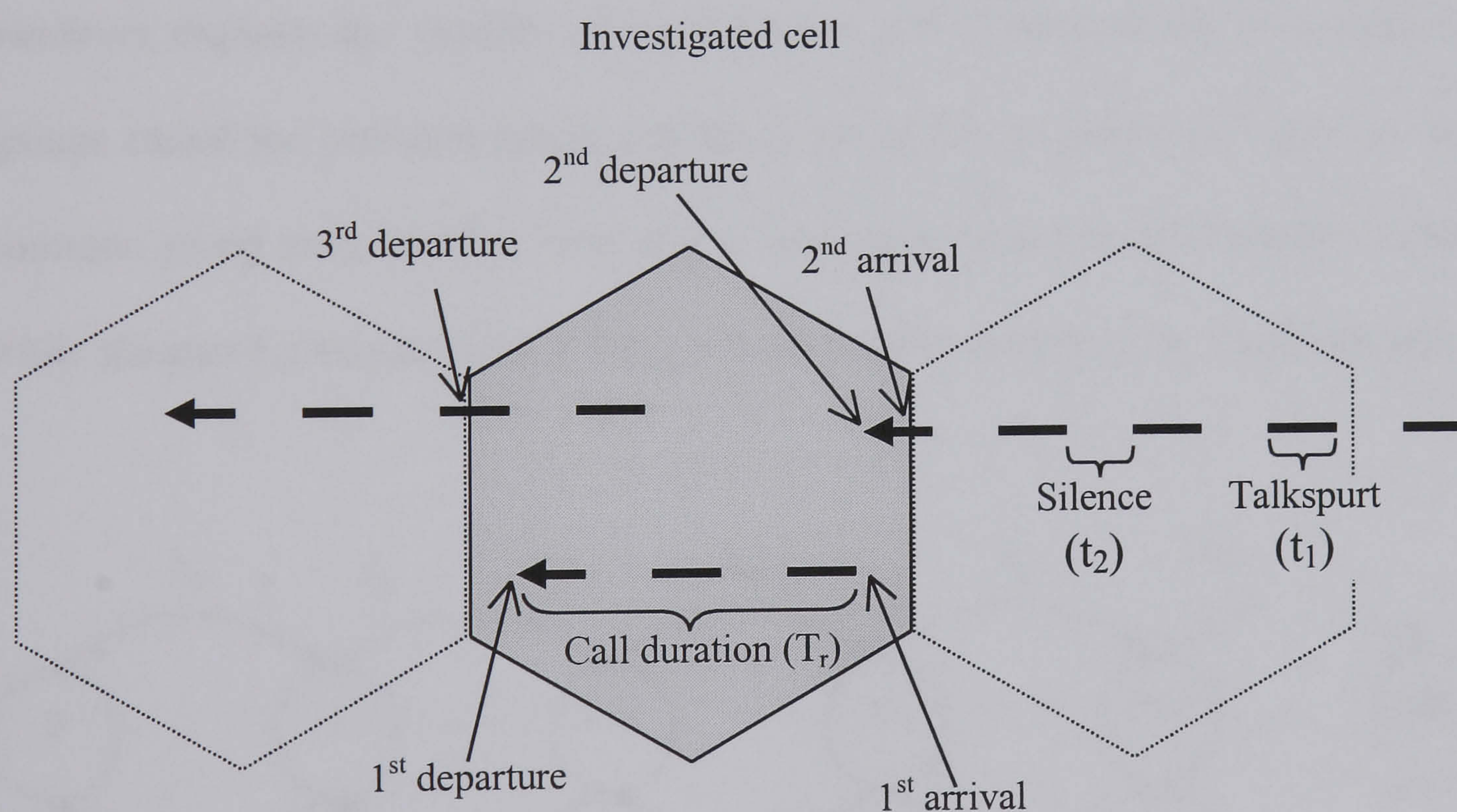


Fig. 6-1 Arrivals and departures within a cell



In case of a call requesting a handover when there is not any slot available then the call will not be blocked immediately but instead it will wait up to a certain tolerable time ( $D_{\max}$ ) for an available slot. During this waiting time packet dropping may occur and the call will eventually be blocked when a specific value of the packet dropping probability is exceeded. Therefore, one can classify the handover mechanism as a hybrid mechanism which is based on both the guard and the queuing schemes.

The queuing model ( $M/M/N/\infty/M_{\max}$ ), consisting of two arrival talkspurt processes and three departure talkspurt processes, can represent a single cell. The states of one cell, which denote the total supported number of TUs during a channel frame, can be represented by a stationary one-dimensional Markov-chain. To secure priority for handover requests the number of states of the cell is divided into two different groups called the common group and the guard group, as shown in Fig. 6-2. The common group consists of  $C$  slots and is used from both new and handover calls while the guard group consists of  $(M_{\max}-C)$  slots and is used only for handover calls.

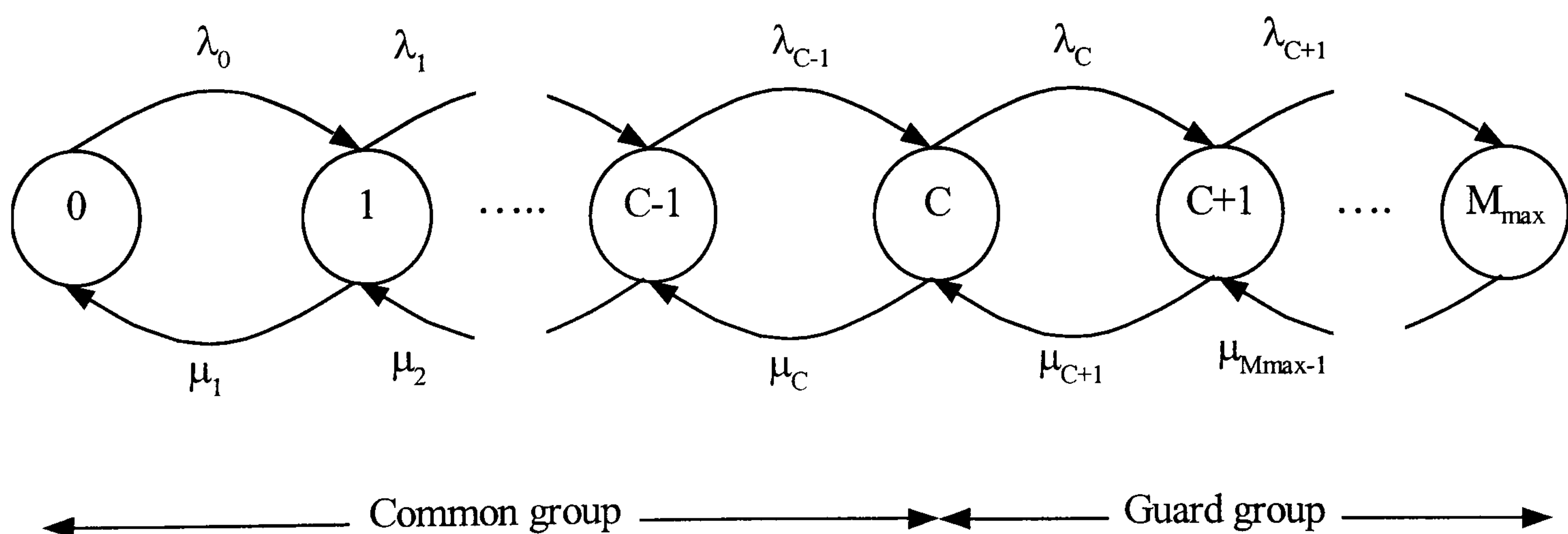


Fig. 6-2 One dimensional Markov-chain state transition diagram

The flow of a handover request is as follows:

- Initially, the MAC protocol looks for a free place in the common group. If there is one then it is assigned to the handover call

- ELSE

It looks for a free place in the guard group. If there is one, it is assigned.

- ELSE

The handover call is forced to terminate.

As illustrated in Fig. 6-1, the first part (1<sup>st</sup> arrival) of the arrival process arises due to talkspurts that are originated within the cell under investigation. The second part (2<sup>nd</sup> arrival) arises due to talkspurts that are originated within the neighbouring cells and request a handover into the cell under investigation. Thus, the transition rate from a state  $n$  to a state  $n+1$  is written as

$$\lambda_n = \begin{cases} (M-n)\lambda_N + (T-M)\lambda_H & 0 \leq n < C \\ (T-M)\lambda_H & C \leq n < M_{\max} \\ 0 & n \geq M_{\max} \end{cases} \quad (6.3)$$

Where  $\lambda_N$  is the new mean arrival rate of talkspurts per TU per unit time and is given by

$$\lambda_N = \frac{T_C}{t_2(T_C + T_r)} \quad (6.4)$$



$T_c$  is the average call duration without any premature termination due to handover failure and  $T_r$  is the average time between call arrivals. In (6.3)  $\lambda_H$  is the mean value of the handover arrival rate

$$\lambda_H = \lambda_N(1 - P_b)P_H \quad (6.5)$$

Where  $P_b$  is the new call blocking probability that is derived below and  $P_H$  is the probability that a call needs a handover.  $P_H$  is given by

$$P_H = \frac{\alpha}{\alpha + (1/T_{cd})} \quad (6.6)$$

$T_{cd}$  is the average slot holding time by a nonblocked call and is the product of the source activity and the call duration,  $\alpha = 1/T_h$  is the number of cell crossings per unit time. Where  $T_h$  denotes the mean sojourn time of a TU within the cell. From the handover arrival expression (6.5) one can see that the new call arrival process is a fully independent process while the handover arrival process depends on the new call arrival process.

The departure processes are shown in Fig. 6-1. The first part of the departure process (1<sup>st</sup> departure) arises due to natural termination of talkspurts that are originated within the cell under investigation. The second part (2<sup>nd</sup> departure) arises due to natural termination of handover accepted talkspurts and can be represented by

$\lambda_H(1 - P_{HB})P_H$ , where  $P_{HB}$  is the handover blocking probability and it will be derived below. The third part (3<sup>rd</sup> departure) arises due to new attempts that are accepted in the cell and now require a handover request, this part is similar to  $\lambda_H$ . Because of the sort of talkspurt duration we assume that only one handover is attempted for each talkspurt. In other words, it is unlikely for a TU to change more than one cell within  $t_1$  time. The total departure rate or mean service rate of talkspurts per unit time per TU is

$$\mu = (1/t_1) + \lambda_H + \lambda_H(1 - P_{HB})P_H \quad (6.7)$$

Thus, the transition rate from a state  $n$  to a state  $n-1$  can be written as

$$\mu_n = \begin{cases} n\mu & 0 \leq n < N \\ N\mu & N \leq n \leq M_{\max} \end{cases} \quad (6.8)$$

The steady-state probability ( $P_n$ ) of the queuing model can be now derived using the birth-death theory processes as

$$P_n = \begin{cases} P_0 \prod_{i=1}^n \frac{(M-i+1)\lambda_N + (T-M)\lambda_H}{i\mu} & 0 \leq n < N \\ P_0 \prod_{i=1}^{N-1} \frac{(M-i+1)\lambda_N + (T-M)\lambda_H}{i\mu} \times \prod_{i=N}^n \frac{(M-i+1)\lambda_N + (T-M)\lambda_H}{N\mu} & N \leq n < C \\ P_0 \prod_{i=1}^{N-1} \frac{(M-i+1)\lambda_N + (T-M)\lambda_H}{i\mu} \times \prod_{i=N}^{C-1} \frac{(M-i+1)\lambda_N + (T-M)\lambda_H}{N\mu} \left[ \frac{(T-M)\lambda_H}{N\mu} \right]^{n-C+1} & C \leq n \leq M_{\max} \end{cases} \quad (6.9)$$

Where  $P_M$  is the average probability that  $M$  TUs stay within a cell. To find  $P_M$  first the number of all distributions of  $M$  mobile TUs to  $Z$  cells must be determined, when exactly  $n$  of them stay in a particular cell. When one TU is in the cell under investigation then the remaining  $T-1$  TUs can be distributed in  $Z-1$  cells. So there are  $(Z-1)^{T-1}$  distributions. Therefore, for  $T$  mobile TUs the number of combinations with one subscriber located in the cell is

$$C_d(1) = T(Z-1)^{T-1} \quad (6.10)$$



For  $M$  TUs staying in the cell under investigation the number of possible distributions of the remaining  $(T-M)$  TUs to  $(Z-1)$  cells is  $(Z-1)^{T-M}$ . Now the number of all combinations of any  $M$  TUs out of  $T$  is

$$\binom{T}{M} = \frac{T!}{(T-M)! M!} \quad (6.11)$$

Therefore, all possible distributions of  $T$  TUs to the  $Z$  cells with exactly  $M$  TUs remaining in the cell under consideration is written as

$$C_d(M) = \binom{T}{M} (Z-1)^{T-M} \quad (6.12)$$

To obtain the average probability that exactly  $M$  TUs stay in the cell (6.12) must be divided by the total number of possible distributions of the mobile TUs to the cells, which is  $Z^T$

$$P_M = \frac{\binom{T}{M} (Z-1)^{T-M}}{Z^T} \quad (6.13)$$

Considering the extreme case that  $M$  can vary from 0 to  $T$  the steady-state probability of the system consists of all probabilities for an  $n$  with 0 to  $T$  TUs inside multiplied by the probability that this certain number of TUs really stays within the cell. Thus, (6.9) is written as

$$P_n' = \begin{cases} \sum_{M=n}^T P_0 \prod_{i=1}^n \frac{(M-i+1)\lambda_N + (T-M)\lambda_H}{i\mu} P_M & 0 \leq n < N \\ \sum_{M=n}^T P_0 \prod_{i=1}^{N-1} \frac{(M-i+1)\lambda_N + (T-M)\lambda_H}{i\mu} \times \\ \prod_{i=N}^n \frac{(M-i+1)\lambda_N + (T-M)\lambda_H}{N\mu} P_M & N \leq n < C \\ \sum_{M=n}^T P_0 \prod_{i=1}^{N-1} \frac{(M-i+1)\lambda_N + (T-M)\lambda_H}{i\mu} \times \\ \prod_{i=N}^{C-1} \frac{(M-i+1)\lambda_N + (T-M)\lambda_H}{N\mu} \left[ \frac{(T-M)\lambda_H}{N\mu} \right]^{n-C+1} P_M & C \leq n \leq M_{\max} \end{cases} \quad (6.14)$$

In (6.14) the sum runs from  $n$  rather than 0 because the steady-state probability for less than  $n$  TUs in the cell is always zero. Recalling the boundary condition

$$\sum_{n=0}^T P_n' = 1 \quad (6.15)$$

$P_0$  is written as



$$\begin{aligned}
P_0 = & \left[ \sum_{n=1}^{N-1} \sum_{M=n}^T \prod_{i=1}^n \frac{(M-i+1)\lambda_N + (T-M)\lambda_H}{i\mu} P_M + \right. \\
& \sum_{n=N}^{C-1} \sum_{M=n}^T \prod_{i=1}^{N-1} \frac{(M-i+1)\lambda_N + (T-M)\lambda_H}{i\mu} \prod_{i=N}^n \frac{(M-i+1)\lambda_N + (T-M)\lambda_H}{N\mu} P_M + \\
& \left. \left( \sum_{N=C}^{M_{\max}} \sum_{M=n}^T \prod_{i=1}^{N-1} \frac{(M-i+1)\lambda_N + (T-M)\lambda_H}{i\mu} \prod_{i=N}^{C-1} \frac{(M-i+1)\lambda_N + (T-M)\lambda_H}{N\mu} \times \right. \right. \\
& \left. \left. \left[ \frac{(T-M)\lambda_H}{N\mu} \right]^{n-C+1} P_M \right) \right]^{-1}
\end{aligned}
\tag{6.16}$$

### 6.3 Packet Dropping Probability

As mentioned before  $P_{\text{drop}}$  which is the probability that the generated voice packets experience a service delay over  $D_{\text{max}}$  is the most important parameter from the TU's point of view. This is because  $P_{\text{drop}}$  is directly related to the voice quality of an accepted new or handover call. Following the analysis in section 5.4  $P_{\text{drop}}$  is written as

$$P_{\text{drop}} = \int_{(D_{\text{max}}+2T_{\text{cf}})}^{(D_{\text{max}}+t_1)} f_D(D, t_1) \frac{D - D_{\text{max}}}{t_1} dD
\tag{6.17}$$

Where  $D$  is the delay experienced by the TU and  $f_D(D, t_1)$  is the probability density function (pdf) of delay with average talkspurt length of  $t_1$ . Here, the cumulative distribution function (cdf) of the delay, denoted by  $F_D(D, t_1)$ , is written as

$$F_D(D, t_1) = 1 - \sum_{n=N}^{M-1} q_n \sum_{i=0}^{n-N} \frac{(\mu ND)^i}{i!} \exp(-\mu ND) \quad (6.18)$$

Where  $q_n$  relates the general-time probability  $P_n$  to the probability that an arrival finds  $n$  TUs in the system

$$q_n = \frac{[(M-n)\lambda_N + (T-M)\lambda_H]P_n}{(M-L)\lambda_N + (T-M)\lambda_H} \quad (6.19)$$

Where  $L$  is the average number of TUs in the system and is given by

$$L = \sum_{n=0}^{M_{\max}} nP_n \quad (6.20)$$

Now  $f_D(D, t_1)$ , the derivative of  $F_D(D, t_1)$ , is given by

$$f_D(D, t_1) = \frac{(e^{-\mu ND}) \mu N}{(M-L)\lambda_N + (T-M)\lambda_H} \sum_{n=N}^{M-1} p_n [(M-n)\lambda_N + (T-M)\lambda_H] \frac{(\mu ND)^{n-N}}{(n-N)!} \quad (6.21)$$

Recalling that  $M$  can vary from 0 to  $T$  then



$$f_D(D, t_1)' = \sum_{M=0}^T f_D(D, t_1) P_M \quad (6.22)$$

Considering again the fact that  $P_{\text{drop}}$  reduces the received voice quality while at the same time it reduces the average talkspurt duration, (5.26) must be utilised again for a desired number of iteration steps to calculate the exact value of  $P_{\text{drop}}$  and of the steady-state probability.

## 6.4 System Throughput

Following the analysis in section 5.5 the throughput ( $\eta$ ) is again defined as the number of the reserved slots in the uplink channel frame over the number of total slots in the same channel frame. We can calculate the throughput using the equilibrium values as follows

$$\eta = \frac{E[n_r]}{N} = \frac{1}{N} \sum_{n_r=0}^N \sum_{n_c=0}^{M-n_r} P(n_r, n_c) n_r \quad (6.23)$$

Where  $E[x]$  is the statistical expected value of the random variable  $x$ ,  $n_r$  is the number of reserved slots in the channel frame,  $n_c$  is the number of contending terminals,  $P(n_r, n_c)$  is the probability that there are  $n_c$  contending TUs in the

system and  $n_r$  reserved slots. Since a TU that waits in the queue will be served as soon as a slot becomes free, the throughput of the system can be expressed as

$$\eta = \frac{1}{N} \left( \sum_{n=0}^{N-1} nP_n + N \sum_{n=N}^{M_{\max}} P_n \right) \quad (6.24)$$

## 6.5 Average Access Delay

Knowing the average number of TUs in the system we can calculate the average access delay that they will experience while waiting in the queue. This is directly calculated by utilising Little's formula as

$$\bar{D} = \frac{L}{\mu(L - L_q)} - \frac{1}{\mu} \quad (6.25)$$

$L_q$  represents the average number of TUs that are waiting in the queue to be served and is given by

$$L_q = \sum_{n=N}^{M_{\max}} (n - N)P_n \quad (6.26)$$

## 6.6 New Call Blocking Probability

A new call will be blocked if more than  $C-1$  TUs are in the system, therefore, the



blocking probability ( $P_b$ ) for new calls is the sum of the steady state probabilities for  $C$  to  $M_{\max}$  TUs in the cell

$$P_b = \sum_{n=C}^{M_{\max}} P_n \quad (6.27)$$

Substituting (6.14) into (6.27)

$$P_b = \sum_{n=C}^{M_{\max}} \left( \sum_{M=n}^T P_0 \prod_{i=1}^{N-1} \frac{(M-i+1)\lambda_N + (T-M)\lambda_H}{i\mu} \times \prod_{i=N}^{C-1} \frac{(M-i+1)\lambda_N + (T-M)\lambda_H}{N\mu} \left[ \frac{(T-M)\lambda_H}{N\mu} \right]^{n-C+1} P_M \right) \quad (6.28)$$

## 6.7 Handover Blocking Probability

A handover attempt will be blocked if in the cell under investigation there are  $M_{\max}$  TUs being served at the same time. Therefore, the expression for such a probability will be the same with the steady state probability for  $M_{\max}$  TUs in the system,  $P_{hb} = P_{M_{\max}}$ . Handover blocking also happens when a TU requests handover more often than once every time limit ( $t_{\min}$ ). Such a restriction will be inevitable for very small cell networks in order to keep the signalling load moderate. Thus, the probability that the time to the last handover is less than  $t_{\min}$  must be found. This probability is similar to the probability of a distance less than  $d_{\min} = v t_{\min}$  which the TU has covered within the cell, where  $v$  is the speed of the mobile TU. Assuming that the

speed of a TU remains constant during the travel in a cell and following the approach in [115], where a hexagonal cell is approximated by a circular one, this part of handover probability can be written as

$$P_{hb}' = \frac{2F_1}{F_{tot}} = \frac{r^2 \arcsin\left(\frac{d_{min}}{2r}\right) - \frac{rd_{min}}{4} \sqrt{4 - \frac{d_{min}^2}{r^2}}}{\pi r^2} \quad (6.29)$$

$F_1$  is the area in the circle where each covered distance is smaller than  $d_{min}$  and  $F_{tot}$  is the total area of the circular approximated cell. Therefore, the total handover blocking probability will be the sum of the two different part handover probabilities described above

$$P_{HB} = P_{hb} + P_{hb}' \quad (6.30)$$

## 6.8 Forced Termination Probability

If there is any handover failure during the lifetime of a call, it will be forced into termination. The probability for occurrence of one handover is given by (6.6). Then the probability that the first handover fails is  $(P_H P_{HB})$ . If the second handover fails obviously before one handover has been successful hence, the probability for this event is  $P_H^2 P_{HB} (1 - P_{HB})$ . Therefore, the probability that the  $(k+1)$ -th handover fails



is  $P_H^{k+1}P_{HB}(1 - P_{HB})^k$ . Since the forced termination probability is the probability that any handover fails the expression is written as

$$P_F = P_H P_{HB} \sum_{k=0}^{\infty} P_H^k (1 - P_{HB}) = \frac{P_H P_{HB}}{1 - P_H (1 - P_{HB})} \quad (6.31)$$

To run the analysis we need initially to calculate  $\lambda_H$  and  $\mu$ . To do so an initial value is assigned for both parameters  $P_b$  and  $P_{HB}$  (e.g., 0.3), then we run the analysis to obtain  $P_b$  from (6.28) and  $P_{HB}$  from (6.30). Then we run the analysis again but now using the new values of  $P_b$  and  $P_{HB}$  in order to calculate  $\lambda_H$  and  $\mu$ . The procedure repeats until  $P_b$  and  $P_{HB}$  converge.

## 6.9 Performance

To obtain numerical results of the handover-based MAC protocol the LAN specifications in Table 6-1 are used. As in Ch. 5 the radius of a cell is taken to be  $r = 3$  meters, this is a satisfactory size between the interference-limited region and noise-limited region according to [57]. To prevent performance degradation due to cochannel interference the channel reuse factor is taken to be  $J = 7$ , this results in a distance of 13.7 meters between two neighbouring cells. Such a distance is large enough to ignore cochannel interference because the latter is much lower than the noise produced by the ambient and artificial light sources. Using OOK modulation at a transmission bit rate  $\leq 10 \text{ Mb/s}$  the intersymbol interference effects due to



multipath phenomenon can be ignored [53]. Therefore, ensuring that the physical layer transmits and receives data at a desired BER, usually  $10^{-9}$ , the IR-LAN performance depends mainly on the MAC protocol structure. The average duration of speech activities taken from [108] and video activities (e.g. videoconference) taken from [93] are shown in Table 6-1.

Variable	Notation	Value
Channel bit rate	$R_c$	8 Mb/s
Source bit rate	$R_s$	64 kb/s
Uplink/downlink frame duration	$T_f$	1 ms
R slot duration	$R$	150 bits
ACK slot duration	ACK	$R+T_d(N+1)$
Downlink timing signal	$T_d$	4 bits
Speech mean ON duration	$t_1$	1 s
Speech mean OFF duration	$t_2$	1.35 s
Speech cell maximum time delay	$D_{max}$	20 ms
Channel reuse factor	$J$	7
Header of an IWC (compressed ATM header, DLC field, MAC field, guard band)	$H$	65 bits
Minimum tolerant time between two consecutive handovers	$t_{min}$	1 s
TU speed	$v$	1 m/s
Call duration	$T_r$	2 min
Number of cells	$Z$	4
Total number of TUs	$T$	30
Maximum supported number of TUs during a channel frame	$M_{max}$	8
Mean sojourn time of a TU within a cell	$T_h$	5 s

Table 6-1 System parameters

The bandwidth allocated during the uplink/downlink frame within a cell is again given by



$$B_c = (T_{cf} R_c) / 2 T_f \quad (6.32)$$

This bandwidth can be used to serve constant bit rate (CBR), variable bit rate (VBR), unspecified bit rate (ABR) and available bit rate (UBR) ATM services. For ABR/UBR services, (such as text) free slots are assigned by means of a dynamic slot allocation algorithm.

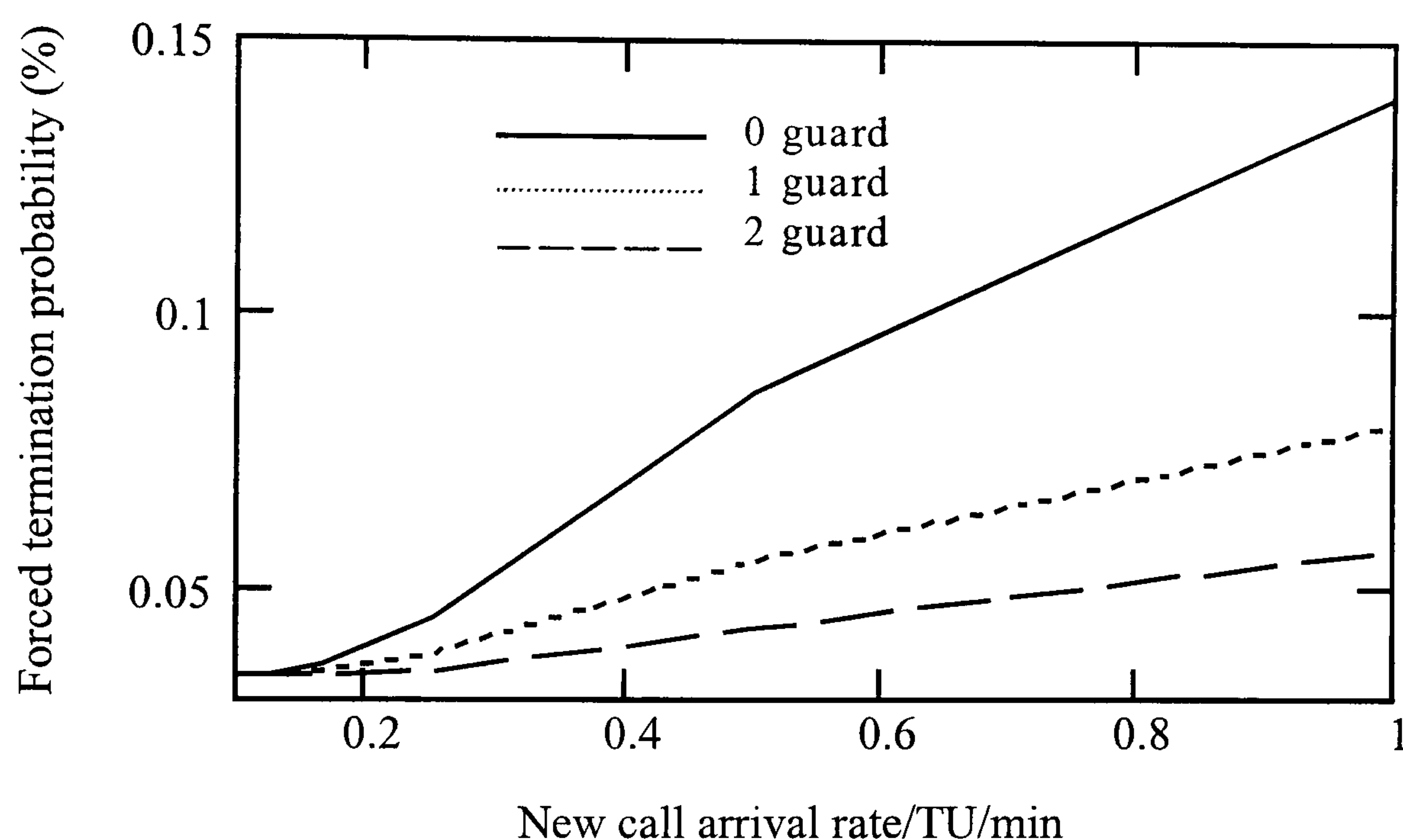


Fig. 6-3 Forced termination probability versus new call arrival rate /TU/min

Figures (6.3-6.7) show the performance characteristics associated with the hybrid handover priority scheme. Fig. 6-3 clearly shows the advantage of the scheme when compared to the nonpriority scheme, zero guard case in the figure. When the guard group is increased from zero to two the forced termination probability is correspondingly decreased at any specific value of the new call arrival rate. For all

cases the forced termination never gets zero but instead its lowest value is a floor level which is due to minimum tolerant time ( $t_{\min}$ ) between two consecutive handovers.

As mentioned before there is a trade-off effect present in guard schemes among the two parameters of new call blocking ( $P_b$ ) and forced termination ( $P_F$ ). Therefore, when the  $P_F$  decreases the  $P_b$  increases. This is because by increasing the guard group the number of available places for new calls is reduced and this in turn will cause an increase of  $P_b$ . This effect is clearly illustrated in Fig. 6-4. Also it is seen that the three curves exhibit almost a constant difference between each other as the call arrival rate increases, this difference starts from as low arrival rates as 0.1 and it shows the immediate effect of the guard group on the MAC performance.

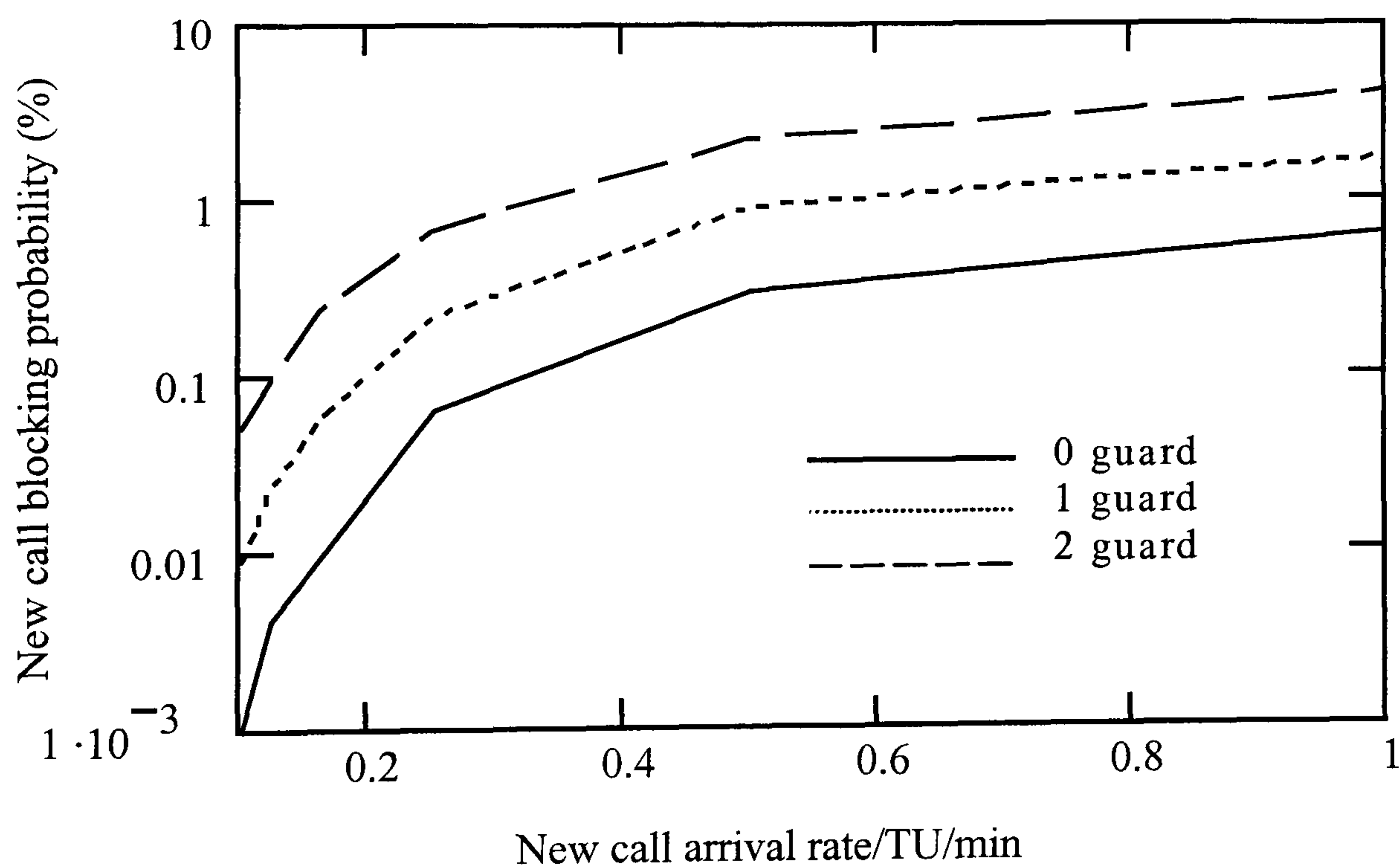


Fig. 6-4 New call blocking probability versus new call arrival rate /TU/min



When a call is assigned a handover request, a place in the handover group is held until the talkspurt, which happened to be served while handover was requested, is finished. The next talkspurt of the call can request a reservation only in the common group. Thus, during a handover procedure the handover group assists to finish servicing the talkspurt that initiated the handover requested and then the common group will be responsible to serve the rest of the call. Hence, most part of the packet dropping probability during the dwell time of a TU in the cell is mainly due to traffic in the common group. So, by increasing the handover group the  $P_b$  increases, implying less TUs served by the common group and this in turn decreases the magnitude of both average packet dropping probability ( $P_{drop}$ ) and average access delay ( $\bar{D}$ ). This is observed in Fig. 6-5 and Fig. 6-6 respectively. The waiting time for a TU to get served increases as the new call arrival rate increases and when a voice packet experiences a delay service longer than  $D_{max}$  it is dropped. Speech  $P_{drop}$  with which speech quality degradation is almost not perceptible must be  $\leq 1\%$  [75].

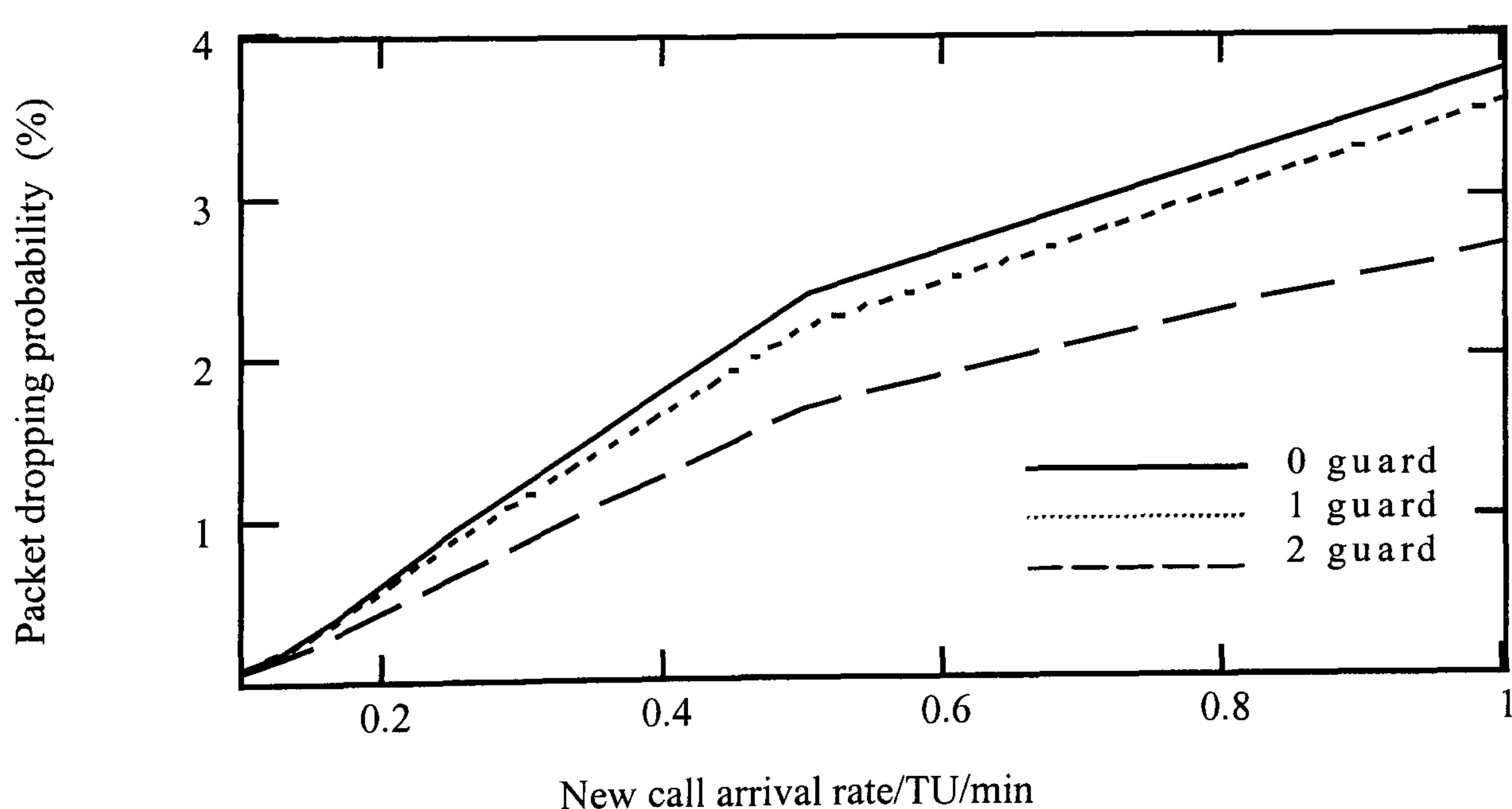


Fig. 6-5 Packet dropping probability versus new call arrival rate /TU/min

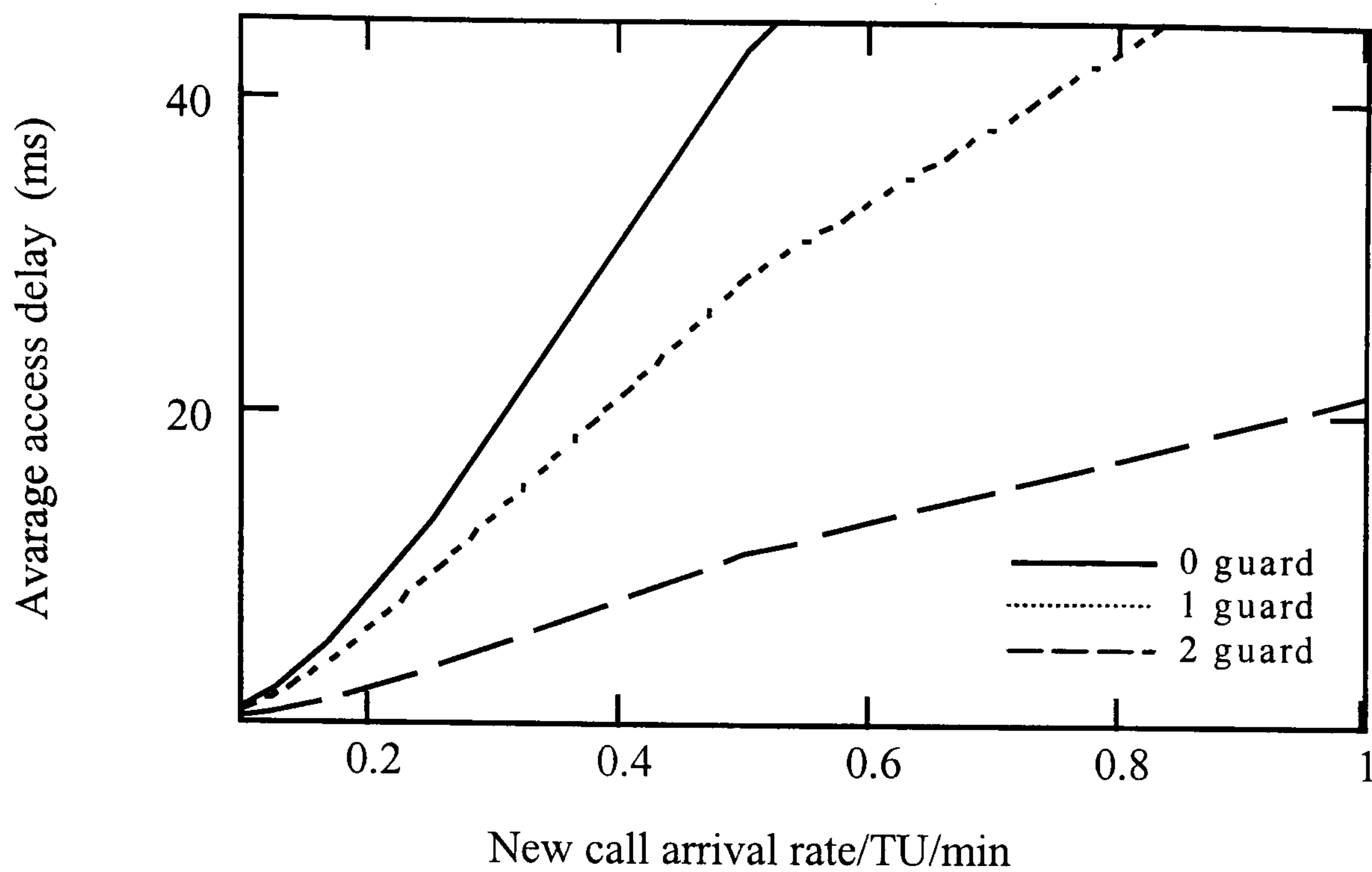


Fig. 6-6 Average access delay versus new call arrival rate /TU/min

In Fig. 6-7 it is shown that for various values of the guard group the throughput parameter almost overlaps with this of the nonpriority scheme. Because the factor of improvement of  $P_F$  is smaller than the factor of degradation of  $P_b$  and because throughput is directly related to these two parameters, one would expect to get a lower value of throughput while the guard group increases. However, this does not happen for arrival values smaller than 0.6. A handover call always looks at the common group for a place first and there will be many instances when it will occupy a place in this group, despite the fact that there are available places in the guard group. When the size of the guard group increases the possibility of a handover request to find a free place in the common group decreases hence, a place in the guard group is most possibly assigned. Therefore, the throughput remains almost the same for all cases since in any case the handover request is served. This feature



demonstrates a general improved performance of the network. It is suggested that further work on the MAC protocol including dynamic allocation of the places in both groups will result in a further improvement of the system capacity.

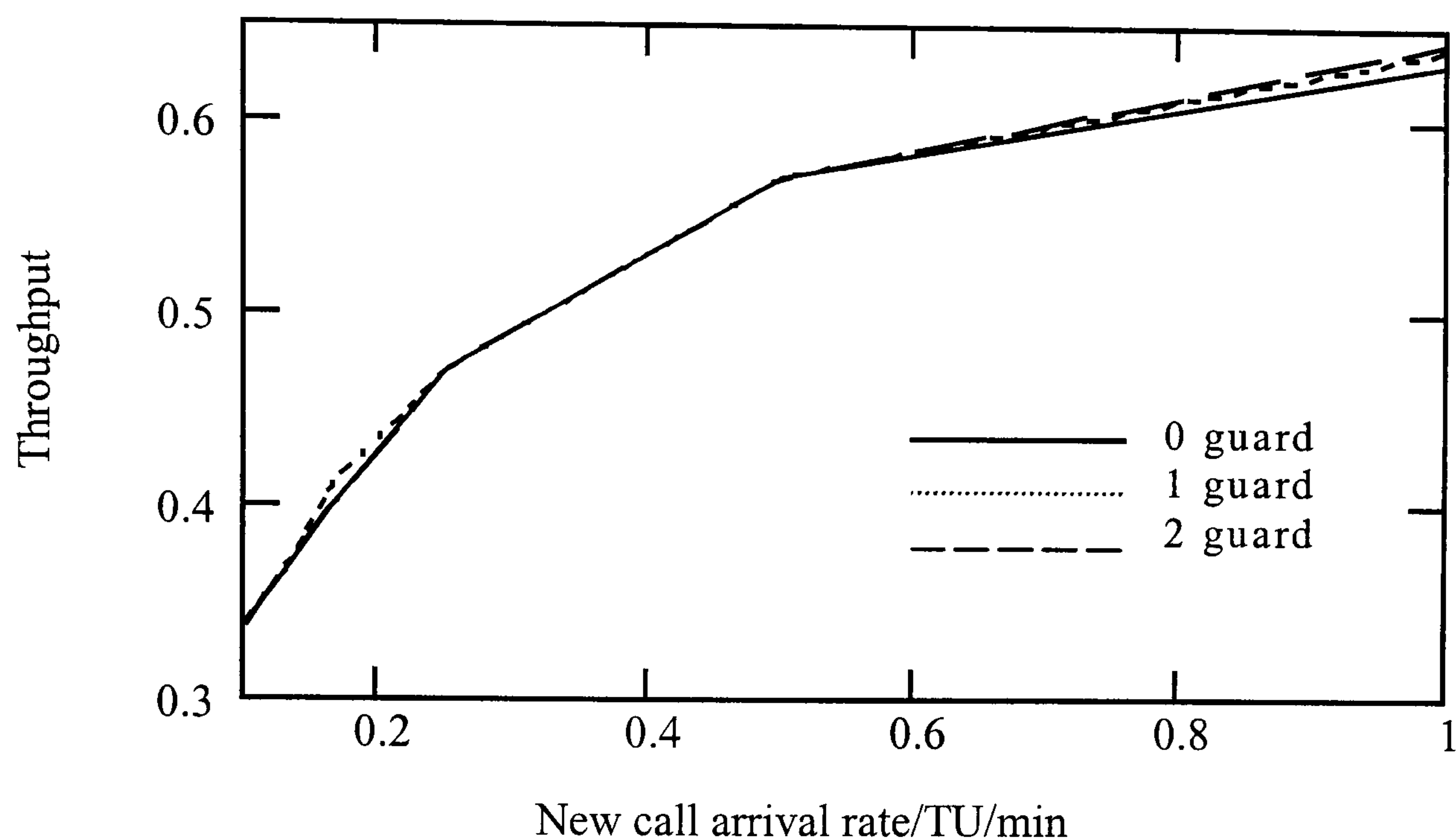


Fig. 6-7 Throughput versus new call arrival rate /TU/min

## 6.10 Summary

In this chapter, a hybrid handover priority-based MAC protocol to support ATM voice services over the IR wireless LANs was proposed. Carrying out mathematical analysis its performance measures were derived for fixed slot assignment. Using the information in link design a LAN example where VBR voice TUs are served was presented. It was shown that the forced termination probability was improved over the nonpriority handover scheme in return of increasing the new call blocking

probability. For  $P_{\text{drop}} = 1\%$  the new call blocking probability is less than 1% while the forced termination probability is less than 0.05 %, these values exhibit a very satisfactory performance. Moreover, the value of the throughput parameter has just slightly changed over the nonpriority scheme only for high new call arrival rates, this fact demonstrates a general improved performance of the network.



# CHAPTER SEVEN:

## SIMULATION OF THE MODEL

## 7 SIMULATION OF THE MODEL

### 7.1 Introduction

In this chapter a simulation process is used to evaluate the system performance measures such as packet dropping probability, throughput, average access delay, statistical multiplexing gain and compare them with the mathematical evaluation in Ch. 5. In digital communication networks the transmission of a bit, a byte or a fixed-size cell can be considered as the basic unit of time or the basic event. Similarly, in the examined system the arrival and departure process fit in with the arrivals and departures of speech packets. Therefore, the transmission of a speech packet is considered as the basic event and the packet duration is considered as the basic time unit.

There are two basic ways to simulate such a digital communication network: the discrete time process and the discrete event process [116]. In the first one the simulator counter increases by one basic unit time regardless of whether new packets have arrived. In discrete event process the simulator counter is advanced to the next time where there is change in the state of the system, e.g. packet arrival. Although the latter process can run more quickly because it will cut out the time in which there is not transmission. We will use the former process to observe the packet dropping probability, the system throughput, and the statistical multiplexing gain. This is because it is easier to implement for these particular parameters and to understand since it models the buffer in a TU from the point of view of the server process, i.e.



considering both arrivals of talkspurts and silences. However, to observe the average access delay is a time consuming process and therefore the discrete event process is used.

The rest of this chapter is organised as follows. The next section shows the basic block diagrams of the simulation model. Section 7.3 deals with the modelling of the speech source considering Poisson distributed packet arrivals while in section 7.4 the MAC mechanism is presented and analysed. Finally, in section 7.5 simulation results are obtained for packet dropping probability, throughput, average access delay and statistical multiplexing gain are compared with those taken by mathematical analysis in Ch. 5. To implement the simulation model the mathematical program MATHCAD 8.0 Prof. by MathSoft, Inc. was used.

## **7.2 Block Diagram of the Simulation Model**

The discrete time model, which is shown in Fig. 7-1, can be considered of two main phases, the traffic generation (talkspurts and silences) and the MAC mechanism. The process of the first phase comes down to the analysis where the time axis, consisting of talkspurts and silences, is segmented into a contiguous sequence of basic time units. To implement this, the Monte Carlo approach is [106,116-118] used that is one in which it is necessary to generate at least one stream of random numbers from some specified probability distribution. We know that the inter-arrival and service times of a VBR speech source follow the exponential distribution or, equivalently,

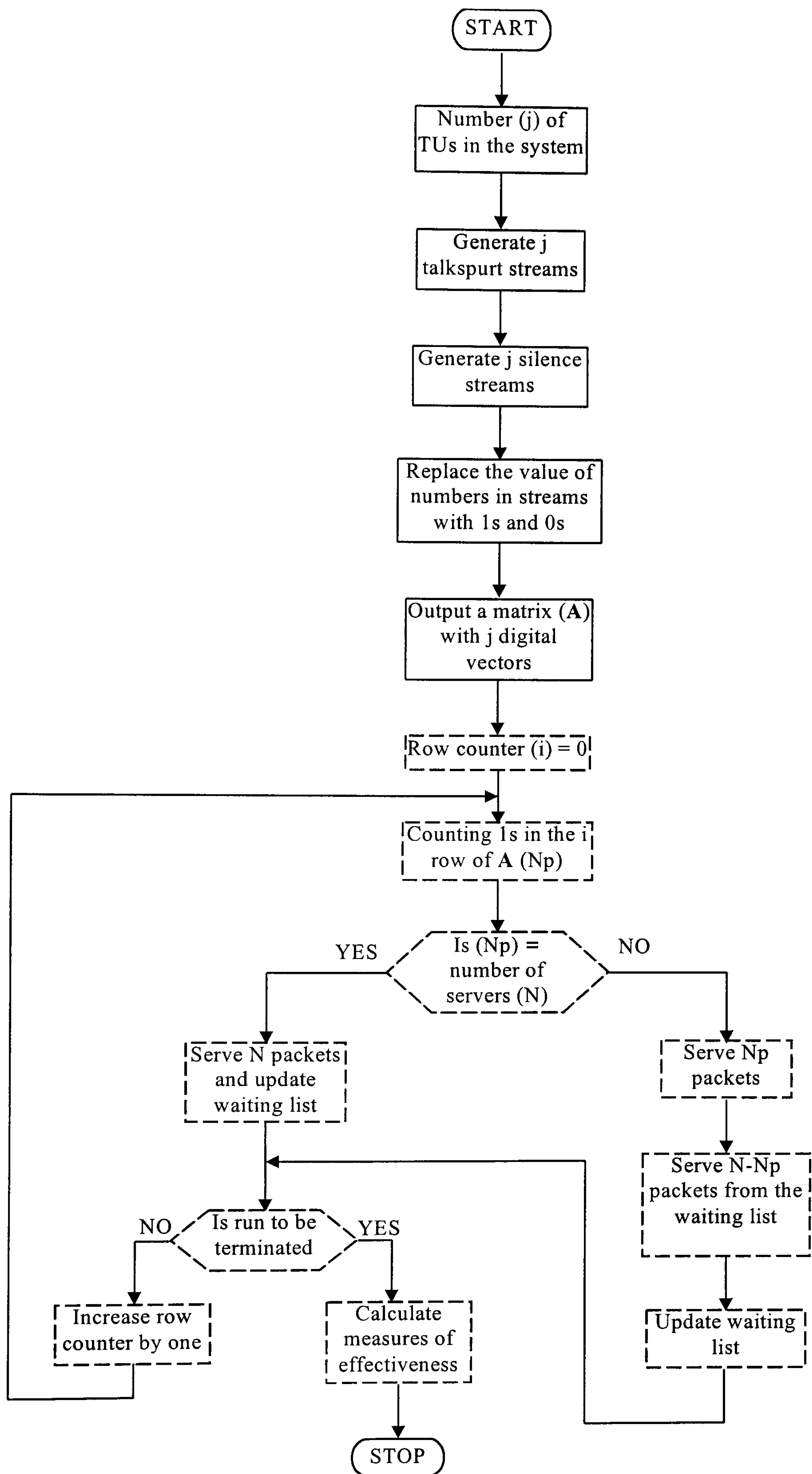


Fig. 7-1 Basic block diagram of the discrete time simulation model



the number of arrivals and number of service completions of speech packets follows a Poisson distribution. Therefore, the generated random numbers must follow the exponential distribution. Each number represents a talkspurt or silence interval and its value denotes the number of basic time units contained in the interval.

The talkspurt stream is generated separately from the silence stream, hence they are statistically independent. Therefore, for each TU (a TU utilises a slow speech activity detector) the simulation process generates a stream of talkspurts and a stream of silences. After rearranging both streams on a single time axis so that the first silence is followed by the first talkspurt and so on the basic time units of talkspurts are marked as 1s while the basic time units of silences are marked as 0s.

The vector of binary elements produced represents the output of a TU in terms of arrival and departure speech packets. For more than one TUs the program generates a matrix (A) in which each vector represents a particular TU.

The MAC mechanism phase where in the block diagram are shown as dashed lines, deals with the service of speech packets each time the row counter increases by one. The served packets can be newly arrived packets or packets that have been waited, in the previous rows, for less than a time limit ( $D_{\max}$ ).

Initially, the simulation process observes the number of packets ( $N_p$ ) in each examined row of the matrix (A) and then the result ( $N_p$ ) is compared with the

number of servers ( $N$ ). This comparison results in two different ways in which the simulation can progress:

1. If the number of packets is smaller than  $N$  then all the packets of the examined row get served. However, because  $N - N_p$  servers are free the counter will go backwards so many time units as they do not exceed  $D_{\max}$  and serve  $N - N_p$  packets. These packets were left in previous rows due to lack of available servers,  $N_p > N$ . When the service of the waiting packets is finished the waiting list is updated and the counter returns to the row in which it was before move backwards.
2. If the number of packets is greater than the number of servers then  $N$  packets are served and the rest are placed in the waiting list.

In any case, if at the end there are more rows to be examined then the counter increases by one and the procedure repeats, otherwise the run stops. During the run quantities of interest such as idle time, waiting time and packets left in the waiting lists are monitored and recorded so that parameters of the MAC effectiveness can be calculated.

The discrete event model to observe the average access delay, shown in Fig. 7-2, is also considered in two phases. The traffic generation phase, which is similar to that of the discrete time model, and the MAC protocol phase (dashed line text boxes) that is responsible to serve each TU in the system regardless of its waiting time. Obviously in a real system a TU that waits more than a certain time period without having accessed the system will switch off.



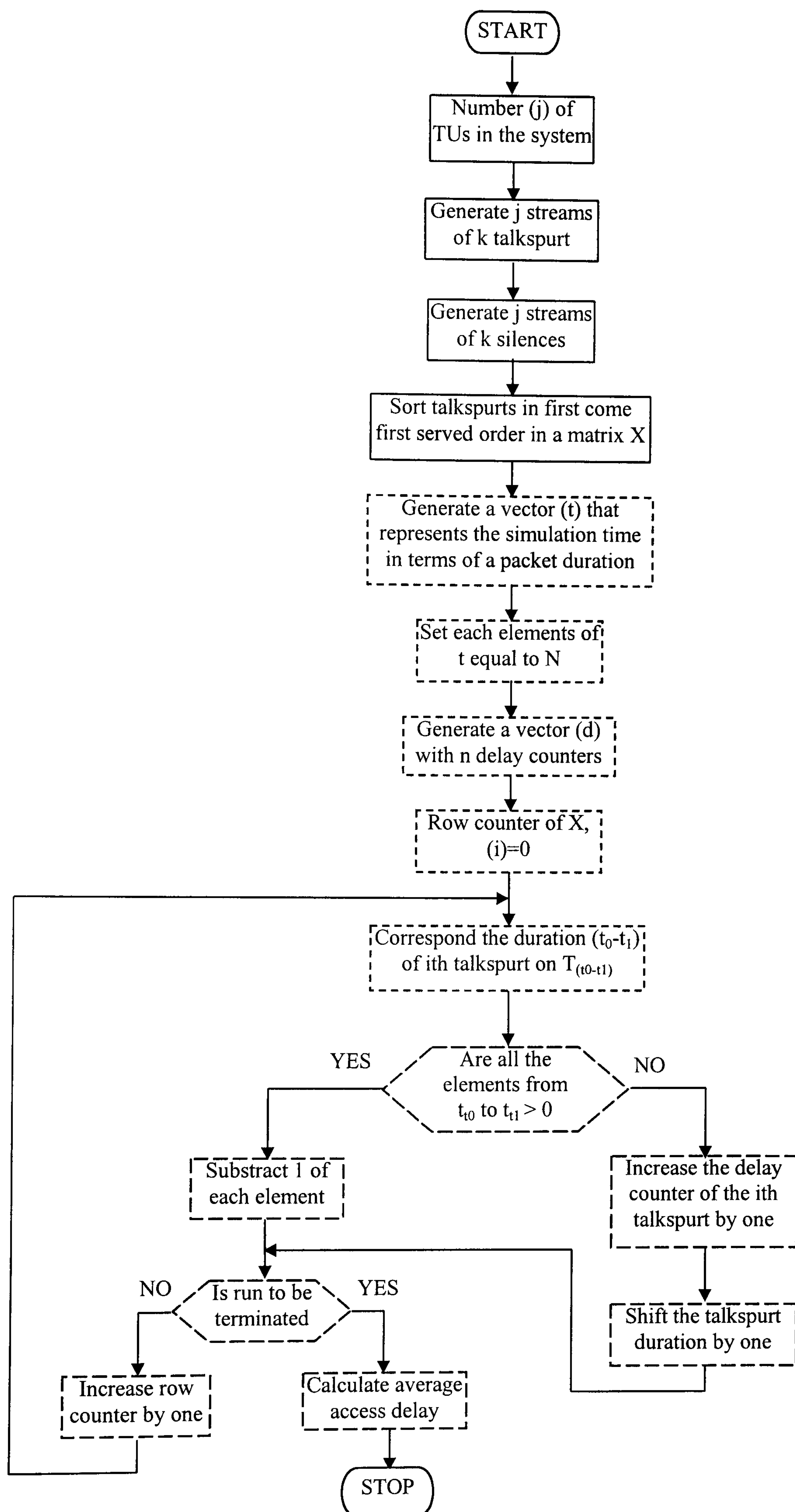


Fig. 7-2 Basic block diagram of the discrete event simulation model

### 7.3 The Source

Initially, we must generate two streams of random numbers that follow the exponential distribution. This is achieved by using the random-number-generator function from the MATHCAD program library

$$\sigma^{(j)} := \text{rexp}(k, \mu) \quad (7.1)$$

The function returns  $j$  statistically independent vectors of  $k$  random numbers that follow the exponential distribution. Each vector represents talkspurt intervals of a TU. Where  $\mu$  is the mean service rate of talkspurt and is given by

$$\mu := \frac{1}{t_1} \quad (7.2)$$

Where  $t_1$  is the mean talkspurt duration. Each talkspurt duration is divided by the packet duration ( $T_p$ ), which is the basic time unit for the discrete time simulation model, in order to generate a vector of speech packet arrivals.  $T_p$  is given by

$$T_p := \frac{R_c \cdot T_{cf} - H \cdot N}{N \cdot R_s} \quad (7.3)$$

The random numbers in the second stream represent silence intervals and are generated using again the random number generator from the MATHCAD program library



$$\tau^{\langle j \rangle} := \text{rexp}(k, \lambda) \quad (7.4)$$

With

$$\lambda := \frac{1}{t_2} \quad (7.5)$$

Where  $\lambda$  is the mean arrival rate of talkspurts and  $t_2$  is the mean silence duration time. Again the silence time intervals are segmented into basic time units by dividing each one with the packet duration ( $T_p$ ). In (7.1) and (7.4) the parameter  $k$  that specifies the number of random observances in each vector ( $j$ ) is taken to be  $k = 2000$ . This value results in each vector a mean value that has a deviation about 0.2% of the theoretical expected value. A smaller deviation can be achieved by increasing the value of  $k$ , however higher values of  $k$  often result in a large (A) matrix which can not be held by the MATHCAD.

We recall again that talkspurt duration is equivalent to service time of a message while silence duration is equivalent to inter-arrival time of messages. Therefore  $\sigma^{\langle j \rangle}$  is an array that represents talkspurt arrivals segmented into basic time units (speech packets) and  $\tau^{\langle j \rangle}$  is an array that represents silence arrivals segmented into basic time units. In order to generate the output of the speech source these two arrays must be combined onto one time axis, so that after the first talkspurt the first silence arrives, then the second talkspurt arrives, then the second silence arrives and so on. This algorithm is depicted by the flow chart shown in Fig. 7-3.

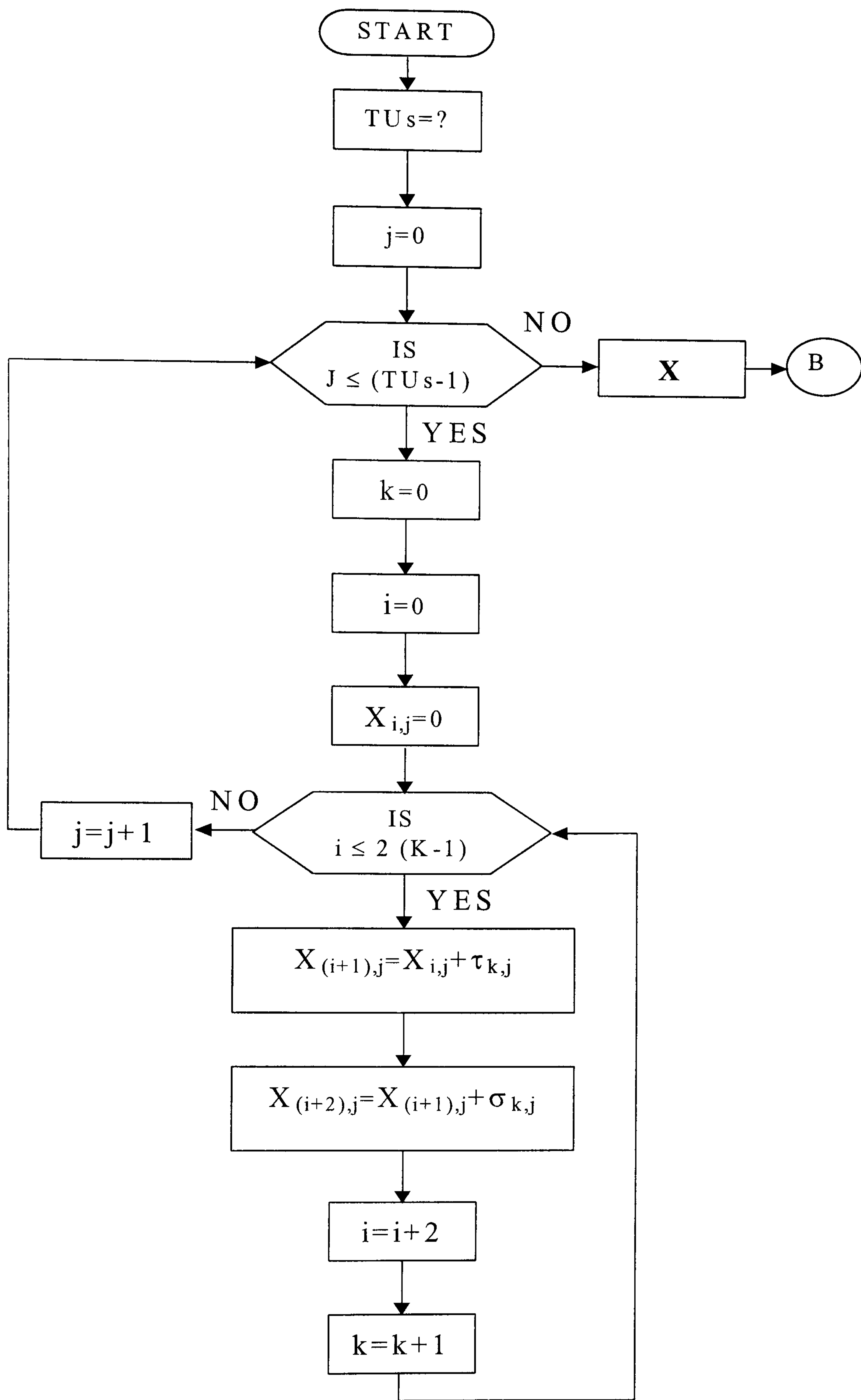


Fig. 7-3 Flow chart for arranging talkspurt and silence streams of each TU on the same time axis



The next and final part of the source model is an algorithm that replaces the value of each random number with 1s and 0s. It will mark as “1” the speech packets in the talkspurts and as “0” the basic time unit in the silences. The resulting vector represents the output of a TU in terms of arrived and departed speech packets. The flow chart of the algorithm is shown in Fig. 7-4. The actual MATHCAD code of the voice source, algorithms of Fig. 7-3 and Fig. 7-4, appears in Appendix A.

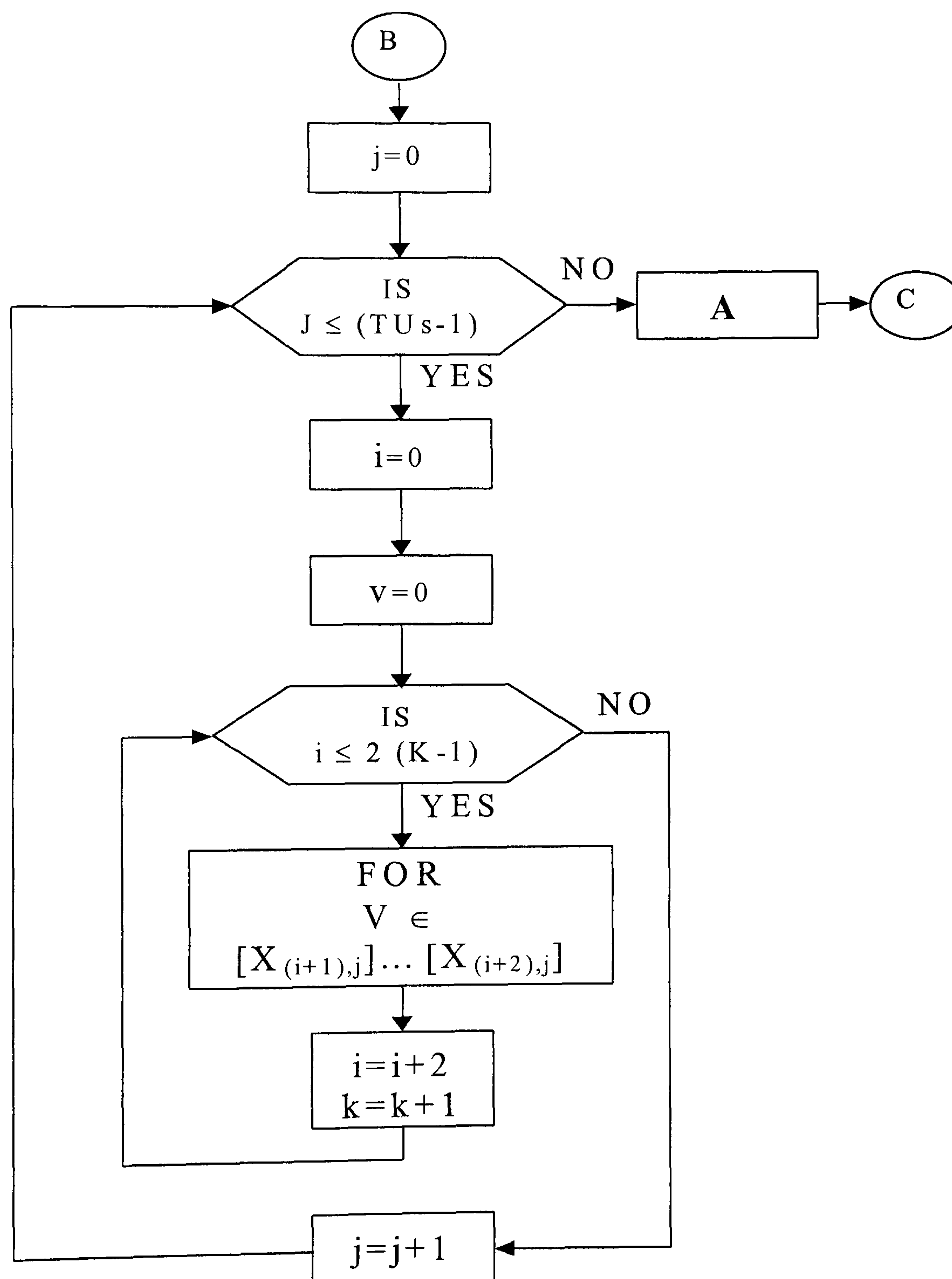


Fig. 7-4 Flow chart that replaces the value of each random number with 1s and 0s.

## 7.4 The MAC Protocol

This section is devoted to the implementation of the flow chart of the MAC protocol mechanism which was described in Ch. 4. As mentioned in the beginning of the chapter this phase of the simulation model deals with book keeping aspects such as how many new packets arrive every time the row counter increases, how many of them get served, how long do they have to wait to be served. Every time the row counter increases by one basic time unit or event the next row of the traffic array is examined and any new arrivals, departures or packet losses will update the records. At the end of the run the effectiveness of the system can be derived according to these recorded data.

Firstly, we will examine the flow chart of the discrete time MAC mechanism which is used to observe the packet dropping probability, system throughput and statistical multiplexing gain and is illustrated in Fig. 7-5. At the beginning the program calculates the number of rows ( $N_r$ ) that correspond to a simulation time equal to  $D_{\max}$ . This information is essential for the row counter when it moves backwards in order to serve waiting packets. For instance, using the system parameters of Table 1 in Ch. 5 we find that  $N_r = 3$ , beyond this number all the packets have been waiting more than  $D_{\max}$  time and therefore are ignored. After this simple but essential calculation the simulation starts running from the  $N_r^{\text{th}}$  row of the matrix. In the simulation algorithm the number of each examined row is denoted by the index  $i$ , for instance the simulation always starts from the  $i = N_r^{\text{th}}$  row. If the packets in the row are more than the servers then  $N_p - N$  packets are placed in the bin ( $\text{BIN}_i$ ) and the



counter moves on to the next row ( $i+1$ ). Here we must mention that each row has its own bin where waiting and dropped packets are stored. In case where the packets are less than the number of servers then  $BIN_i$  gets the value zero and the program registers  $N-N_p$  free servers (FS) to serve waiting packets in the bins of previous rows. Therefore the counter moves back to  $(i- N_p)^{th}$  row and looks for waiting packets in the bin.

1. If the packets in the bin are more than the free servers then FS packets are served and the rest are left in the bin,  $BIN_{(i-N_p)} = [ BIN_{(i-N_p)} - FS ]$ . Since the counter will not serve the same row again, the left packets are said to be speech dropped packets. The program records that no more free servers left ( $FS_i = 0$ ) and it moves on to the  $i+1$  row. Recording the number of the unused free servers every time before the program moves to the next row the throughput of the system can be calculated at the end of the run according to the definition in (5.27).
2. If the number of packets in the  $(i- N_p)^{th}$  bin is less than FS then all the packets get served, the bin gets the value of zero, and the program updates the number of free servers,  $FS = FS - BIN_{(i-N_p)}$ .

The counter now moves to  $i-( N_p-1)^{th}$  row and the procedure from stage 1 repeats till it moves to  $i+1$  row.

The program goes through the whole matrix and at the end outputs two values: the total value of the packets left in all bins (TBIN) and the total value of the unused servers (TFS) during the whole simulation. Based on these two values the system throughput and the packet dropping probability can be revealed. The MATHCAD code of the MAC protocol appears in Appendix B.



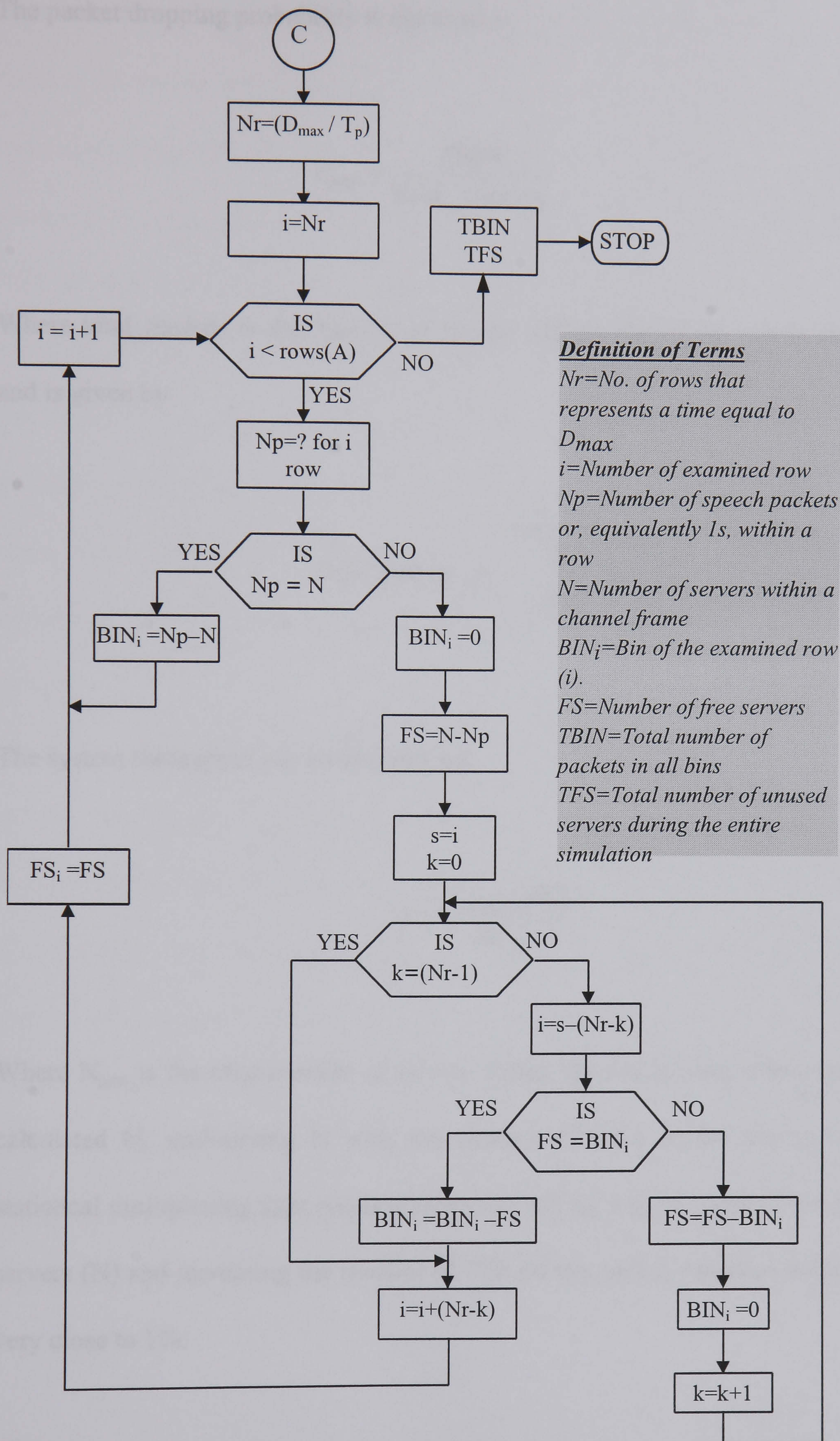


Fig. 7-5 Flow chart diagram for the discrete time MAC mechanism



The packet dropping probability is obtained as

$$P_{\text{drop}} = \frac{\text{TBIN}}{\text{total\_packets}} \quad (7.6)$$

Where total\_packets is the number of speech packets during the whole simulation and is given by

$$\text{Total\_Packets} := \sum_{j=0}^{\text{TUs} - 1} \Sigma A^{<j>} \quad (7.7)$$

The system throughput can be obtained by

$$\eta = \frac{N_{\text{total}} - \text{TFS}}{N_{\text{total}}} \quad (7.8)$$

Where  $N_{\text{total}}$  is the total number of servers during the whole time simulation and is calculated by multiplying  $N$  with the number of rows of the matrix (A). The statistical multiplexing gain (G) is obtained by setting a fixed value of the available servers (N) and increasing the number of TUs till the packet dropping probability is very close to 1%.

$$G = \frac{\text{TUs}_{\text{max}}}{N} \quad (7.9)$$

The flow chart of the discrete event MAC mechanism to observe the average access delay is illustrated in Fig. 7-6. Initially, the program sorts the talkspurts in a first come first served fashion and outputs them in the matrix  $X$ . Then the program generates two new vectors denoted as  $t$  and  $d$ . The length of the vector  $t$  is equal with the number of speech packets that must be served during the run time of the simulation. Thus its length can be determined by obtaining the maximum value of the matrix  $X$ . Each element of  $t$  initially takes the value of the total available servers ( $N$ ) in the system. The vector  $d$  serves as a delay counter for each talkspurt when it is not served immediately. Its length is equal to the number of talkspurts during the simulation, which is the number of rows in matrix  $X$ , and each element is initially set zero.

As the simulation starts running it will firstly examine the duration of the first arrived talkspurt and projects it onto the vector  $t$ . For instance, lets assume that the first talkspurt has a length from 5-15 packets which means that initially 5 silence packets were transmitted then 15 speech packets, then again a number of silence packet follows and so on. Now the simulation process must examine if there are available servers to serve the talkspurt at its arrival time. This is achieved by observing the vector  $t$  and particular if its elements from 5 to 15 have a value higher than 0. The result of this comparison is stored in the variable  $q$  in the simulation flow chart.



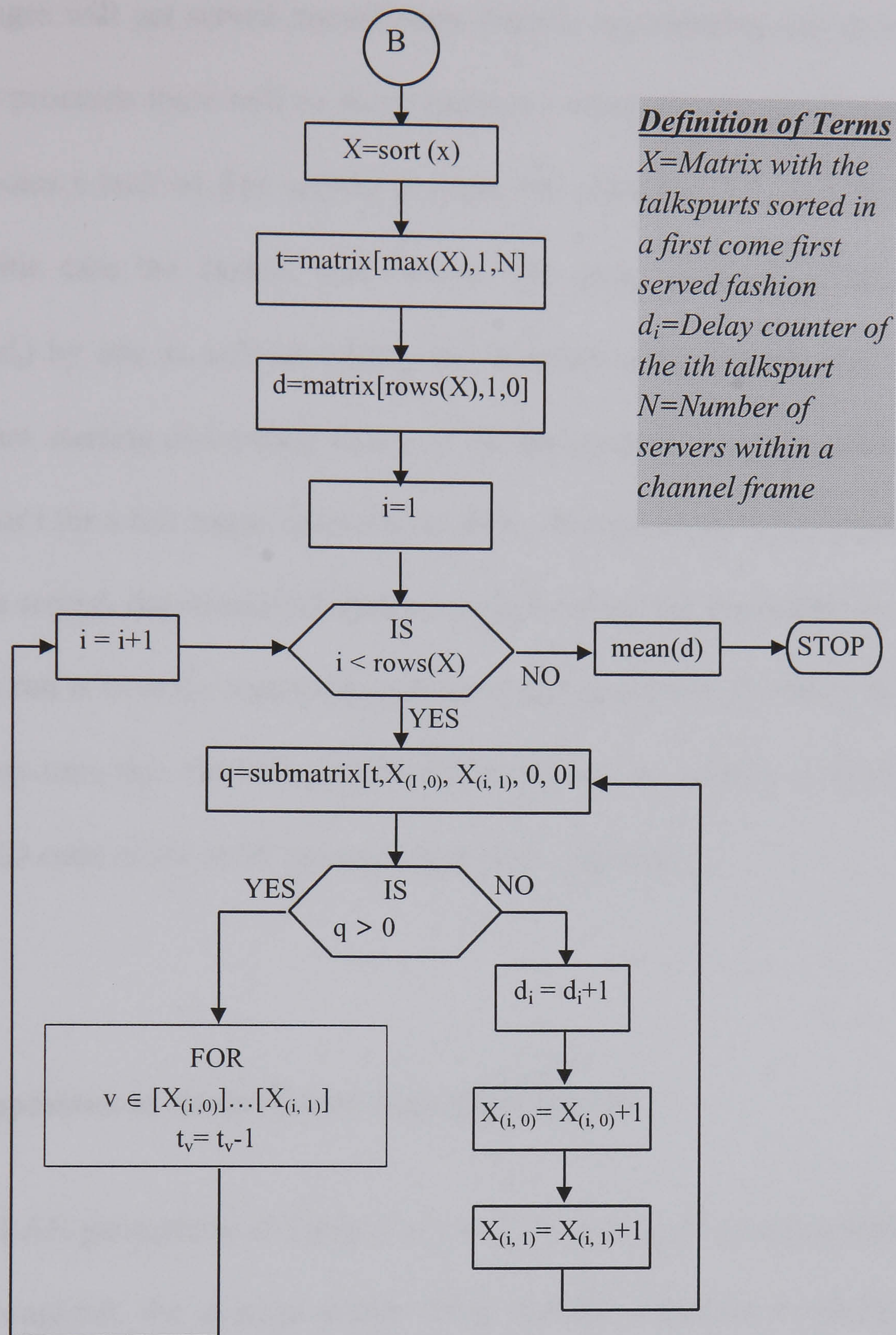


Fig. 7-6 Flow chart diagram for the discrete event MAC mechanism

Therefore if  $q$  is not zero it means that the required number of servers to serve the talkspurt is available and consequently the talkspurt will get served. Then the process will update the vector  $t$  by subtracting 1 from the elements 5 to 15 and will move to the next talkspurt by increasing the row counter ( $i$ ) by one. Obviously the



first messages will get served immediately without experiencing any delay. As the simulation proceeds there will be many instances where the variable  $q$  will be zero which denotes a lack of free servers to serve the particular talkspurt at its arrival time. In this case the system will increase the delay counter of the particular talkspurt ( $d_i$ ) by one as well as shifting the duration of the talkspurt by one. Now with the new starting and ending values of the talkspurt the process will look again at the vector  $t$  for a full length of available slots. This procedure is repeated until the talkspurt is served, the simulation then proceeds to serve the next talkspurt. Once the simulation run is over the mean value of the vector  $D$ , which represents the average access delay time that the TUs experienced to access the system, is observed. The MATHCAD code of the MAC protocol appears in Appendix C.

## 7.5 Comparison of Analysis and Simulation Results

Using the LAN parameters of Table 1 in Ch. 5 the packet dropping probability, the system throughput, the average access delay and the statistical multiplexing gain were simulated when only voice TUs are in the system. To obtain results as accurately as possible and display them within confidence intervals (CI) of 95% the simulation run repeated 10 times. Fig. 7-7 depicts the results of packet dropping probability from both simulation and analysis. It is observed that the results of both processes are fairly close to each other. The fact that there is a small magnitude difference between the two curves is because the simulation runs for a tolerant speech delay time ( $D_{\max}$ ) of 18 ms instead of 20 ms, which is the theoretical value.



This happens because the row counter moves backwards three rows ( $N_r = 3$ ), or equivalently three basic time units, every time it is called to serve waiting speech packets. Hence, from (7.3) three basic time units equal to a real time of 18 ms. To eliminate this problem we must consider a shorter basic time unit, such as a byte or a bit. However, such a modification will increase complexity and running time of the simulation.

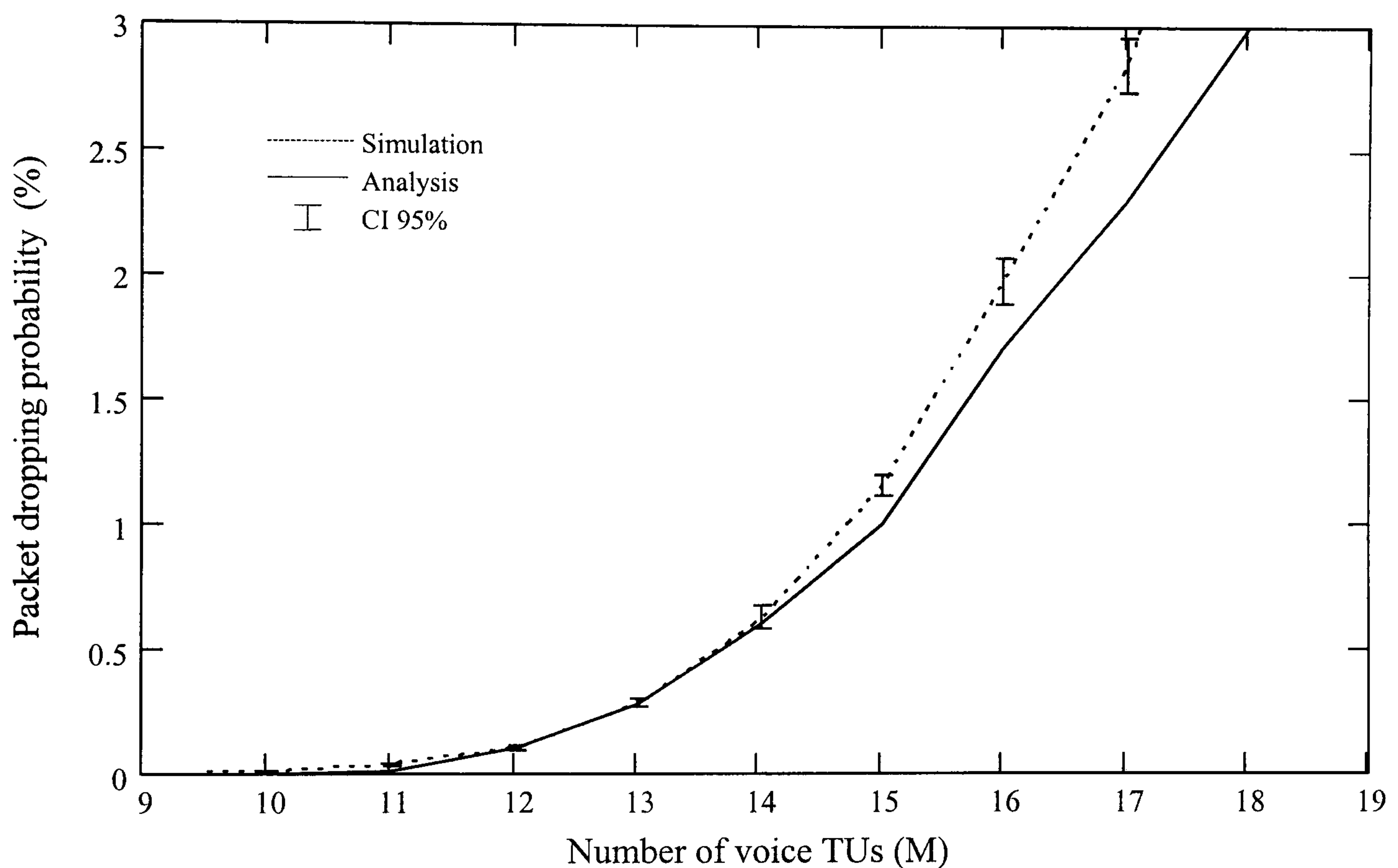


Fig. 7-7 Simulation and analysis results for the packet dropping probability

System throughput results of both simulation and analysis are shown in Fig. 7-8. It is observed that up to 16 TUs in the system the simulation results overlap the analysis ones, however for more than 16 TUs a difference between the two curves is exhibited. This difference is explained as follows. When more than 16 TUs are in the

system and the parameter of random observances ( $k$ ) is equal to 2000 then the data generation algorithm results in a large matrix ( $A$ ), which cannot be held by the MATHCAD. To successfully run the simulation the variable  $k$  was decreased to 1500 for up to 19 TUs, and to 1000 for up to 21 TUs. By decreasing the value of  $k$  the produced digital vectors of talkspurts and silences exhibit mean values that have a deviation of about 1% of the theoretical expected ones. Hence, the magnitude difference of the throughput between the simulated and analysis results.

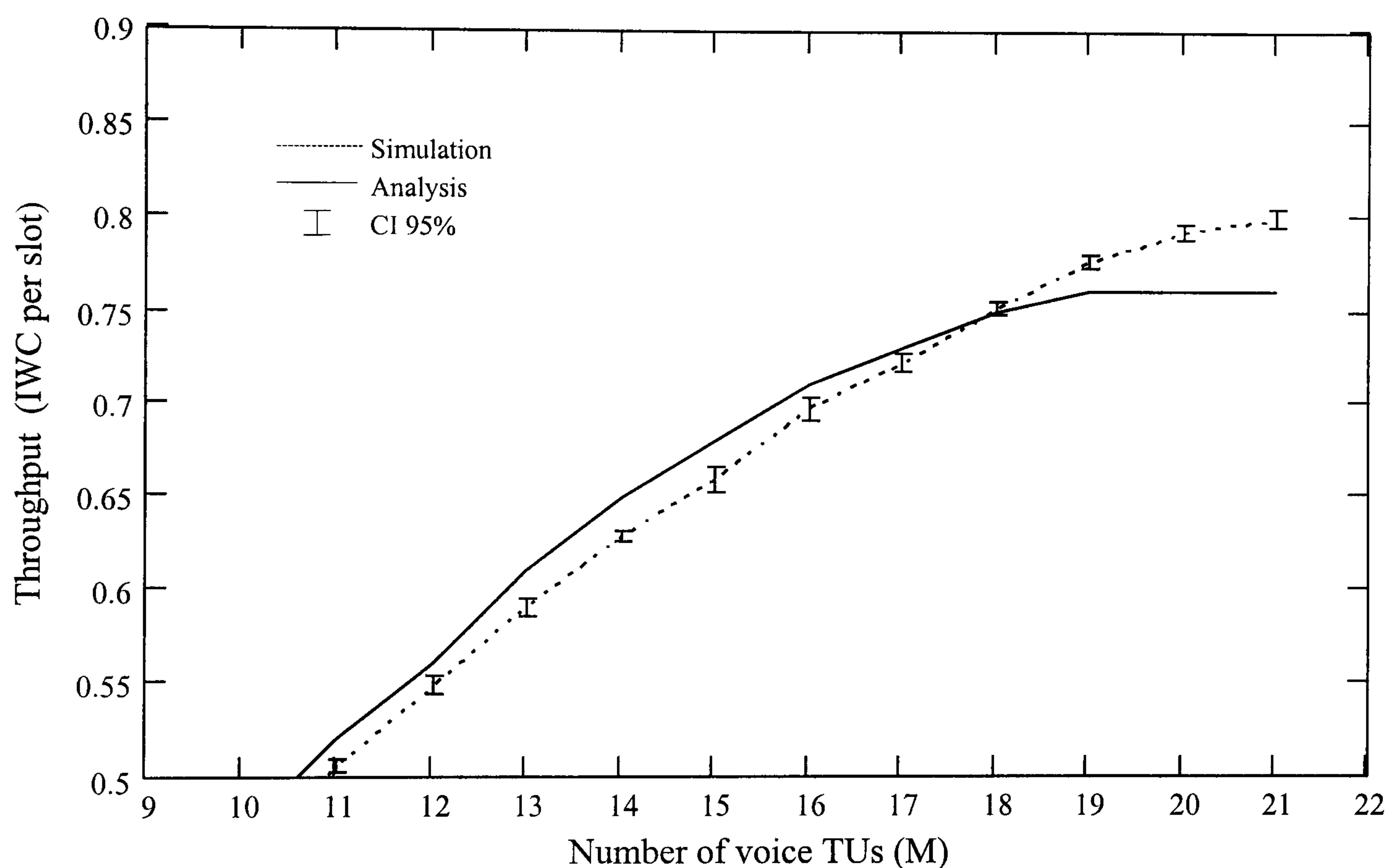


Fig. 7-8 Simulation and analysis results for the throughput system

Average access delay results from both simulation and analysis are depicted in Fig. 7-9. It is shown that when up to 16 voice TUs are in the system the results of both processes are overlap, however when increasing the number of TUs beyond 16 a difference between the two curves is exhibited and the 95% confidence intervals (CI)



increase. This is due to the events occurring during the simulation. For instance, there were always a few messages that would experience very long delays (up to 10 minutes), in the real world a TU would not wait more than 10 to 15 seconds to be connected. This produces a significant rise in the average access delay.

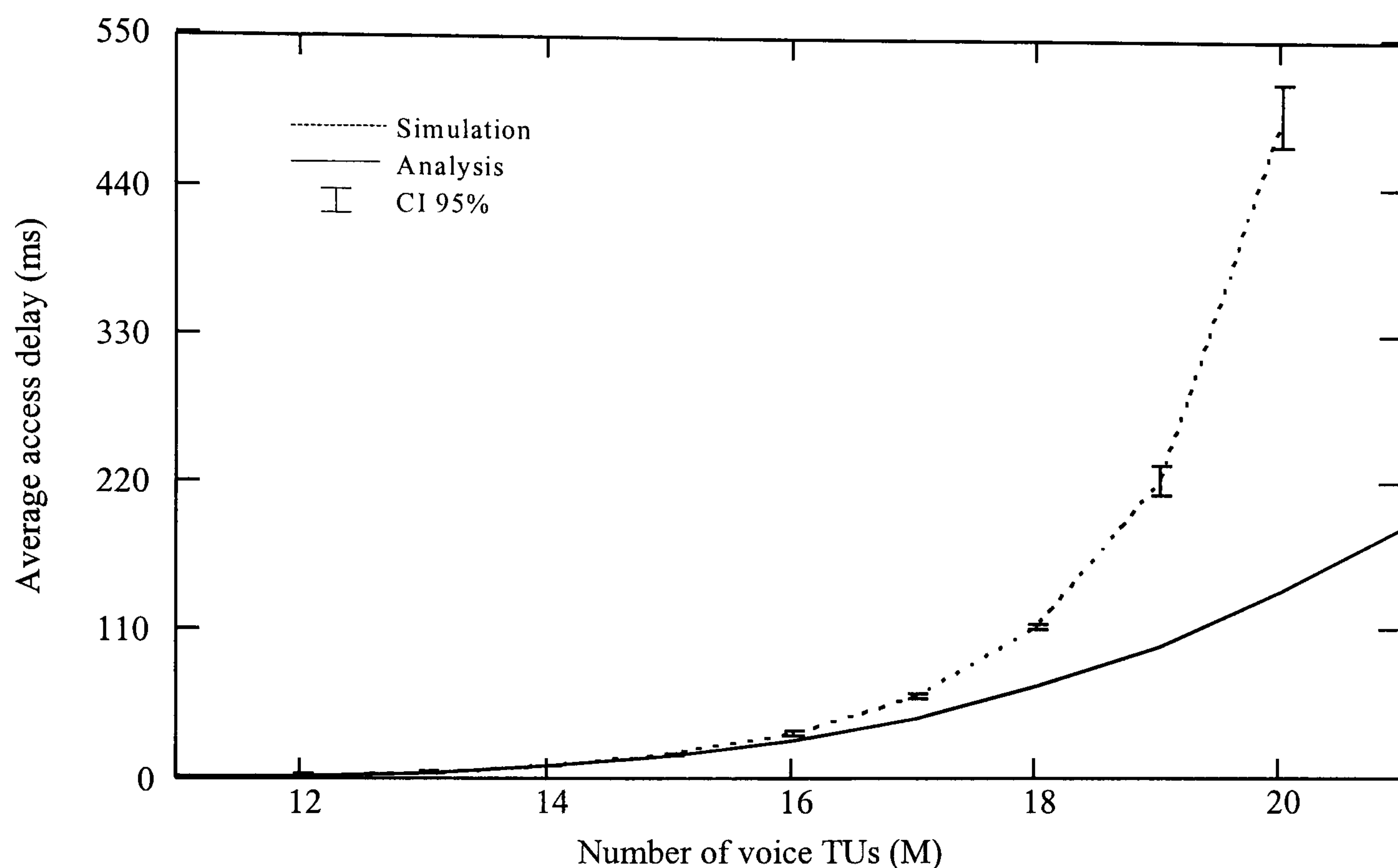


Fig. 7-9 Simulation and analysis results for the average access delay

This particular behaviour of the system can be treated further using the large deviation theory [119-121] however such a treatment is out of the scope of this thesis. Furthermore, in a real indoor IR wireless LAN the cell radius will not be more than a few meters, i.e. in chapter 6 it is taken to be  $r=3$  m, and therefore it is most unlikely to find more than 15 mobile TUs. It can be seen in Fig. 7-9 that for up to 16 TUs the analysis and simulation results correspond very well.

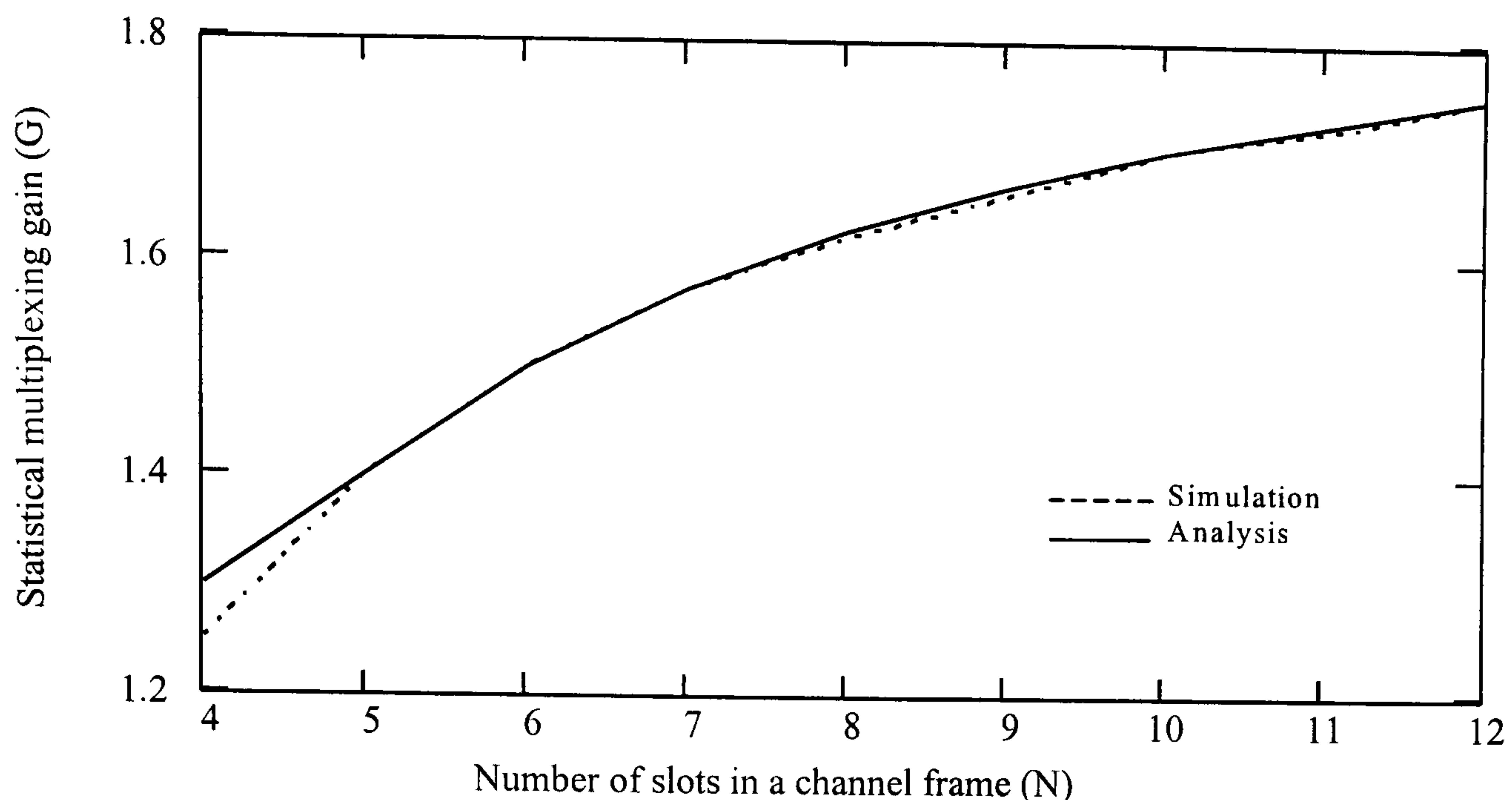


Fig. 7-10 Simulation and analysis results for the statistical multiplexing gain

Fig. 7-10 shows results for the statistical multiplexing gain. It is observed that the results of both simulation and analysis are in very close agreement.

## 7.6 Summary

In this chapter discrete time and event simulation processes were used to evaluate the system performance. The speech packet duration was considered as the basic time unit or event. The simulation model was divided into two main phases, the traffic generation (talkspurts and silences) and the MAC mechanism. Performance parameters such as packet dropping probability, throughput, average access delay and statistical multiplexing gain were simulated and compared with those from the mathematical analysis in Ch. 5. It was shown that the results of both processes are in close agreement.



# DISCUSSION

## CHAPTER EIGHT: PROPOSED EXTENDED WORK

## **8 PROPOSED EXTENDED WORK**

### **8.1 Introduction**

This chapter discusses issues for further work of this project. Although, numerous issues and aspects can be considered for future work presented here are the ones that are the most directly related to work that has been done to this extent. Therefore, issues concerning the slot allocation in the MAC protocol and the performance of the MAC protocol under the several particularities exhibited by the IR channel are discussed. Moreover, the effect of the co-channel interference, the handover initiation, and the further improvement of the discrete simulation model are considered.

### **8.2 Dynamic Slot Allocation of the MAC Protocol**

To this stage the work has mainly been concerned with the evaluation of the model under statistical mode for periodic packet sources. When a video source is required to be served, then the base (BS) station will assign when the required bandwidth is available, to the source its statistical bandwidth. Although the performance of a variable bit rate (VBR) video source may be satisfied when its statistical bandwidth is assigned, the statistical bandwidth does not exactly describe the traffic of the source. In order to precisely allocate the bandwidth for such a source and therefore improve the performance of the system in terms of capacity, dynamic slot allocation



based on the instantaneous bandwidth requirements of the source must be employed. As shown in Fig. 4-5 such information is transmitted to the BS via the SIG field of the IR wireless cell (IWC). Available bit rate (ABR) services, such as text, is a typical example of a dynamic allocation strategy because they are served by dynamically allocating the idle slots (slots that are not used by CBR and VBR services).

Therefore, it is of interest to modify the system in a way that it supports all kind of services in order to extend the ATM facilities into an indoor IR wireless LANs while the maximum MAC dynamic multiplexing gain is obtained. To achieve this the time slots in both uplink and downlink channel frames must be allocated to TUs in a dynamic pattern. This must be done according to burst length of information and residual lifetime of each service. To dynamically allocate the slots to TUs the existing MAC protocol must be controlled from a program. The program will retrieve the instantaneous requirements of each TU by means of the SIG field in each IWC and then will individually allocate the slots for each service. Also, the programme based on the handover-request rate within each individual cell will be responsible to dynamically vary the size of the common group and the guard group.

### **8.3 MAC Performance Under Hybrid FEC/ARQ Techniques**

Since ATM was designed for a medium whose bit error rate (BER) is very low, about  $10^{-9}$ , it is challenging to maintain the QoS for multimedia services while

employing ATM on a diffuse IR wireless links. Such links are characterised by a very noisy and time-varying environment in terms of the multipath phenomenon and intersymbol interference (ISI) with less bandwidth. Hence, the BER of the communication channel increases resulting in increased packet dropping probability and consequently the QoS and number of TUs in the system drop. Possible solutions for improving the IR channel BER must be examined for different sources. For time sensitive sources we will employ forward error controls (FEC) in the data link control (DLC) layer and for time insensitive sources the automatic repeat request (ARQ) can be employed.

ARQ and FEC techniques have been compared for various channels in particular the radio wireless channel, by many authors. The issue is quite complicated for integrated communications in a wireless channel, due to various conflicting requirements. Finding an engineering solution between ARQ and FEC that will reduce complexity and minimise extra bandwidth and delay, while at the same time satisfying all QoS requirements is difficult. Although several hybrid ARQ/FEC techniques have been reported in the literature, the particular characteristics of the diffuse IR medium change many of the boundary conditions. Hence, new research results under these conditions are required.

#### **8.4 Co-channel Interference for Various Reuse Factors**

As mentioned in Ch. 6, by introducing small radius cells (3 to 5 meters) for IR wireless LANs, the system capacity per unit area increases, but, at the same time



both the cochannel interference from the neighbouring cells and the number of handovers per call increase too. Throughout the analysis in chapters 5 and 6 a large channel reuse factor ( $J = 7$ ) is used to prevent co-channel interference. Knowing the lowest reuse factor possible, we can maximise the capacity of the system, however, this would cause an increased co-channel interference with the neighbouring cells that use the same channel. Thus the optimum point between channel reuse factor and co-channel interference must be investigated and determined according to the required system performance such as the area to be covered by each cell; required bandwidth for each cell; QoS to be delivered, etc. Therefore, for different channel reuse factors and under the employment of a hybrid FEC/ARQ scheme, the SNR of the diffuse IR link must be calculated. Based on this SNR the MAC performance as well as the receiver sensitivity will be derived.

## **8.5 Handover Request Initiation**

In a multi-cell environment, a TU travels from one cell to another while a connection is still alive. In such a case handover functions will deal with transferring the live connection while guaranteeing that the QoS requirements will not degrade. In this project a new hybrid handover-priority MAC protocol was proposed and using mathematical analysis its performance parameters under statistical slot allocation were derived. However, the handover initiation has been left unexamined. Such an initiation must be based on SNR measurements of the diffuse IR channel. A channel measurement takes place (when the signal of the old BS which the TU is linked is

weak) to determine whether a handover must be initiated. However, a technique must be adopted to distinguish that the fade of the IR signal is due to increase of the distance between TU and BS and not by any shadowing effects. Such a technique must be based on both signal measurements of the linked BS and signal measurements of the neighbouring BSs. Also, co-channel interference measurements could play an important role in initiating a handover request since the longer the distance between TU and the BS the larger the cochannel interference becomes. Handover initiation, therefore, poses a significant challenge for network control and management in our proposed IR wireless LAN.

## **8.6 Simulation Including Mobility and IR Channel Impairments**

In Ch. 7 discrete time and event simulation process was used to validate the results of the mathematical analysis demonstrated in Ch. 5. The simulation was run for a finite number of TUs within each cell without taking into account mobility issues that will in turn generate handover requests. Therefore, the current programme can be modified to run for mobile TUs within the network and consequently utilise the MAC protocol with the handover priority mechanism which was described in Ch. 6. Also, it would be very interesting if the simulation process were to take into account the IR channel impairments. For fast implementation of such a large and complex simulation algorithm, currently available simulation packages such as OPNET and COMNET can be used.



## 8.7 Summary

In this chapter issues for further work of this thesis are discussed. It is interesting to modify the proposed system in a way that the time slots in both uplink and downlink channel frames are allocated to TUs in a dynamic pattern. To reduce the BER of a diffuse IR channel for different types of services a hybrid FEC/ARQ based on the IR channel particularities must be used. Further work on the co-channel interference for different channel reuse factors would enlighten the adoption of the smallest possible channel reuse factor, and therefore increase the system capacity. In addition, handover initiation poses a significant challenge for network control and management in our proposed IR wireless LAN. Further improvement of the simulation program would include mobility, handover mechanism and the IR channel particularities.

# CHAPTER NINE:

## CONCLUSIONS



## 9 CONCLUSIONS

This thesis has considered the development and evaluation of a new hybrid wireless communication system. Such a system will be able to extend the broadband integrated system networks (B-ISDNs) into indoor optical wireless networks. The primary triggers for evolving toward the B-ISDN include an increasing demand for high bit rate services and the evolution of technology such as optical fibre transmission and switching technology. The transfer of information in these networks uses what is referred to as ATM which is a packet switching technique using fixed length packets, called cells. Each cell consists of a 5-byte header and 48-byte payload. The header carries sufficient information to route the cell across the network. The ATM layer consists of virtual channel and virtual path levels and carries out the routing of the cells using the identification fields of the headers. Above the ATM layer lays the ATM adaptation layer (AAL). This layer performs convergence as well as segmentation and reassembly operations on different types of traffic. Because of the small size cell ATM provides limited error detection and few operations are performed on the short header. Therefore, there is need for using traffic and control techniques in higher layers in order to successfully transfer the information in the network.

There are two viable media in which we can implement indoor wireless B-ISDN systems: radio and IR. Radio links will always find difficulty to deliver high bandwidths which are required for multimedia broadband platforms. However, the very high carrier frequency associated with IR systems (300 THz at  $1\mu\text{m}$ ) promises

high bandwidth channels, in the GHz region. Moreover, IR transmission neither interferes with existing radio systems nor falls under any regulation of the Federal Communication Commission (FCC) and therefore there is no need for any licence. Also, the fact that IR signals do not penetrate walls enables an indoor wireless network to provide both a considerable degree of privacy within an area, and a very large spatial bandwidth at the same spectrum, as the same frequency can be reused in adjacent areas. As the diffused optical signal propagates to the receiver there are two principal limitations caused by interference from ambient light and multipath propagation. The ambient light significantly reduces the SNR and calls for high transmitter powers. Diffuse high powers can be problematic due to eye safety standards that have to be obeyed. Diffuse IR technology is still in its infancy and most of the available systems today employ mainly direct-LOS or hybrid-LOS links.

The network scenario was presented and the structure of the protocol stack that attaches the wireless part onto the wired ATM network was analysed. To reduce complexity and processing time between the two networks the wireless part was designed to provide seamless interworking with the wired ATM network. The concept of a PRMA protocol was utilised to share the IR medium to TUs. Therefore, emphasis was placed on the structure of the MAC protocol that is employed under TDD mode and utilises optical prime codes to prevent collisions when TUs apply for slot reservations. The format of the IR wireless cells for conveying voice services in the user plane was considered and some of the most basic challenges of employing ATM over diffuse IR local area networks were revealed.



The MAC protocol was modelled as a  $M/M/N/\infty/M$  queuing system consisting of exponentially distributed durations of all spurts and gaps,  $N$  parallel servers, infinite storage and  $M$  users. The state probability of the system was derived using the birth-death theory. Then the performance parameters such as throughput, average access delay, packet dropping probability, and statistical multiplexing gain were derived. Using mathematical analysis it was revealed that for  $P_{\text{drop}}$  equal to 1% the MAC is capable of supporting 15 voice TUs simultaneously while the system throughput is 0.68. For  $M$  less than 14 the system is in an insensitive region and the variance of TUs has no effect on the average access delay. When  $M$  exceeds 14 the system is in a sensitive region and the access delay increases rapidly. The statistical multiplexing gain of the MAC is 1.7 conversations per each uplink time slot for  $P_{\text{drop}} = 1\%$ . The multiaccess interference at the correlative receiver was found to be approximately  $10^{-8}$ , which is a satisfactory value.

A hybrid handover priority-based MAC protocol to support ATM voice services over the IR wireless LANs was proposed. Carrying out mathematical analysis its performance parameters were derived for a fixed slot assignment. Using the information in link design a LAN example where VBR voice TUs are served was presented. It was shown that the forced termination probability was improved over the nonpriority handover scheme in return of increasing the new call blocking probability. For  $P_{\text{drop}} = 1\%$  the new call blocking probability is less than 1% while the forced termination probability is less than 0.05 %. These values exhibit a very

satisfactory performance. Moreover, the value of the throughput parameter has just slightly changed over the nonpriority scheme only for high new call arrival rates, this fact demonstrates a general improved performance of the network.

Discrete time and event simulation process was used to evaluate the system performance. The simulation model was divided into two main phases, the traffic generation (talkspurts and silences) and the MAC mechanism. Performance parameters such as packet dropping probability, system throughput, average access delay and statistical multiplexing gain were simulated and compared with them from the mathematical analysis in Ch. 5. It was shown that the results of both processes are in close agreement.

The future work section focuses on improving and investigating the original design of the model including modification of the proposed MAC in a way that the time slots in both uplink and downlink channel frames are allocated to TUs in a dynamic pattern. Other issues concerning the performance of the MAC protocol under the several particularities exhibited by the IR channel are discussed the effect of the co-channel interference, the handover initiation, and the further improvement of the discrete simulation model were discussed.



## APPENDIX A

---

### MATHCAD code for the voice source

```
x := | j ← 0
      | while j ≤ (TUs - 1)
      |   | k ← 0
      |   | i ← 0
      |   | xi,j ← 0
      |   | while i ≤ 2 · (N_messag - 1)
      |   |   | x(i+1),j ← (xi,j + τk,j)
      |   |   | x(i+2),j ← [x(i+1),j + σk,j]
      |   |   | i ← i + 2
      |   |   | k ← k + 1
      |   | j ← j + 1
      | x
```

```
A := | j ← 0
      | while j ≤ (TUs - 1)
      |   | i ← 0
      |   | v ← 0
      |   | while i ≤ 2 · (N_messag - 1)
      |   |   | for v ∈ [x(i+1),j] .. [x(i+2),j]
      |   |   |   | Av,j ← 1
      |   |   | i ← i + 2
      |   | j ← j + 1
      | A
```

## APPENDIX B

### MATHCAD code for the discrete time simulation MAC mechanism

```

MAC := | b_steps ← 3
      | for i ∈ 0 .. (b_steps - 1)
      |   Bini ← 0
      | i ← b_steps
      | while i < rows (A)
      |   | (TUs - 1)
      |   | Np ← ∑j = 0 Ai,j
      |   | Bini ← (Np - N) if Np ≥ N
      |   | otherwise
      |   |   | Bini ← 0
      |   |   | As ← (N - Np)
      |   |   | s ← i
      |   |   | for k ∈ 0 .. (b_steps - 1)
      |   |   |   | i ← s - (b_steps - k)
      |   |   |   | if As ≤ Bini
      |   |   |   |   | Bini ← (Bini - As)
      |   |   |   |   | break
      |   |   |   | otherwise
      |   |   |   |   | As ← (As - Bini)
      |   |   |   |   | Bini ← 0
      |   |   |   | i ← i + (b_steps - k)
      |   |   | TAsi ← As
      |   |   | i ← i + 1
      |   | Total_Bin ← ∑i = 0rows (A) - 1 Bini
      |   | Tas ← ∑ TAs
      |   | [ Total_Bin ]
      |   | [ Tas ]

```



## APPENDIX C

---

### MATHCAD code for the discrete event MAC mechanism

```
x ← x
ts ← matrix [(max (x)) + 1 , 1 , F]
delay ← matrix (rows (x) - 1 , 1 , Z)
i ← 1
while i ≤ rows (x) - 1
  q ← submatrix [ts , x(i, 0) , x(i, 1) , 0 , 0]
  if min(q) > 0
    I ← i
    for i ∈ x(i, 0) .. x(i, 1)
      tsi ← tsi - 1
    i ← I
    i ← i + 1
  otherwise
    delayi ← delayi + 1
    x(i, 0) ← x(i, 0) + 1
    x(i, 1) ← x(i, 1) + 1
  delay
```

## REFERENCES

---

1. Minzer, "*Broadband ISDN and Asynchronous Transfer Mode (ATM)*", IEEE Communications Magazine, pp. 17-24, Sept. 1989.
2. I-series of CCITT draft Recommendations, November 1990.
3. ITU-T Recommendations I.121 Broadband Aspects of ISDN, 1991.
4. ITU-T, "*I-series Recommendations*", 1993.
5. F. A. Tobagi, "*Fast Packet Switch Architectures For Broadband Integrated services Digital Networks*", Proc. IEEE, Vol. 78, No. 1, 1990.
6. C.J. Hughes, A.G. Waters, "*Packet Power: B-ISDN and The Asynchronous Transfer Mode*", IEEE Review, pp. 357-360, October 1991.
7. M. Kawarasaki and B. Jabbari, "*B-ISDN architecture and protocol*", IEEE Journal on Selected Areas in Communications, Vol. 9, No. 9, 1991.
8. P.E. White, "*The role of the Broadband Integrated Services Digital Network*", IEEE Communications Magazine, pp. 116-119, March 1991.
9. A. Day, "*International Standardisation of B-ISDN*", IEEE Lightwave Transmission Systems, pp. 13-20, August 1991.
10. Jean-Yves Le Boudec, "*The Asynchronous Transfer Mode: a tutorial*", Computer Networks and ISDN Systems, Vol. 24, pp. 279-309, 1992.



11. I. Gallagher, “*Broadband ISDN*”, IEEE Data Communications and Networks 3, pp. 76-90, 1994.
12. W. Stallings, “*ISDN and Broadband ISDN with Frame Relay and ATM*”, Prentice Hall, Inc, 1995.
13. U. Black, “*ATM: Foundation For Broadband Networks*”, Prentice Hall, Inc., 1995.
14. S. Dixit, S. Elby, “*Frame Relay and ATM Interworking*”, IEEE Commun. Mag., pp. 64-82, June 1996.
15. Y.T. Hou, L. Tassiulas, H.J. Chao, “*Overview of Implementing ATM-Based Enterprise Local Area Network for Desktop Multimedia Computing*”, IEEE Commun. Mag., pp. 70-76, April 1996.
16. R. Jeffries, “*ATM’s Challenges; Real and Imagined*”, Business Commun. Review, Vol. 26, No. 4, pp. 24-27, 1996.
17. T.K. Lala, “*Broadband Access: What Kind, When and How Much?*”, IEEE Communications Magazine, pp. 112-113, November 1996.
18. J. Anderson, P. Lamy, L. Hue, L.L. Beller, “*Operations Standards for Global ATM Networks: Network Element View*”, IEEE Communications Magazine, pp. 72-84, December 1996.
19. Dave Mustill, “*Quality of Services Guarantees: A Challenge for ATM Networks*”, IEEE GLOBECOM ‘96, Vol. 1, pp. 420-423, 1996.
20. P.L. Clarke, N.J.P. Cooper, D.J. Sutherland, “*ATM-the next generation*”, BT Technol. J., Vol. 16, No. 1, pp. 106-113, 1998.

21. <http://www.atmforum.com/>
22. *"Special Issue on Wireless ATM"*, IEEE Personal Communications, Vol. 3, No. 4, August 1996.
23. *"Special Issue on Introduction to Mobile and Wireless ATM"*, IEEE Communications, Vol. 35, No. 11, November 1997.
24. T. Stock, X. Garcia, *"On the Potentials of Forward Error Correction Mechanisms Applied to Real-Time Services Carried Over B-ISDN"*, Conf: Broadband Communications, International Zurich Seminar '96, pp. 107-118, 1996.
25. S. Aikawa, Y. Motoyama, M. Umehira, *"Forward Error Correction Schemes for ATM Systems"*, IEEE International Conference on Communications '96, Dallas, Texas USA, Vol. 1, pp. 454-458, June 1996.
26. S.H. Lim, D.M. Ahn, D.W. Kim, D.Y. Kim, *"Cell Loss Reduction by Cell Unit Interleaving in Wireless ATM Networks"*, IEEE International Conference on Communications '96, Dallas, Texas USA, Vol. 1, pp. 449-453, June 1996.
27. C. Oliveria, J.B. Kim, T. Suda, *"Quality-of-Service Guarantee in High-Speed Multimedia Wireless Networks"*, IEEE International Conference on Communications '96, Dallas, Texas USA, Vol. 2, pp. 728-734, June 1996.
28. C. Blondia, O. Casals, *"Traffic Profiles in ATM Networks"*, Telecommun. systems J., Vol. 5, pp. 49-69, 1996.



29. D. Gaiti, G. Pujolle, "*Performance Management Issues in ATM Networks: Traffic and Congestion Control*", IEEE/ACM Trans. on Networking, Vol. 4, No. 2, 1996.
30. E.P. Rathgeb, "*Modelling and performance comparison of policing mechanisms for ATM*", IEEE Journal on Selected Areas in Communications, Vol. 9, No. 3, 1991.
31. F.R. Gfeller, U. Bapst, "*Wireless In-House Data Communication via Diffuse Infrared Radiation*", IEEE Proc., Vol. 67, No. 11, 1979.
32. P.P. Smyth, M. McCullagh, D. Wisely, D. Wood, S. Ritchie, P. Eardley, S. Cassidy, "*Optical Wireless Local Area Networks-enabling Technologies*", BT Technol. J., Vol. 11, No. 2, 1993.
33. J.R. Barry, J.M. Kahn. W.J. Krause, E.A. Lee, D.G. Messerschmitt, "*Simulation of Multipath Impulse Response for Indoor Wireless Optical Channels*", IEEE Selected areas in Commun. J., Vol. 11, No. 3, 1993.
34. P. Mckee, D. Wood, J. Towers, P. Smyth, "*Applications of Computer Generated, Free-Space Diffractive Optics From Interconnections and Packaging to Optical Wireless Antennas*" Fourth International Conference on Holographic Systems, Components and Applications, Sept. 1993.
35. H. Hashemi, G. Yun, M. Kavehrad, F. Behbahani, P.A. Galko, "*Indoor Propagation Measurements at Infrared Frequencies for Wireless Local Area Networks Applications*" IEEE Trans. on Vehicular. Technology, Vol. 43, No. 3, pp. 562-576, 1994.
36. J.R. Barry, "*Wireless Infrared Communications*", Boston, Kluwer Academic, 1994.

37. K-C Chen, "*Direct Detected Modulations of High Speed Indoor Diffused Infrared Wireless transmission*", IEEE PIMRC/WCN, Vol. IV, pp. 1096-1100, 1994.
38. R.T. Valadas, A.M. de Oliveira Duarte, "*Sectored Receivers for Indoor Wireless Optical Communication Systems*", IEEE PIMRC/WCN, Vol. IV, pp. 1090-1095, 1994.
39. G.W. Marsh, J.M. Kahn, "*50-Mb/s Diffuse Infrared Free-Space Link Using On-Off Keying with Decision-Feedback Equalization*", IEEE PIMRC'94/WCN, Vol. IV, pp. 1086-1089, 1994.
40. J.J.G. Fernades, P.A. Watson, J.C. Neves, "*Wireless LANs: Physical Properties of Infra-Red Systems vs Mmw Systems*", IEEE Commun. Mag., pp. 68-73, August 1994.
41. L.G. Kazovsky, T. Fong, T. Hofmeister, "*Optical Local Area Network Technologies*", IEEE Commun. Mag., pp.50-54, December 1994.
42. M.D. Audeh, J.M. Kahn, "*Performance evaluation of baseband OOK for wireless indoor infrared LAN's operating at 100 Mb/s*", IEEE trans. Commun., Vol. 43, no. 6, pp. 2085-2094, 1995.
43. A.J.C. Moreira, R.T. Valadas, A.M. de Oliveira Duarte, "*Characterisation and Modelling of Artificial Light Interference in Optical Wireless Communication systems*", IEEE PIMRC'95, Toronto, pp. 326-331, 1995.
44. J.M. Kahn, W.J. Krause, J.B. Carruthers, "*Experimental Characterisation of Non-Directed Indoor Infrared Channels*", IEEE Trans. on Commun., Vol. 43, No. 2/3/4, pp. 1613-1623, 1995.



45. J.M. Kahn, W.J. Krause, J.B. Carruthers, "*Experimental Characterisation of Non-Directed Indoor Infrared Channels*", IEEE Trans. on Commun., Vol. 43, No. 2/3/4, pp. 1613-1623, 1995.
46. R. Narasimhan, M.D. Audeh, J.M. Kahn, "*Effect of electronic-ballast fluorescent lighting on wireless infrared links*" IEE Proc.-Optoelectron., Vol. 143, No. 6, pp. 347-354, 1996.
47. P.L. Eardley, D.R. Wisely, D. Wood, P. McKee, "*Holograms for optical wireless LANs*" IEE Proc.-Optoelectron., Vol. 143, No. 6, pp. 365-369, 1996.
48. M.R. Pakravan, E. Simona, M. Kavehrad, "*Holographic Diffusers for Infrared Communication systems*", IEEE GLOBECOM '96, Vol. 3, pp. 1608-1612, 1996.
49. A.C. Boucouvalas, "*Indoor ambient light noise and its effect on wireless optical links*" IEE Proc.-Optoelectron., Vol. 143, No. 6, pp. 334-338, 1996.
50. A.J.C. Moreira, R.T. Valadas, A.M. de Oliveira Duarte, "*Performance of infrared transmission systems under ambient light interference*" IEE Proc.-Optoelectron., Vol. 143, No. 6, pp. 339-346, 1996.
51. G.N. Bakalidis, E. Glavas, Ph. Tsalides, "*Optical power distribution in wireless infrared LANs*", IEE Proc.-Commun., Vol. 143, No. 2, pp. 93-97, 1996.
52. J.M.H. Elmirghani, H.H. Chan, R.A. Cryan, "*Sensitivity evaluation of optical wireless PPM systems utilising PIN-BJT receivers*" IEE Proc.-Optoelectron., Vol. 143, No. 6, pp. 355-359, 1996.
53. J.M. Kahn, J.R. Barry, "*Wireless Infrared communications*", IEEE Proc., Vol. 85, No. 2, pp. 263-298, 1997.

54. J.B. Carruthers, J.M. Kahn, "*Modelling of Nondirect Wireless Infrared Channels*", IEEE Trans. On Commun., Vol. 45, No. 10, pp. 1260-1268, 1997.
55. A.M. Street, P.N. Stavrinou, D.C. O'Brien, D.J. Edwards, "*Tutorial Review: Indoor optical wireless systems - a review*", Optical and Quantum Electronics, 29, pp. 349-378, 1997.
56. Pavlos Theodorou, J.M.H Elmirghani, R.A. Cryan, "*Concept and architecture for Indoor Optical Wireless Multimedia Systems*", The International Society for Optical Engineering (SPIE) All-Optical Communication Systems: Architecture, Control and Network Issues Conference, Vol. 3230, pp. 104-108, Dallas, Texas, November 1997.
57. G. W. Marsh, J. M. Kahn, "*Channel Reuse Strategies for Indoor Infrared wireless Communications*", IEEE Trans. Commun., Vol. 45, No. 10, pp. 1280-1290, 1997.
58. Pavlos Theodorou, J.M.H Elmirghani, and R.A. Cryan "*ATM Infrared Wireless LANs: A proposed architecture*", IEEE Communications Magazine, Vol. 36, No. 12, pp. 118-123, Dec. 1998.
59. Pavlos Theodorou, J.M.H Elmirghani and R.A. Cryan, "*Packet Voice Transmission for Indoor Optical wireless Networks*", IEEE Global Communications Conference (GLOBECOM'98), Sidney, Australia, Vol. 1, pp.288-233, 1998.
60. Infrared Data Association: <http://www.irda.org/>
61. Pavlos Theodorou, J.M.H. Elmirghani, and R.A. Cryan, "*Broadband Optical Wireless ATM LANs With Fixed Time Slot Assignment*", 3rd IEEE International



Workshop on Broadband Switching Systems, Queen's University, Kingston, Ontario, Canada, June 1-3, 1999.

62. Pavlos Theodorou, J.M.H. Elmirghani, and R.A. Cryan, "*Performance Analysis of ATM Traffic on Optical Wireless LANs*", Proc. IEE Colloquium on Optical Wireless Communications, pp. 11/1-11/6, London 1999.
63. Pavlos Theodorou, J.M.H. Elmirghani, and R.A. Cryan "*Performance of Fixed Slot Assignment MAC Protocol for ATM Infrared Wireless LANs*", Accepted for publication in the Journal of Optical Communications, 1999.
64. Colloquium on "*Optical Wireless Communications*", IEE, London, 22 June 1999.
65. S.H. Khoo, E.B. Zyambo, G. faulkner, D.C. O'Brien, D.J. Edwards, M. Ghisoni, J. Bengtsson, "*Eyesafe optical link using a holographic diffuser*", IEE Colloq. on Optical Wireless Communications, pp. 3/1-3/6, London, June 1999.
66. V. Pohl, V. Jungnickel, R. Hentges, C. von Helmolt, "*Integrating Sphere Diffuser for Wireless Infrared Communication*", IEE Colloq. on Optical Wireless Communications, pp. 4/1-4/6, London, June 1999.
67. Int. Electrotech. Commission, CEI/IEC825-1: *Safety of Laser Products*, 1993.
68. Safety of Laser products, EN 608 25-1:1994, British Standards Institution, London.
69. IEEE 802.11 Wireless LAN Standard
70. <http://www.spectrixcorp.com/>

71. M. Kadoch, “*ATM Signalling: a Tutorial*”, 1995 Canadian Conference on Electrical and Computer Engineering, pp. 420-423, 1995.
72. E. Gelenble, X. Mang, R. Onvural, A. Telesyn, “*Bandwidth Allocation and Call Admission Control in High-Speed Networks*”, IEEE Communications Magazine, pp. 122-129, May 1997.
73. R. Bolla, F. Davoli, M. Marchese, “*Bandwidth Allocation and Admission Control in ATM Networks with Service Separation*”, IEEE Communications Magazine, pp. 130-137, 1997.
74. S.S. Lam, “*Packet Broadcast Networks: A Performance Analysis of the R-ALOHA Protocol*”, IEEE Trans. on Communications, Vol. 29, No. 7, pp. 596-603, 1980.
75. D.J. Goodman, R.A. Valenzuela, K.T. Gayliard, B. Ramamurthi, “*Packet Reservation Multiple Access for Local Wireless Communications*”, IEEE Trans. on Commun., Vol. 37, No. 8, pp. 885-890, 1989.
76. S. Nanda, D.J. Goodman, U. Timor, “*Performance of PRMA: A Packet Voice Protocol for Cellular Systems*”, IEEE Trans. Veh. Techn., Vol. 40, NO. 3, pp. 584-598, 1991.
77. N. Amitay, S. Nanda, “*Resource Auction Multiple Access (RAMA) for Statistical Multiplexing of Speech in Wireless PCS*”, IEEE, Trans. Veh. Techn., Vol. 43, No. 3, pp. 584-596, 1994.
78. G. Wu, K. Mukumoto, A. Fukuda, “*Analysis of an Integrated Voice and Data Transmission System Using Packet Reservation Multiple Access*”, IEEE Trans. Veh. Techn., Vol. 43, No. 2, pp. 289-297, 1994.



79. M.J. McTiffin, A.P. Hulbert, T.J. Ketseoglou, W. Heimsch, G. Crisp, “*Mobile Access to an ATM Network Using a CDMA Air Interface*”, IEEE, JSAC, Vol. 12, NO. 5, pp. 900-908, 1994.
80. D. Raychaudhuri, N.D. Wilson, “*ATM-Based Transport Architecture for Multiservices Wireless personal Communication Networks*”, IEEE, JSAC, Vol. 12, No. 8, pp. 1402-1414, 1994.
81. D.M. Chhitre, D.S. Gokhale, T. Henderson, J.L. Lunsford and N. Mathews, “*Asynchronous Transfer Mode (ATM) Operation Via Satellite: Issues, Challenges and Resolutions*”, International Journal of Satellite Communications, Vol. 12, pp. 211-222, 1994.
82. J. Dunlop, J. Irvine, D. Robertson, P. Cosimini, , “*Performance of Statistically Multiplexed access Mechanisms for a TDMA Radio Interface*”, IEEE Personal Commun., Vol. 2, pp.56-64, June 1995.
83. W. Zhuang, “*Medium Access Control Protocol for Multimedia Wireless Networks*”, PIMRC’95, Vol. 3, pp. 1094-1098, 1995.
84. D. Petras, “*Medium Access Protocol for wireless, transparent ATM access*”, IEEE Wireless Communication systems Symposium 1995, <http://www.comnets.rwth-aachen.de/~petras>, 1995.
85. H.F Chou, K.C. Chen, “*Performance of Group Randomly addressed Polling with Reservation in Wireless Integrated services Networks*”, IEEE GLOBECOM ‘95, Vol. 2. pp. 1497-1501, 1995.
86. G. Sfikas, R. Tafazolli, B.G. Evans, “*ATM Cell Transmission Over The IEEE 802.11 Wireless MAC Protocol*”, IEEE, 7<sup>th</sup> Int. Symposium, on Personal, Indoor and Mobile Radio Communications (PIMRC), pp. 173-177, 1996.

87. D. Petras, A. Kramling, A. Hettich, "*Design Principles for a MAC protocol of an ATM Air Interface*", <http://www.comnets.rwth-aachen.de/~petras>, 1996.
88. M. Umehira, M. Nakura, H. Sato, A. Hashimoto, "*ATM Wireless Access for Mobile Multimedia: Concept and Architecture*", IEEE Personal Communications, pp. 39-48, October 1996.
89. G. Anastasi, D. Grillo, L. Lenzini, "*An Access Protocol for Speech/Data/Video Integration in TDMA-Based Advanced Mobile Systems*", JSAC, Vol. 15, No. 8, pp. 1498-1510, 1997.
90. J. Sanchez, R. Martinez, M.W. Marcellin, "*A Survey of MAC Protocols Proposed for Wireless ATM*", IEEE Network, pp. 52-62, Nov./Dec. 1997.
91. S. Jiang, D. H. K. Tsang, "*On Architectures for Broadband Wireless Systems*", IEEE Commun. Magazine, pp. 132-140, October 1997.
92. W. Ren, C. Fan, "*Study of Frame-Based PRMA Protocol under Time-Division Duplex*", Globecom'97, Vol. 3, pp. 1630-1634, 1997.
93. X. Wu, S. Wu, H. Sun, L. Li, "*Dynamic Slot allocation Multiple access protocol for Wireless ATM Networks*", ICC'97, Vol. 3, pp. 1560-1565, 1997.
94. G. Anastasi, L. Lenzini, E. Mingozzi, A. Hettich, A. Kramling, "*MAC Protocols for Wideband Wireless Local Access: Evolution Toward Wireless ATM*", IEEE, Personal Communicatios, pp. 53-64, October 1998.
95. R. Ramjee, T.F. La Porta, J. Kurose, D. Towsley, "*Performance Evaluation of Connection Rerouting schemes for ATM-Based Wireless Networks*", IEEE/ACM Trans. on Networking, Vol. 6, No. 3, 1998.



96. J.A. Salehi, "Code Division Multiple-Access Techniques in Optical Fiber Networks-Part I: Fundamental principles", IEEE Trans. on Commun. Vol. 37, No. 8, pp. 824-833, 1989.
97. F.R.K. Chung, J.A. Salehi, V.K. Wei, "Optical Orthogonal Codes: Design, Analysis and Applications", IEEE Trans. on Information. Theory, Vol. 35, No. 3, pp. 595-604, May 1989.
98. J.A. Salehi, "Code Division Multiple-Access Techniques in Optical Fiber Networks-Part II: Systems Performance Analysis", IEEE Trans. on Commun. Vol. 37, No. 8, pp. 834-842, 1989.
99. A.S. Holmes, R.R. A. Syms, "All-Optical CDMA Using "Quasi-Prime" Codes", J. of Lightwave Techn., Vol. 10, No. 2, pp. 279-286, 1992.
100. J.M.H. Elmirghani, R.A. Cryan, "Hybrid PPM-CDMA Optical Orthogonal Codes for Indoor Wireless Infrared Communication", Microwave and Optical Techn. Lett., Vol. 8, No. 1, 1995.
101. Jian-Guo Zhang, Wing C. Kwong, Stelly Mann, "All-Optical code-division multiple-access applications:  $2n$  extended-prime codes", Applied Optics, Vol. 36, No. 26, 1997.
102. J.G. Zhang, W.C. Kwong, A.B. Sharma, " $2^n$  modified prime codes for use in fibre optic CDMA networks", Electr. Lett., Vol. 33, No. 22, pp. 1840-1841, 1997.
103. J.G. Zhang, W.C. Kwong, A.B. Sharma, "Effective design of optical code-division multiple access networks by using the midified prime code", Electr. Lett., Vol. 33, No. 3, pp. 229-230, 1997.

104. D. Petras, A. Hettich, "*Performance evaluation of the ASR-ARQ Protocol for wireless ATM*", IEEE Wireless Communication systems Symposium 1995, <http://www.comnets.rwth-aachen.de/~petras>, 1995.
105. D.S. Eom, M. Sugano, M. Murata, H. Miyahara, "*A Combination Scheme of ARQ and FEC for Multimedia Wireless ATM Networks*", IEICE Trans. Commun. Vol. E81-B, No. 5, pp. 1016-1024, 1998.
106. D. Gross, C. M. Harris, "*FUNDAMENTALS OF QUEUEING THEORY*", John Wiley & Sons, pp. 118-120, 1974.
107. P. Taaghol, R. Tafazolli, B.G. Evans, "*Statistical Upper Bounds and Performance Evaluation of packet Reservation-Based Multiple Access Protocols in Cellular Communications Systems*", PIMRC'95, Vol. 1, pp. 348-53, 1995.
108. D.J. Goodman, S.X. Wei, "*Efficiency of Packet Reservation Multiple Access*", IEEE Trans. Veh. Techn., Vol. 40, No. 1, 1991.
109. H.G. Perros, K.M. Elsayed, "*Call Admission Control Schemes: A Review*", IEEE Communications Magazine, pp. 82-91, November 1996.
110. R. Guerin, H. Ahmadi, M. Naghshineh, "*Equivalent Capacity and Its Application to Bandwidth Allocation in High-Speed Networks*", IEEE JSAC, Vol. 9, No. 7, pp. 968-981, 1991.
111. G.-C. Yang, W.C. Kwong, "*Performance analysis of optical CDMA with prime codes*", IEE Electr. Letters, Vol. 31, No. 7, pp. 569-570, 1995.



112. D. Hong, S.S. Pappaport, "*Traffic Model and performance Analysis for Cellular Mobile Radio telephone systems with Prioritized and Nonprioritized Handoff Procedures*", IEEE Trans. Veh. Techn., Vol. 35, No. 3, pp. 77-92, 1986.
113. M.D. Kulavaratharajah, A.H. Aghvami, "*Teletraffic Performance Evaluation of Microcellular Personal Communication Network (PCN's) with Prioritised Handoff Procedures*", IEEE Trans. Veh. Techn., Vol. 48, No. 1, pp. 137-152, 1999.
114. Y. Lin, S. Mohan, A. Noerpel, "*PCS Channel Assignment Strategies for Hand-off and Initial Access*", IEEE Personal Communications, 3rd Quarter, pp. 47-56, 1994.
115. S. Mayer, "*A new method to determine blocking probabilities in micro-and picocellular wireless communications networks*", GLOBECOM'97, Vol. 2, pp. 1001-1005, 1997.
116. E. Gelenble, G. Pujolle, "*Introduction to Queueing Networks*", John Wiley & Sons, 1998.
117. J.M. Pitts, J.A Schormans, "*Introduction to ATM: Design and Performance*", John Willey & Sons, 1996.
118. J. Walrand, "*Communication Networks; A First Course: 2<sup>nd</sup> Edition*", McGraw-Hill, 1998.
119. M. Cottrell, J. C. Fort, G. Malgouyres, "*Large deviations and rare events in the study of stochastic algorithms*", IEEE Trans. on Automatic Control, vol.AC-28, no.9, pp.907-20, 1983.

120. N. Sowski, "*Large deviation theory and efficient simulation of excessive backlogs in a GI/GI/m*", IEEE Trans. on Automatic Control, vol.AC-36, no.12, 1997.
121. S. Deman, R.K. Boel, "*Estimation of the probabilities of rear events and the sensitivity using importance sampling*", 5th Proceedings of the fifth IFIP Workshop on Performance Modelling and Evaluation of ATM Networks, Ilkley, pp. 80/1-80/10, 1997.